

Proceedings of the  
*11<sup>th</sup> International Symposium on  
Vibrations of Continuous Systems*

*Royal Victoria Hotel, Llanberis,  
Snowdonia, Wales, UK,  
July 16-22, 2017*





## Preface

The International Symposium on Vibrations of Continuous Systems (ISVCS) is a forum for leading researchers from across the globe to meet with their colleagues and to present both old and new ideas in the field. Each participant has been encouraged either to present results of recent research or to reflect on some aspect of the vibration of continuous systems, which is particularly interesting, unexpected or unusual. This type of presentation is meant to encourage participants to draw on understanding obtained through many years of research in the field.

ISVCS focuses on the vibrations of the fundamental structural elements: strings, rods, beams, membranes, plates, shells, bodies of revolution and other solid bodies of simple geometry. Structures composed of assemblies of structural elements are also of interest, especially if such structures display interesting or unusual response.

The ISVCS started 20 years ago, at Stanley Hotel, Estes Park, Colorado, USA August 11-15, 1997. It comes every two years, the present 11th Symposium takes place on 16-22 July 2017 at the Victoria Hotel, Llanberis, Snowdonia, Wales UK. Typical days at the Symposium will consist of morning technical presentations, afternoon hikes or excursions in the local area and, in the evening, further technical discussions and social gatherings. The various outings and social gatherings provide important opportunities for relaxed and informal discussion of technical and not-so-technical topics surrounded by the natural beauty of the Snowdonia National Park.

This volume of Proceedings contains 20 short summaries of the technical presentations to be made at the Symposium, as well as short biographical sketches of the participants.

The present edition is the first one without the presence of Art Leissa, founder and Honorary Chairman of ISVCS. We all miss Art. Many others senior board members are absent (Y. Narita, J. Wauer, S. Dickinson, P. Hagedorn); we hope that some of them will join again in the next Symposia.

Last but not least we remember with pain that Ali Nayfeh, a frequent attendee of past Symposia, left us unexpectedly on March 27 at the age of 83. An obituary by Prof Walter Lacarbonara is currently in press in Journal of Sound and Vibration.

*General Chairman* Erasmo Carrera  
*Editorial Chairman* Ilanko Ilanko  
*Local Arrangements Chairman* David Kennedy  
*Publicity Chairman* Yoshihiro Narita  
*Honorary Chairman* Art Leissa

## **Past Symposia**

The 1st International Symposium:

The Stanley Hotel, Estes Park, Colorado, USA

August 11-15, 1997

The 2nd International Symposium:

The Sunstar Hotel, Grindelwald, Switzerland

July 11-16, 1999

The 3rd International Symposium:

Jackson Lake Lodge, Grand Teton National Park, Wyoming, USA

July 23-27, 2001

The 4th International Symposium

Keswick, Lake District, England

July 23-27, 2003

The 5th International Symposium:

Berchtesgaden at Lake Königssee, Germany

July 25-29, 2005

The 6th International Symposium:

PlumpJack Squaw Valley Inn, Olympic Valley, California, USA

July 23-27, 2007

The 7th International Symposium:

Zakopane, Poland

July 19-25, 2009

The 8th International Symposium:

Whistler, British Columbia, Canada

July 18-22, 2011

The 9th International Symposium:

Courmayeur, Italy

July 22-26, 2013

The 10th International Symposium:

Stanley Hotel, Estes Park, Colorado, USA,

July 26-31, 2015

Details of the Proceedings of the past Symposia can be found at

<http://www.isvcs.org>

# Table of Contents

## Presentation Summaries (Presenting author is shown underlined)

1. **The Vibration Correlation Technique Revisited**  
H. Abramovich, K. Kalnins page 1
2. **Veering and modes aberration of structures subjected to in-plane loadings according to linearized and full nonlinear formulations**  
Erasmus Carrera, Alfonso Pagani page 4
3. **3D vibrations of multilayered hollow spheres in complex fluids**  
Weiqiu Chen, Bin Wu page 7
4. **A Wavelet-decomposed Semi-analytical Model for Acoustic Black Hole Effect Analyses**  
Liling Tang, Li Cheng page 10
5. **On the application of the spectral theory of linear operators to the natural vibration analysis of continuous systems**  
Piotr Cupiał page 13
6. **Investigations on the Similitudes of Stiffened Cylinders**  
G. Petrone, S. De Rosa and F. Franco page 16
7. **The Necessity of the Timoshenko Beam Theory for modeling Gyroscopic Continua**  
Hu Ding page 19
8. **Vibrations of plates with rectangular cutouts**  
Moshe Eisenberger and Aharon Deutsch page 22
9. **Shear Coefficients for Symmetric Bending Vibration of Thin, Shallow, Circular Cylindrical, Rectangular-planform Shells**  
Mark Ewing page 25
10. **Rotordynamics analyses using a node-dependent unified formulation**  
Matteo Filippi, Enrico Zappino, Erasmus Carrera page 28

- 11. Comparison of the Dynamic and Stability behaviour of Guided Spline Circular Saws and Collared Circular Saws**  
Stanley G. Hutton, Ahmad Mohammadpanah, page 31
- 12. The effect of roving rotary inertia as it passes a crack**  
S. Ilanko, J. De Los Rios, S. Caddemi, D. Kennedy page 34
- 13. Exact Strip Modelling and Vibration Based Identification of Damage in Plate Assemblies**  
David Kennedy, Carol A. Featherston, Basem Suliman, Yulin Luo page 37
- 14. A novel analytical method for highly efficient and accurate modal analysis of plates and plate assemblies with general boundary conditions**  
Xiang Liu, J. Ranjan Banerjee page 40
- 15. Wave propagation in resonant structural metamaterials: continuum and discrete models**  
Brian R Mace, Yi Yang, Michael J Kingan page 43
- 16. Stability of in-plane vibration of an elastically supported rotating thin ring, revisited**  
Tao Lu, Apostolos Tsouvalas, Andrei V. Metrikine page 46
- 17. Vibration Localization of Imperfect Circular Cylindrical Shells**  
Francesco Pellicano, Antonio Zippo, Marco Barbieri, Matteo Strozzi page 49
- 18. Numerical method to calculate 1D impact problems by approximating the geometry with piecewise constant cross sections and applying d'Alembert's solution**  
Jens Burgert, Wolfgang Seemann page 52
- 19. Free Vibration of Piezoelectric Composites using NURBS for Geometric and Response Field Functions**  
Anand V. Singh, Vijai Raj page 54
- 20. Eigenvalues and eigenvectors of a system of Bernoulli Euler beams connected together in a tree topology**  
Andrew Watson, W. Paul Howson page 57

## **Biosketches of participants page**

Haim Abramovich .....	page 60
Ranjan Banerjee .....	page 61
Erasmo Carrera .....	page 62
Weiqiu Chen .....	page 63
Li Cheng .....	page 64
Piotr Cupial .....	page 65
Sergio De Rosa .....	page 66
Hu Ding .....	page 67
Moshe Eisenberger .....	page 68
Mark Ewing .....	page 69
Matteo Filippi .....	page 70
Stanley G. Hutton .....	page 71
Sinniah Ilanko .....	page 72
David Kennedy .....	page 73
Xiang Liu .....	page 74
Brian R Mace .....	page 75
Andrei V. Metrikine .....	page 76
Wolfgang Seemann .....	page 77
Alfonso Pagani .....	page 78
Francesco Pellicano .....	page 79
Anand Singh .....	page 80
Andrew Watson .....	page 81

## The Vibration Correlation Technique Revisited

H. Abramovich<sup>\*</sup>, K. Kalnins<sup>#</sup>

<sup>\*</sup> Faculty of Aerospace Engineering  
Technion, I.I.T.,  
32000 Haifa, Israel  
haim@technion.ac.il

<sup>#</sup> Institute of Materials  
and Structures, Riga Technical  
University, Riga, Latvia  
kaspars.kalnins@sigmanet.lv

### Abstract

The vibration correlation technique, the VCT, consists of measuring the natural frequencies of a loaded structure, and monitoring their change, while increasing the applied load. Assuming that the vibrational modes are similar to the buckling ones, one can draw a curve, displaying the natural frequencies squared vs. the applied load, and extrapolating the curve to zero frequency would yield the predicted buckling load of the tested structure. Singer et. al [1], dedicated a whole chapter in his book, to review the VCT approach and its applications.

Besides its capability to nondestructively predict the buckling load of thin walled structures, the approach can also determine the actual in situ boundary condition of the structures, and therefore the VCT is usually classified in two main groups according to their approach: (1) determination of in situ boundary conditions, and (2) direct prediction of buckling loads.

The VCT method has been successfully applied to beam and columns axially loaded, (see for example References 2-6), yielding a straight line between the frequency squared and the compressive load. This relationship can be written as:

$$\left(\frac{f}{f_0}\right)^2 + \left(\frac{P}{P_{cr}}\right) = 1 \quad (1)$$

where  $f$  and  $P$  are the natural frequency (in Hz) and the applied compressive load, respectively,  $f_0$  is the natural frequency at zero load and  $P_{cr}$  is the buckling load of the column. It was shown analytically that Equation (1) is valid for a column on simply supported boundary conditions, while for other boundary conditions, the straight line would be a slightly curved one. Following this successful application, the VCT method was used to define both boundary conditions and to predict the buckling loads of plates and shell type structures. Since the early seventies (last decade) an extensive work has been performed at the Laboratory of Aeronautical Structures, Faculty of Aerospace Structures, the Technion, I.I.T., Haifa, Israel, to better define the in situ actual boundary conditions of stringer stiffened aluminum cylindrical shells, and thus better predicting the experimental buckling loads [6,7]. The direct prediction of the buckling loads of compressively loaded shells, using the VCT method yielded in most of the cases, loads higher than the experimental ones, and it was shown that in the vicinity of the buckling load, the curve of frequency squared vs. the compressive load, ceases to be linear and performs a sharp bend towards the actual buckling (zero frequency) due to initial geometric imperfections of the specimens [7]. Recently, new studies [8] have shown again that the use of VCT method for direct predictions of buckling loads in composite shells is not yet mature to be applied in industrial applications, like space launchers. To overcome the above described shortcomings of the method, when applied to structures, like shell type ones, presenting non-stable behavior in

the post buckling region, a new relationship between the natural frequency and the applied compressive load was proposed by Souza et. al [9,10], yielding the following:

$$(1 - p)^2 + (1 - \xi^2)(1 - f^4) = 1 \tag{2}$$

where  $p=P/P_{cr}$ ,  $f=f/f_0$ ,  $P$  and  $f$  being the measured applied axial load and the natural frequency, respectively,  $f_0$  is the natural frequency at zero load and  $P_{cr}$  is the extrapolated buckling load based on the curve  $f^2$  vs.  $p$ .  $\xi^2$  is the “experimentally” knock-down factor based on the results of the test at relatively low loads (up to 60% from the predicted buckling load). The process is depicted in Figure 1.

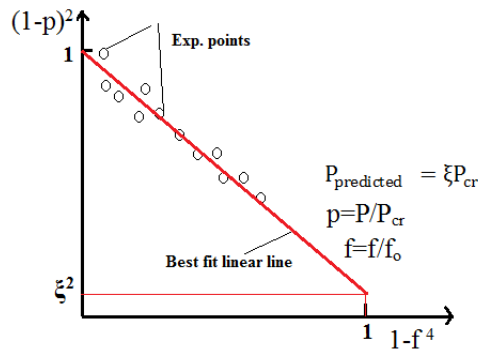


Figure 1 The calculation of the predicted buckling load ( $P_{predicted}$ ) for a shell

A similar approach is presented in [8] where graphs presenting the  $(1-p)^2$  vs  $(1-f^2)$ , where obtained by measuring the natural frequency and nondimensionalising it by division of the natural frequency at zero axial load, yielding the variable  $f$ . The nondimensional variable  $p$ , is defined as the ratio between the axial load divided by the numerical buckling load. A second degree polynomial curve is then fitted to the experimental data. Then the polynomial equation is once derived to yield the value of the  $\xi^2$ . The predicted value of the VCT approach would then be  $P_{cr} (VCT) = \xi P_{cr}$  (numerical buckling load) (see Figure 2).

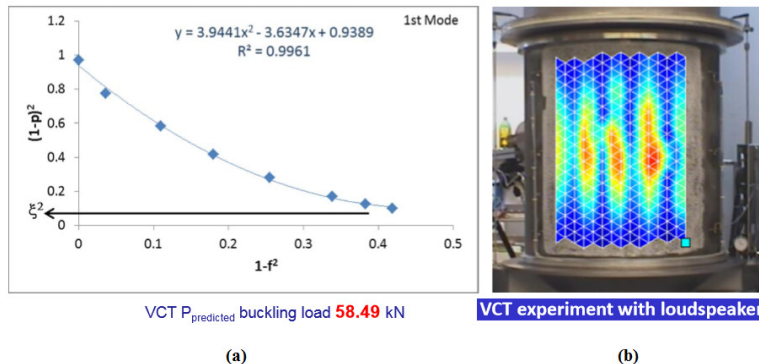


Figure 2 Experimental results using VCT - DLR Shell Z36 : (a) prediction of the buckling load. (b) the shell mode shape at 450 aperture, as projected by the RTU laser Doppler vibrometer.

The VCT is revisited, reviewing the main achievements of the method, and presenting recent applications to laminated curved stringer stiffened cylindrical panels (see Figure 3-  $D_{com1}$  a hybrid panel with laminated composite skin and two aluminum longerons) using a new excitation method, as well as experimental results performed on laminated composite cylindrical

shell, excited by a shaker and loudspeaker, while the response is monitored using a laser based system. The review is concluded by providing adequate guidelines for successful application of the VCT approach.

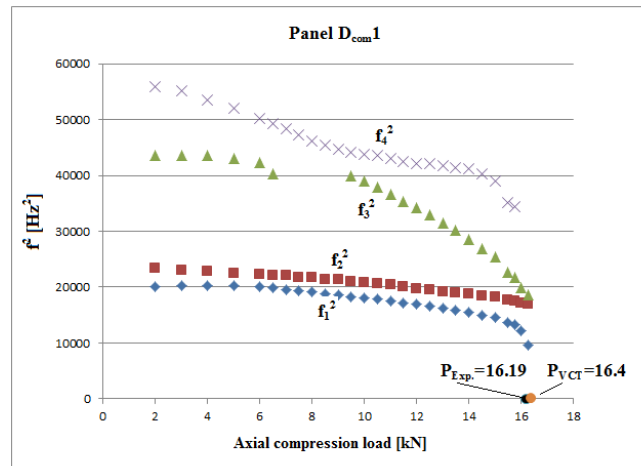


Figure 3 Determination of first buckling load using VCT : 16.4 kN (compared with 16.19kN experimental value)– Panel D<sub>com1</sub>

## References

- [1] Singer, J.; Arbocz, J.; Weller, T.: Buckling Experiments: Experimental methods in Buckling of Thin-Walled Structures, Vol. 2: Shells, Built-up Structures and Additional Topics, Ch. 15.2 Vibration Correlation Techniques (VCT), John Wiley & Sons, Inc., Aug. 2002.
- [2] Lurie, H.: Lateral vibrations as related to structural stability, Ph.D. thesis, California Institute of Technology, Pasadena, California, 1950.
- [3] Plaut, R. H.; Virgin, L.N.: Use of frequency data to predict buckling, Journal of Engineering Mechanics, 116 (10), 1990, 2330-2339
- [4] Virgin, L.N.; Plaut, R.H.: Effect of axial load on for CED vibrations of beams, Journal of Sound and Vibration, 168 (3), (1993, 395-405.
- [5] Virgin, L.N.; Plaut, R.H.; Via, C. E.: Axial load effects on the frequency response of a clamped beam, Proc. of 21<sup>st</sup> IMAC Conference and Exposition 2003 (IMAC XXI): A Conference and Exposition on Structural Dynamics, 3-6 February 2003, Kissimmee, Florida, ISBN 9781604238037 (5p).
- [6] Singer, J.; Abramovich, H.: Vibration correlation techniques for definition of practical boundary conditions in stiffened shells. AIAA J., 17(7): 762- 769, 1979.
- [7] Rosen, A.; Singer, J.: Effect of axisymmetric imperfections on the vibrations of cylindrical shells under axial compression. AIAA Journal 1974; 12:995–7.
- [8] Arbelo, M.A.; de Almeida, S.F.M.; Donadon, M.V.; Rett, S.R.; Degenhardt, R.; Castro, S.G.P.; Kalnins, K.; Ozolins, O.: Vibration correlation technique for the estimation of real boundary conditions and buckling load of unstiffened plates and cylindrical shells, Thin Walled Structures, 79, 119-128, 2014.
- [9] Souza, M.A.; Fok, W.C.; Walker, A.C.: Review of experimental techniques for thin-walled structures liable to buckling, Part I-Neutral and unstable buckling, Experimental Techniques, 7(9): 21-25, 1983.
- [10] Souza, M.A.; Fok, W.C.; Walker, A.C.: Review of experimental techniques for thin-walled structures liable to buckling, Part II-Stable Buckling, 7(10), 36-39, 1983.

## Veering and modes aberration of structures subjected to in-plane loadings according to linearized and full nonlinear formulations

Erasmus Carrera, Alfonso Pagani

Mul2, Department of Mechanical and Aerospace Engineering  
Politecnico di Torino  
Corso Duca Degli Abruzzi 24, 10129 Torino, Italy  
erasmo.carrera@polito.it, alfonso.pagani@polito.it

### Abstract

This research work was originated and inspired by a presentation made by Professor Arthur W. Leissa at ISVCS 9, Courmayeur, Italy, on July 2013 [1]. According to his talk, authors realized that the interesting phenomena related to mode aberration have rarely been investigated in the recent years.

During service and due to the nature of applied loadings, structural components, such as stiffeners, panels, ribs and boxes in aerospace constructions, for example, are subjected to stress fields. Those stresses, and especially compression ones, may significantly modify the equilibrium state of the structures and, thus, affect their dynamic response, eventually in a catastrophic manner. For this reason, the evaluation and the analysis of the natural frequencies and mode shapes changing as the elastic system is subjected to operational loads is of primary interest.

By employing a refined beam model with higher-order capabilities, this work, thus, investigates the eigenvalue loci veering, crossing, coalescence and eventual buckling events due to mode degeneration of metallic and composite structures undergoing pre-stress states and, eventually, large displacements and rotations. The proposed models are based on the Carrera Unified Formulation (CUF), according to which each theory of structures (either 1D or 2D) can be expressed as a degenerated form of the three-dimensional equilibrium equations in a hierarchical manner [2]. As an example, 1D beam theories can be formulated from the three-dimensional displacement field ( $\mathbf{u}$ ) as an arbitrary expansion of the generalized unknowns ( $\mathbf{u}_\tau$ ); i.e.,

$$\mathbf{u}(x, y, z) = F_\tau(x, z)\mathbf{u}_\tau(y), \quad \tau = 1, 2, \dots, M \quad (1)$$

where  $F_\tau$  are generic functions on the beam cross-section domain,  $M$  is the number of expansion terms, and  $\tau$  denotes summation. Depending on the choice of  $F_\tau$  and the number of expansion terms  $M$ , different classes of beam models can be formulated and, thus, implemented in a straightforward manner. Namely, in this work, low- to higher-order beam models with only pure displacement variables are implemented by utilizing Lagrange polynomials expansions of the unknowns on the cross-section.

Give a structure subjected to a pre-stress state  $\sigma_0$ , it can be easily demonstrated that the linearization of the virtual variation of the work of internal strains can be approximated as follows:

$$\delta(\delta L_{\text{int}}) \approx \langle \delta \boldsymbol{\varepsilon}^T \boldsymbol{\sigma} \rangle + \langle \delta(\delta \boldsymbol{\varepsilon}^T) \boldsymbol{\sigma}_0 \rangle \quad (2)$$

or, in other words,

$$\mathbf{K}_T^{ij\tau s} \approx \mathbf{K}^{ij\tau s} + \mathbf{K}_{\sigma_0}^{ij\tau s} \quad (3)$$

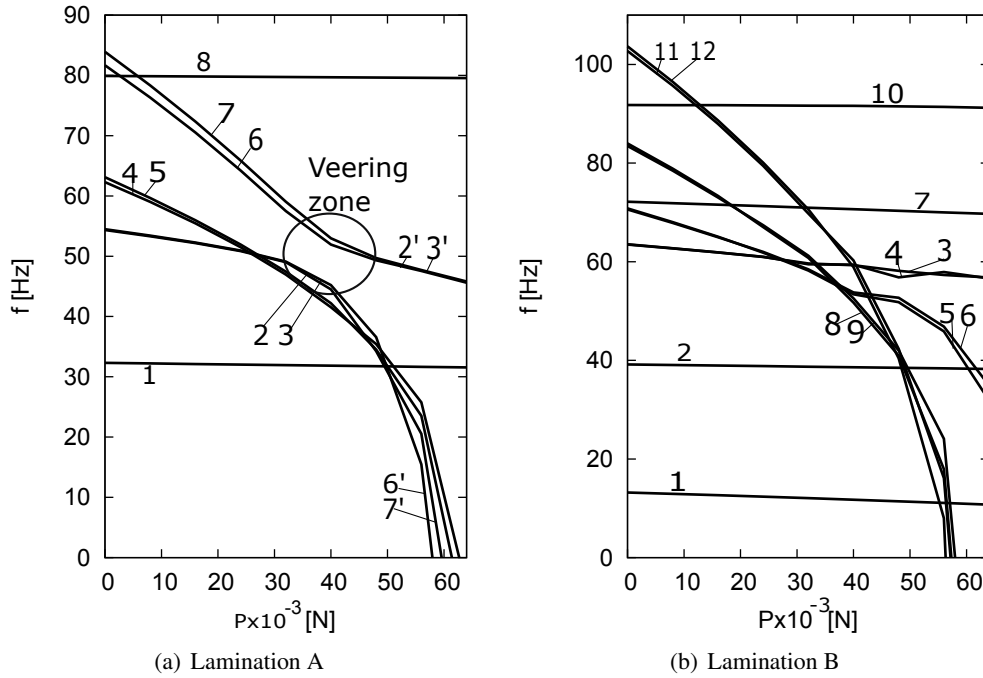


Figure 1: Mode aberration of a composite box beam subjected to compression.

In Eq. (2),  $\varepsilon$  and  $\sigma$  are the vectors of strain and stress components, whereas  $\langle \cdot \rangle = \int_V (\cdot) dV$ . In contrast, Eq. (3) shows that the *fundamental nucleus* (FN) of the tangent stiffness matrix,  $\mathbf{K}_T^{ij\tau s}$ , can be approximated as the sum of the FNs of the linear stiffness,  $\mathbf{K}^{ij\tau s}$ , and the geometric stiffness,  $\mathbf{K}_{\sigma_0}^{ij\tau s}$ . According to CUF and in the framework of the finite element method, as in the case of this work, finite element arrays of generally refined structural models can be formulated in a straightforward manner by expanding the FNs versus the indexes  $(\tau, s = 1, \dots, M)$  and  $(i, j = 1, \dots, N)$ , where  $N$  is the number of nodes of the finite element employed. For the sake of brevity, the derivation and the complete expressions of the FNs in Eq. (3) are not given here, but they can be found in [2] and [3]. Once the global tangent stiffness matrix  $\mathbf{K}_T$  is known, the natural frequencies and mode shapes of the structure can be evaluated by solving the usual eigenvalue problem  $(\mathbf{K}_T - \omega^2 \mathbf{M}) \mathbf{u} = 0$ , where  $\mathbf{M}$  is the mass matrix. However, it is important to underline that Eqs. (2) and (3) are based on the fundamental hypotheses that the equilibrium state is linear and the structure undergoes infinitesimal strains and displacements/rotations [4].

For representative purposes, a numerical example is shown here. We consider a cantilever single-cell, two-bay composite box beam subjected to compression load  $P$ . The box is made of two layers of carbon/epoxy material on each flange. In lamination A, the fibre orientation is 0 deg in the top and bottom flanges and  $\pm 15$  deg in the right and left flanges. On the other hand, in lamination B, an angle-ply lamination  $\pm 45$  deg is employed for all the flanges. Figure 1 shows the variation of the natural frequencies for the first important modes and for different values of the load  $P$ . Also, for the sake of completeness, Fig. 2 depicts some mode shapes of the box in the case of  $P = 0$ . The analysis clarifies that, independently of the lamination angles, buckling occurs approximately for the same compression loading. Nevertheless, Fig. 1 shows that, in the case of lamination A, veering phenomena appear as a consequence of severe mode aberrations. Moreover, Fig. 2 demonstrates the importance of employing adequate structural models when dealing with this kind of analysis, especially if composite and thin-walled structures are considered. From this point of view, due to its higher-order and enhanced capabilities, CUF is a good candidate for mode aberration investigations.

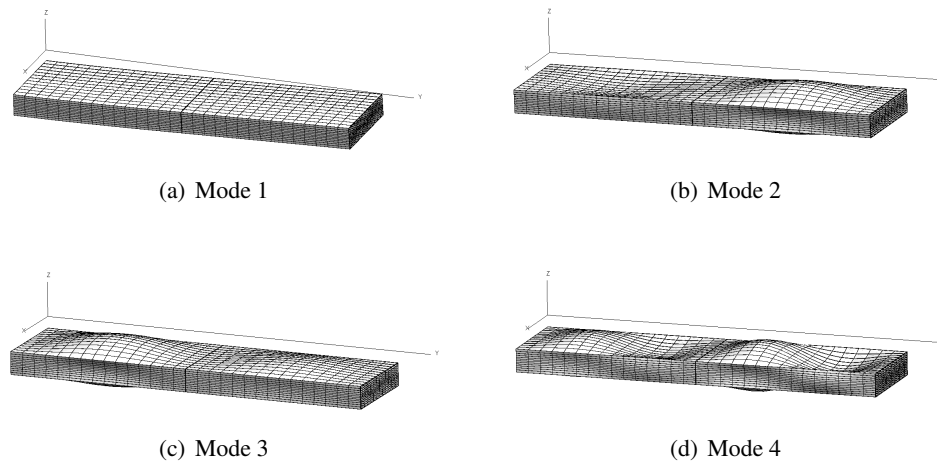


Figure 2: Representative mode shapes of the composite box structure. Lamination A.

As a final comment, it must be underlined that the hypotheses according to which the approximation in Eq. (2) holds may be too much limiting in the case of problems that involve moderate or large displacements, e.g. for analyses and investigations that go beyond the first buckling load. In this case, and by assuming that the nonlinear equilibrium state is reached with infinitesimal and consecutive load steps (i.e., dynamic effects are not accounted for), the tangent stiffness to be employed for the linear, free-vibration eigenvalue problem comes from the following expression of the internal strain energy:

$$\delta(\delta L_{\text{int}}) = \langle \delta \varepsilon^T \delta \sigma \rangle + \langle \delta(\delta \varepsilon^T) \sigma_0 \rangle \quad (4)$$

or rather

$$\mathbf{K}_T^{ij\tau s} = \mathbf{K}^{ij\tau s} + \mathbf{K}_{T_1}^{ij\tau s} + \mathbf{K}_{\sigma_0}^{ij\tau s} \quad (5)$$

where  $\mathbf{K}_{T_1}^{ij\tau s}$  represents the contribution due to the *secant* stiffness and  $\mathbf{K}_{\sigma_0}^{ij\tau s}$  takes into account both the linear and geometrical nonlinear stress components. Accordingly, the differences between linearized and full nonlinear vibration problems will be discussed during the *11th International Symposium on Vibrations of Continuous Systems*.

## References

- [1] Leissa, A.W.: Looking Back at Curve Veering. ISVCS9 - Proceedings of 9th International Symposium on Vibrations of Continuous Systems, pp. 46–48, 2013.
- [2] Carrera, E.; Cinefra, M.; Petrolo, M.; Zappino, E.: Finite Element Analysis of Structures through Unified Formulation. John Wiley & Sons, 2014.
- [3] Pagani, A.; Carrera, E.: Unified formulation of geometrically nonlinear refined beam theories. Mechanics of Advanced Materials and Structures, 2017. DOI: 10.1080/15376494.2016.1232458.
- [4] Carrera, E.; Pagani, A.: Veering, crossing and coalescence phenomena in compressed composite box structures. In preparation.

**3D vibrations of multilayered hollow spheres in complex fluids****Weiqiu Chen<sup>\*</sup>, Bin Wu<sup>#</sup>**

<sup>\*</sup> State Key Laboratory of Fluid  
Power and Mechatronic Systems  
Zhejiang Unveristy  
38# Zheda Road, 310027 Hangzhou,  
China  
chenwq@zju.edu.cn

<sup>#</sup> Department of Engineering  
Mechanics  
Zhejiang Unveristy  
38# Zheda Road, 310027 Hangzhou,  
China  
wubinlongchang@163.com

**Abstract**

Acoustic vibrations of elastic bodies in fluid media are related to design of underwater acoustic wave devices, characterization of mechanical properties of materials, understanding of mechanical and biological sensing mechanism, developing methods to destroy virus, etc. A few experimental and analytical studies have been carried out, but mostly for various structures in Newtonian fluids [1-3]. Recently, the researches carried out by the group led by Sader showed that the viscoelastic properties of the surrounding fluid play a significant role in the dynamics of the submerged nanostructures [4-6], and non-Newtonian fluid models should be employed to predict the experimentally observed phenomena that would not appear in a Newtonian fluid.

Sader et al. only presented exact solutions for the simple breathing modes of elastic isotropic nanowires or nanospheres [5,6]. Also, at the nanoscale, the surface effect may become very important [7]. Therefore, in this study, we will present a three-dimensional exact free vibration analysis of a multilayered spherically isotropic hollow sphere submerged in a Maxwell fluid. The layered structure could be easily adapted to a sphere with a surface effect [8].

To deal with the solid phase (i.e. the multilayered hollow sphere), we employ the state-space approach developed by Chen and Ding [9]. In fact, two independent state equations with varying coefficients and partial operators could be derived as

$$\nabla_2 \begin{Bmatrix} \Sigma_1 \\ \psi \end{Bmatrix} = \begin{bmatrix} -2 & -c_{66}(\nabla_1^2 + 2) + r^2 \rho \partial^2 / \partial t^2 \\ \frac{1}{c_{44}} & 1 \end{bmatrix} \begin{Bmatrix} \Sigma_1 \\ \psi \end{Bmatrix} \quad (1)$$

$$\nabla_2 \begin{Bmatrix} \Sigma_{rr} \\ \Sigma_2 \\ G \\ w \end{Bmatrix} = \begin{bmatrix} 2\beta - 1 & \nabla_1^2 & k_1 \nabla_1^2 & -2k_1 + r^2 \rho \partial^2 / \partial t^2 \\ \beta & -2 & k_2 \nabla_1^2 - 2c_{66} + r^2 \rho \partial^2 / \partial t^2 & -k_1 \\ 0 & \frac{1}{c_{44}} & 1 & 1 \\ \frac{1}{c_{33}} & 0 & \beta \nabla_1^2 & -2\beta \end{bmatrix} \begin{Bmatrix} \Sigma_{rr} \\ \Sigma_2 \\ G \\ w \end{Bmatrix} \quad (2)$$

where  $\psi$  and  $G$  are two displacement functions, and  $\Sigma_1$  and  $\Sigma_2$  are two stress functions. They are related to the displacement components ( $u_i$ ) and the modified stress components ( $\Sigma_{ij}$ ) by

$$u_\theta = -\frac{1}{\sin \theta} \frac{\partial \psi}{\partial \varphi} - \frac{\partial G}{\partial \theta}, \quad u_\varphi = \frac{\partial \psi}{\partial \theta} - \frac{1}{\sin \theta} \frac{\partial G}{\partial \varphi} \quad (3)$$

$$\Sigma_{r\theta} = -\frac{1}{\sin \theta} \frac{\partial \Sigma_1}{\partial \varphi} - \frac{\partial \Sigma_2}{\partial \theta}, \quad \Sigma_{r\varphi} = \frac{\partial \Sigma_1}{\partial \theta} - \frac{1}{\sin \theta} \frac{\partial \Sigma_2}{\partial \varphi} \quad (4)$$

Also, we have denoted  $u_r = w$ , and the modified stresses are defined as  $\Sigma_{ij} = r\sigma_{ij}$ , with  $\sigma_{ij}$  being the usual stresses.  $c_{ij}$  and  $\rho$  in Eqs. (1) and (2) are the elastic moduli and mass density, respectively;  $\beta$  and  $k_i$  are all material constants expressed in terms of  $c_{ij}$ ;  $\nabla_1^2$  is the two-dimensional Laplacian defined on a spherical surface.

Equations (1) and (2) could be solved analytically by making use of the following series expansions:

$$\left. \begin{aligned} \Sigma_1 &= ac_{44}^{(1)} \sum_{m=0}^n \sum_{n=0}^{\infty} \Sigma_{1n}(\xi) S_n^m(\theta, \varphi) e^{i\omega t}, & \psi &= a \sum_{m=0}^n \sum_{n=0}^{\infty} \psi_n(\xi) S_n^m(\theta, \varphi) e^{i\omega t} \\ \Sigma_{rr} &= ac_{44}^{(1)} \sum_{m=0}^n \sum_{n=0}^{\infty} \Sigma_{rn}(\xi) S_n^m(\theta, \varphi) e^{i\omega t}, & \Sigma_2 &= ac_{44}^{(1)} \sum_{m=0}^n \sum_{n=0}^{\infty} \Sigma_{2n}(\xi) S_n^m(\theta, \varphi) e^{i\omega t} \\ G &= a \sum_{m=0}^n \sum_{n=0}^{\infty} G_n(\xi) S_n^m(\theta, \varphi) e^{i\omega t}, & w &= a \sum_{m=0}^n \sum_{n=0}^{\infty} w_n(\xi) S_n^m(\theta, \varphi) e^{i\omega t} \end{aligned} \right\} \quad (5)$$

where  $S_n^m(\theta, \varphi)$  are the surface spherical harmonic functions,  $\omega$  is the circular frequency,  $a$  is the inner radius of the multilayered hollow sphere, and  $c_{44}^{(1)}$  is the elastic constant for the innermost layer (the first layer). Substitution of Eq. (5) into Eqs. (1) and (2) leads to two state equations in ordinary differential form, which can be easily solved. In fact, in view of the solutions thus obtained, we can establish the relationships between the state variables at the inner surface and those at the outer surface of each layer. By virtue of the continuity conditions between two adjacent layers, two sets of linear algebraic equations about the state variables at the innermost and outermost surfaces of a multi-layered hollow sphere are obtained:

$$\mathbf{V}_k(\eta) = \mathbf{T}_{kn} \mathbf{V}_k(1) \quad (k=1, 2; n=1, 2, 3, \dots) \quad (6)$$

$$\begin{Bmatrix} \Sigma_{r0}(\eta) \\ w_0(\eta) \end{Bmatrix} = \mathbf{T}_{20} \begin{Bmatrix} \Sigma_{r0}(1) \\ w_0(1) \end{Bmatrix} \quad (n=0) \quad (7)$$

where  $\eta = b/a$  is the radius ratio, with  $b$  being the outer radius,  $\mathbf{V}_1 = [\Sigma_{1n}, \psi_n]^T$  and  $\mathbf{V}_2 = [\Sigma_{rn}, \Sigma_{2n}, G_n, w_n]^T$  are two state vectors, and  $\mathbf{T}_{kn}$  are the corresponding transfer matrices.

The effect of the surrounding Maxwell fluid could be written as certain generalized spring-like (in the frequency domain) boundary conditions applied to the outer spherical surface:

$$\Sigma_{1n}(\eta) = f_{1n} \psi_n(\eta) \quad (8)$$

$$\Sigma_{rn}(\eta) = f_{2n} G_n(\eta) + f_{3n} w_n(\eta), \quad \Sigma_{2n}(\eta) = f_{4n} G_n(\eta) + f_{5n} w_n(\eta) \quad (9)$$

where  $f_{in}$  and  $g_n$  are coefficients depending on the fluid parameters as well as the frequency.

In view of Eqs. (8) and (9) as well as the tractions-free conditions on the inner surface, we finally derive the following frequency equations for the free vibrations of the submerged multilayered hollow sphere:

$$f_{1n}T_{1n22} - T_{1n12} = 0 \quad (n=1,2,3,\dots) \quad (10)$$

$$\begin{vmatrix} f_{2n}T_{2n33} + f_{3n}T_{2n43} - T_{2n13} & f_{2n}T_{2n34} + f_{3n}T_{2n44} - T_{2n14} \\ f_{4n}T_{2n33} + f_{5n}T_{2n43} - T_{2n23} & f_{4n}T_{2n34} + f_{5n}T_{2n44} - T_{2n24} \end{vmatrix} = 0 \quad (n=1,2,3,\dots) \quad (11)$$

$$f_{3n}T_{0n22} - T_{0n12} = 0 \quad (n=0) \quad (12)$$

Equation (12) is for the breathing mode, which is shown to be identical to that obtained by Sader in the case of a homogeneous isotropic sphere. Since the free vibrations are damping, the roots ( $\omega$ ) of these frequency equations are complex, and will be searched numerically.

## References

- [1] Ding, H.J.; Chen, W.Q.: Natural Frequencies of an Elastic Spherically Isotropic Hollow Sphere Submerged in a Compressible Fluid Medium. *Journal of Sound and Vibration*, Vol. 192, No. 1, pp. 173-198, 1996.
- [2] Ding, H.J.; Chen, W.Q.: Exact Shell Theory Analysis of Free Vibrations of Submerged Thin Spherical Shells. *International Journal of Solids and Structures*, Vol. 35, No. 33, pp. 4381-4389, 1998.
- [3] Chen, W.Q.; and Bian, Z.G.: Wave Propagation in Submerged Functionally Graded Piezoelectric Cylindrical Transducers with Axial Polarization. *Mechanics of Advanced Materials and Structures*, Vol. 18, No. 1, pp. 85-93, 2011.
- [4] Chakraborty, D., Leeuwen, E. van; Pelton, M.; Sader, J.E.: Vibration of Nanoparticles in Viscous Fluids. *Journal of Physical Chemistry C*, Vol. 117, No. pp. 8536-8544, 2013.
- [5] Yu, K.; Major, T.A.; Chakraborty, D.; Devadas, M.S.; Sader, J.E.; Hartland, G.V.: Compressible Viscoelastic Liquid Effects Generated by the Breathing Modes of Isolated Metal Nanowires. *Nano Letters*, Vol. 15, No., pp. 3964-3970, 2015.
- [6] Chakraborty, D.; Sader, J.E.: Constitutive Models for Linear Compressible Viscoelastic Flows of Simple Liquids at Nanometer Length Scales. *Physics of Fluids*, Vol. 27, No., pp. 052002, 2015.
- [7] Cammarata, R.C.: Surface and Interface Stress Effects on Interfacial and Nanostructured Materials. *Materials Science and Engineering A*, Vol. 237, No. , pp. 180-184, 1997.
- [8] Chen, W.Q.; Wu, B.; Zhang, C.L.; Zhang, Ch.: On Wave Propagation in Anisotropic Elastic Cylinders at Nanoscale: Surface Elasticity and its Effect. *Acta Mechanica*, 225(10): 2743-2760, 2014.
- [9] Chen, W.Q.; Ding, H.J.: Free Vibration of Multi-layered Spherically Isotropic Hollow Spheres. *International Journal of Mechanical Sciences*, Vol. 43, No. 3, pp. 667-680, 2001.

**A Wavelet-decomposed Semi-analytical Model for Acoustic Black Hole Effect Analyses****Liling Tang, Li Cheng\***Department of Mechanical Engineering, The Hong Kong Polytechnic  
University, Hong Hom, Kowloon, Hong Kong

\*Corresponding author, e-mail: li.cheng@polyu.edu.hk,

**Abstract**

The Acoustics Black Holes (ABH) effect results from the manipulation of bending wave propagation inside a thin-walled structure through thickness changes. With a tailored power-law thickness variation ( $h(x)=\varepsilon x^m$ , where  $\varepsilon$  is an constant and  $m$  the power index), the phase velocity of the bending wave gradually reduces to zero in the ideal scenario, resulting in zero wave reflection and high energy concentration at the wedge tip [1]. The ABH effect attracts increasing attention as a promising passive vibration control method because vibration energy can be channeled and only a very small amount of damping material is required within the energy focalization region to achieve efficient damping to flexural waves [2]. In addition, it also shows potential in sound radiation control and energy harvesting due to the high energy concentration within a confined area [3, 4]. In these applications, however, the addition of vibration control or energy harvesting elements may affect the formation of the ideal ABH through their coupling with the host structure on one hand; topological or system optimizations may be needed to achieve the maximum performance on the other hand. To this end, a flexible model, which allows the consideration of the full coupling between the host ABH structure and various control or energy-harvesting elements to be embedded, is of paramount importance.

We propose a semi-analytical model to analyze an Euler-Bernoulli beam with an embedded ABH feature and its full coupling with the damping layers coated over its surface [5]. By decomposing the transverse displacement field of the beam over the basis of a set of Mexican Hat wavelets, the extremalization of the Hamiltonian via Lagrange's equations yields a set of linear equations, which can be solved for structural responses. Highly consistent with the FEM and experimental results (as shown in Figs. 1 and 3), numerical simulations demonstrate that the proposed wavelet-based model is particularly suitable to characterize the ABH-induced drastic wavelength fluctuation phenomenon. The ABH feature as well as the effect of the wedge truncation and that of the damping layers on the vibration response of the beam is analyzed. It is shown that the conventionally neglected mass of the damping layers needs particular attention when their thickness is comparable to that of the ABH wedge around the tip area. Due to its modular and energy-based feature, the proposed framework offers a general platform allowing embodiment of other control or energy harvesting elements into the model to guide ABH structural design for various applications.

Meanwhile, manufacturing an ideally tailored power-law profile of a structure with an embedded ABH feature can hardly be achieved in practice. Past research showed that the inevitable truncation at the wedge tip of the structure can significantly weaken the expected ABH effect by creating wave reflections. On the premise of the minimum achievable truncation thickness by the current manufacturing technology, exploring ways to ensure and achieve a better ABH effect becomes important. Therefore, we investigate this issue by using this

developed model on an Euler-Bernoulli beam with a modified power-law profile and an extended platform of constant thickness [6]. The so-called extended platform is an add-on portion of the beam at the truncated ABH tip. Its thickness is the same as the truncated ABH tip thickness. Through comparisons with the conventional ABH profile in terms of system loss factor and energy distribution, numerical results show that the modified thickness profile brings about a systematic increase in the ABH effect at mid-to-high frequencies, especially when the truncation thickness is small and the power index  $m$  is large. The use of an extended platform further increases the ABH effect to broaden the frequency band whilst providing room for catering to particular low frequency applications (shown in Fig. 2).

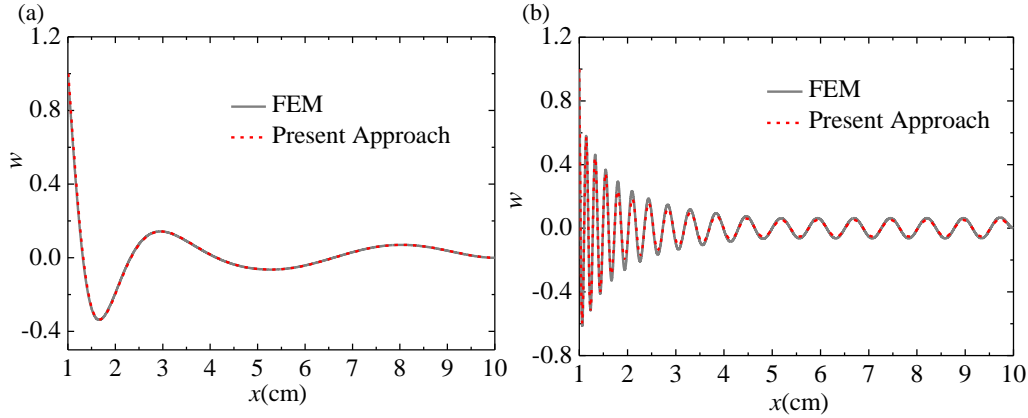


Fig. 1 Mode shape comparison between FEM and present approach when  $x_0=1$  cm for (a) first mode, and (b) thirty-fifth mode.

It is worth pointing out that although the ABH effect exists as a broadband phenomenon based on wave propagation theory in structures of semi-infinite size, we demonstrate the disappearance of the ABH effect in a finite beam in specific frequency ranges above the cut-on frequency, both experimentally and theoretically (shown in Fig. 3) [7]. Analyses show that the phenomenon takes place at frequencies which are close to the low order local resonant frequencies of the beam portion, demarcated by the excitation point. These frequencies can be predicted so that the phenomenon can be avoided for the targeted frequency ranges in ABH applications.

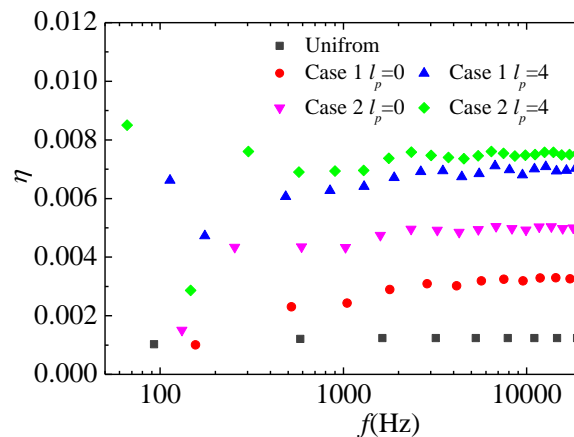


Fig. 2 System loss factors ( $\eta$ ) for three different beam cases with and without extended platform for damping layers of the same length applied. Case 1 has a conventional ABH profile; Case 2 uses a modified thickness profile detailed in [6].  $L_p$  is the length of the extended platform.

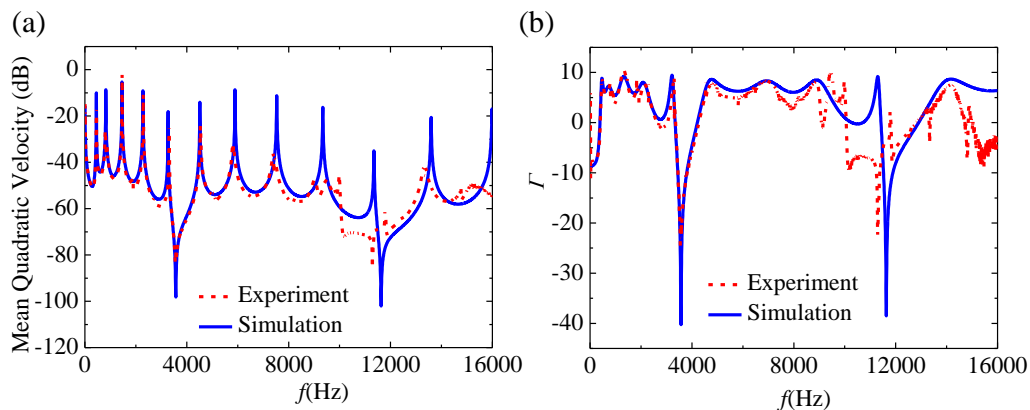


Fig. 3. (a) The mean quadratic velocity of the ABH part and (b) the ratio of mean quadratic velocity of the ABH part to that of the uniform beam part from experimental and numerical simulations.

Finally the established model is extended to deal with a 1D lattice comprising periodic ABH cells. Results show remarkable locally resonant band gaps [8]

### Acknowledgements

This work was supported by Research Grants Council of Hong Kong Special Administrative Region, China (PolyU 152026/14E and PolyU 152009/15E), National Science Foundation of China (No. 11532006) and the NUA State Key Laboratory Program under Grant MCMS-0514K02 for financial support.

### References

- [1] Mironov M.A., Propagation of a flexural wave in a plate whose thickness decreases smoothly to zero in a finite interval, *Soviet Physics: Acoustics*, Vol. 34, No.3, pp.318-319, 1988.
- [2] Krylov V.V., Tilman F. J. B. S., Acoustic ‘black holes’ for flexural waves as effective vibration dampers, *Journal of Sound and Vibration*, Vol. 274, pp. 605-619, 2004.
- [3] Conlon S.C., Fahnline J.B., Numerical analysis of the vibroacoustic properties of plates with embedded grids of acoustic black holes, *Journal of the Acoustical Society of America*, Vol. 137, No. 1, pp. 447-457, 2015.
- [4] Zhao L.X., Conlon S.C., Semperlotti F., Broadband energy harvesting using acoustic black hole structural tailoring, *Smart Materials and Structures* Vol. 23, pp. 065021, 2014.
- [5] Tang L.L., Cheng L., Ji H.L., Qiu J.H., Characterization of Acoustic Black Hole effect using a one-dimensional fully-coupled and wavelet-decomposed semi-analytical model, *Journal of Sound and Vibration*, Vol. 374, pp.172-184, 2016.
- [6] Tang L.L., Cheng L., Enhanced Acoustic Black Hole effect in beams with a modified thickness profile and extended platform, *Journal of Sound and Vibration*, Vol. 391, pp. 116-126, 2017.
- [7] Tang L.L., Cheng L., Loss of acoustic black hole effect in a structure of finite size, *Applied Physics Letters*, Vol. 109, pp. 014102, 2016.
- [8] Tang L.L., Cheng L., Broadband locally resonant band gaps in periodic beam structures with embedded acoustic black holes, *Journal of Applied Physics*, in press, 2017.

## On the application of the spectral theory of linear operators to the natural vibration analysis of continuous systems

Piotr Cupiał\*

\*Faculty of Mechanical Engineering and Robotics, AGH University of Science and Technology,  
Al. Mickiewicza 30, 30-059 Kraków, Poland. Email: [pcupial@agh.edu.pl](mailto:pcupial@agh.edu.pl)

### 1. Introduction

The standard approach to obtaining the natural frequencies and the corresponding eigenmodes of lumped-parameter systems is to solve the algebraic eigenvalue problem. In the natural vibration analysis of continua, nontrivial solutions of differential equations are sought, subject to appropriate boundary conditions. By this approach the solutions of any particular problem can be obtained in the most straightforward way.

A different method allowing the study of eigenvalue problems has been developed within the framework of the spectral theory of linear operators [1,2]. This theory deals with eigenvalue problems for linear operators, including the important case of operators with non-constant coefficients. The approach relies on the analysis of the resolvent, through the use of the theory of functions of complex variable. The spectral theory of linear operators can provide results that, for distributed-parameter systems, may be difficult to obtain by other methods. One of the advantages of this theory is that it offers a unified approach to the study of the character of the spectrum of linear operators. It provides an efficient means of analyzing whether the spectrum of a linear operator is discrete or continuous, with methods of finding in either case the spectral representation of the operator. For a discrete spectrum, which is encountered in the vibration analysis of continuous systems (as opposed to wave propagation problems), the theory can be used to justify the fact that the solutions of vibration problems can be expanded into series of natural vibration modes.

An important application of the spectral theory of linear operators is in perturbation analysis [3,4]. Unlike the approaches usually found in quantum mechanics books, the spectral method provides mathematically rigorous perturbation results for distributed parameter systems. Being of the analytical character, it also furnishes tools for investigating the convergence of the perturbation series. Moreover, the scope of application of spectral theory is broader than that covered in most physics books, since it is not limited to the case of self-adjoint operators.

The aim of the present study is to apply the abstract mathematical concepts described in Refs. [1–4] to a simple example of a distributed-parameter vibrating system, with a view to making the theory better understandable.

### 2. Spectral analysis of a rod with a spring at one end

The main elements of the natural vibration analysis using spectral theory will be illustrated by the longitudinal vibrations of a prismatic rod, fixed at the left end, with a spring acting on its other end. For this system, the eigenvalue problem, when written in non-dimensional form, is formulated as follows :

$$-\frac{d^2u}{dx^2} = \lambda u, \quad u(0) = 0, \quad u_x(1) + \kappa u(1) = 0 \quad (1)$$

where:

$$\lambda = \frac{\rho l^2}{E} \omega^2, \quad \kappa = \frac{kl}{EA} \quad (2)$$

Here:  $l$  is the length of the rod;  $\rho, E, A$  are, respectively, the mass density, Young's modulus and the rod cross-section area;  $k$  stands for the stiffness of the spring that acts on the right end of the rod;  $\omega$  is the circular frequency,  $u$  – the non-dimensional displacement along the rod axis, and  $0 \leq x \leq 1$ . Subscript  $x$  in the boundary condition denotes differentiation with respect to  $x$ .

The resolvent (as defined in Ref. [3]) of the problem in hand is an integral operator, with the kernel (Green's function) given by the solution of the following differential equation:

$$-\frac{d^2 G}{dx^2} - \lambda G = \delta(x - \xi) \quad (3)$$

with the boundary conditions:

$$G(0, \xi; \lambda, \kappa) = 0, \quad G_x(1, \xi; \lambda, \kappa) + \kappa G(1, \xi; \lambda, \kappa) = 0 \quad (4)$$

Dirac's  $\delta$ -function appears on the right-hand side of Eq. (3). The Green's function, defined in the rectangular region  $0 \leq x \leq 1, 0 \leq \xi \leq 1$ , is given for  $x \leq \xi$  by the formula:

$$G(x, \xi; \lambda, \kappa) = \frac{\sin \lambda^{1/2} x [\cos \lambda^{1/2} (1 - \xi) + \kappa \lambda^{-1/2} \sin \lambda^{1/2} (1 - \xi)]}{\lambda^{1/2} \cos \lambda^{1/2} + \kappa \sin \lambda^{1/2}} \quad (5)$$

For  $x \geq \xi$  one needs to interchange  $x$  and  $\xi$  in Eq. (5). The Green's function is continuous when  $x = \xi$ , whereas its first derivative suffers a jump there.

Let us take the case with  $\kappa = 0$ , first. In this case, Green's function (5) reduces to:

$$G(x, \xi; \lambda) = \begin{cases} \frac{\sin \lambda^{1/2} x \cos \lambda^{1/2} (1 - \xi)}{\lambda^{1/2} \cos \lambda^{1/2}} & \text{for } x \leq \xi \\ \frac{\sin \lambda^{1/2} \xi \cos \lambda^{1/2} (1 - x)}{\lambda^{1/2} \cos \lambda^{1/2}} & \text{for } x \geq \xi \end{cases} \quad (6)$$

The eigenvalues are obtained as the poles of (6). One can show, e.g., by expanding Green's function (6) in series around  $\lambda = 0$ , that 0 is not a pole. The poles of (6) are simple and they satisfy the equation:  $\cos \lambda_k^{1/2} = 0, k = 1, 2, \dots$ . The solutions  $\lambda_k$  are the eigenvalues of a fixed-free rod.

In order to find the eigenmodes, one needs to calculate the projection operator, given by the following expression [3]:

$$Pv(x) = - \int_0^1 \text{res}_{\lambda_k} [G(x, \xi; \lambda)] v(\xi) d\xi \quad (7)$$

where the residue at a simple pole is equal to:

$$\text{res}_{\lambda_k} [G(x, \xi; \lambda)] = \frac{N(\lambda_k)}{D'(\lambda_k)} = -2 \sin \lambda_k^{1/2} x \sin \lambda_k^{1/2} \xi \quad (8)$$

Here,  $N(\lambda)$  and  $D(\lambda)$  denote, respectively, the numerator and denominator of Green's function (6), and the comma stands for differentiation with respect to  $\lambda$ . Result (8) is symmetrical with respect to the interchange of  $x$  and  $\xi$ , therefore the formula that defines the projector is valid both when  $x \leq \xi$  and  $x \geq \xi$ , irrespective of the ordering of  $x$  and  $\xi$  in the expression of Green's function (6).

By combining Eqs. (7) and (8) one obtains:

$$Pv(x) = \left[ 2 \int_0^1 \sin(\lambda_k^{1/2} \xi) v(\xi) d\xi \right] \sin \lambda_k^{1/2} x \quad (9)$$

It can be seen that projection (9) of an arbitrary function  $v(x)$  onto the eigenspace (which is one-dimensional in our case) is proportional to the eigenvector  $\sin \lambda_k^{1/2} x$ , corresponding to eigenvalue  $\lambda_k$ . In particular, when  $v(x) = C \sin \lambda_k^{1/2} x$ , where  $C$  is an arbitrary constant, the coefficient in the square brackets in Eq. (9) is equal to  $C$ , so that the eigenvector is not altered when projected onto the eigenspace of  $\lambda_k$ .

Returning to the general case of a rod with a spring acting on its right end, setting the denominator of kernel (5) to be equal to zero, the characteristic equation of the rod with the spring is as follows:

$$\lambda^{1/2} \cos \lambda^{1/2} + \kappa \sin \lambda^{1/2} = 0 \quad (10)$$

The projection operator can be obtained in a way similar to that described for the case with no spring, and it can be brought to the following form:

$$Pv(x) = \left[ \frac{2(\lambda_k^{1/2} \sin \lambda_k^{1/2} - \kappa \cos \lambda_k^{1/2})}{\lambda_k^{1/2} \sin \lambda_k^{1/2} - (1 + \kappa) \cos \lambda_k^{1/2}} \int_0^1 \sin(\lambda_k^{1/2} \xi) v(\xi) d\xi \right] \sin \lambda_k^{1/2} x \quad (11)$$

where  $\lambda_k$  is the  $k$ -th eigenvalue obtained from characteristic equation (10).

One of the important applications of this theory is the perturbation calculation of the eigenvalues and eigenvectors of linear operators. This will be discussed during the symposium, by treating the force from the spring as a perturbation term. It is to be noted that this perturbation appears in the boundary condition, rather than in the governing equation. When using the standard perturbation approach described in many physics books, some complications arise in such a case. That is the justification why this example has been chosen for the study. The analytical approach described above is capable of dealing with such a problem in a rigorous way.

## References

- [1] Dunford, N., and J.T.Schwartz, *Linear Operators, Part I: General Theory*, Interscience, New York, 1958.
- [2] Lorch, E.R., *Spectral Theory*, Oxford University Press, New York, 1962.
- [3] Kato, T., *Perturbation Theory for Linear Operators*, Springer-Verlag, Berlin/Heidelberg/New York, 2<sup>nd</sup> ed., 1980.
- [4] Baumgärtel H., *Analytic Perturbation Theory for Matrices and Operators*, Akademie-Verlag, Berlin, 1984.

## Investigations on the Similitudes of Stiffened Cylinders

G. Petrone, S. De Rosa and F. Franco

pasta-lab, Laboratory for Promoting experiences in Aeronautical Structures and Acoustics  
Department of Industrial Engineering, Aerospace Section  
University of Napoli "Federico II", Via Claudio 21, 80125 Napoli, Italy  
giuseppe.petrone@unina.it, sergio.derosa@unina.it, francesco.franco@unina.it

### Abstract

Scaling laws provide the relationship between a full-scale structure and its scaled models. They can be used to extrapolate the experimental data from a small, inexpensive, and easy to be tested model into design information for the full -scale structure.

In some engineering fields, like in the aerospace or naval ones where the structures are huge, practical applications of scaled down models are suitable and the importance of establishing a similarity and finding proper scaling laws is evident, [1]-[4].

This work presents an investigation on the definition and applicability of distorted similitudes and the related scaling laws for the analysis of the dynamic response of stiffened cylinders. Such responses are determined from a generalization of the modal approach, which allows the use of the mode shapes and natural frequencies to establish the proper scaling laws. The complete procedure is named SAMSARA (Similitude and Asymptotic Models for Structural Acoustic Research and Applications).

The previous theoretical and numerical studies, based on Modal Analysis, Finite Element Approach and Energy Distribution Approach, allowed to use modal sets to produce both the original and distorted forced responses for a class of test-cases: the sequence of works is from [5] to [12].

Important experimental evidences for the vibroacoustic response of plates are already available to demonstrate the feasibility of pursued approach [10] and [12]. Recently, the problem of random excitation has been analyzed, [13]. Also the preliminary analytical investigations for the cylinders were successful [9]. To highlight the opportunities offered by the similitudes, the laboratory tests are considered an unavoidable successive step. The identification of the principal scaling laws can be a difficult step as consequence of the large number of design parameters in stiffened cylindrical shells; some limitations of the similitude relationships may be encountered during the design of parent (small-scale) stiffened shells.

Thus, having in mind to apply the laws defined in [9], two classes of stiffened cylinders (indicating as *A* and *B*), consisting of 6 rectangular-shaped ribs and 5 square-shaped stringers, are investigated, Table 1. The cylinders are made of aluminium:  $E = 70$  GPa,  $\mu = 0.33$ ,  $\rho = 2750$  kg/m<sup>3</sup>. The *A* and *B* test-articles indicate the two reference cylinders and  $A_1$ ,  $A_2$ ,  $B_1$  and  $B_2$  are the *avatars*, that is the cylinders in distorted similitude. Article *C* one is an attempt to find a sort of intermediate configuration between *A* and *B* test-articles. The aim is to use  $A_i$  and  $B_i$  to recover the forced response of *A* and *B* ones. The response of *C* will be carefully investigated to recover *A* and *B*: this will be the most challenging goal. In particular, the *B* test-article has a *tube* configuration; on the contrary, in the *A* one, the circular shape prevails.

Preliminary numerical models and investigations of the cited cylinders are performed and several

Table 1: Cylinders

label	A	A <sub>1</sub>	A <sub>2</sub>	B	B <sub>1</sub>	B <sub>2</sub>	C
	mm						
length	2500	1250	1250	2500	1250	1250	850
diameter	1000	500	500	400	200	200	400
skin thickness	2	2	2	1	1	1	1
area	mm <sup>2</sup>						
long. stiffener	10 × 10	10 × 10	10 × 5	10 × 10	10 × 10	10 × 5	10 × 10
circ. stiffener	30 × 10	30 × 10	30 × 15	30 × 10	30 × 10	15 × 10	30 × 10

considerations, useful for the best use of the experimental tests, are acquired. It is verified with a replica (i.e. a domain whose dimensions are scaled according a unique similitude rate) that it is always possible to switch from the original model to the parent model and vice-versa. In this sense, the terms 'original' and 'parent' are interchangeable. On the other hand, in the case of distorted parents, the distribution of natural frequencies is altered and only a partial similitude is achieved. It has, thus, tested the use at same time of more than a single scaling law; these scaling laws are tailored on several frequency ranges. For the replica, the response is correctly obtained applying just a single scaling law, as expected.

The experimental test bench is set-up in order to facilitate the cross correlation with the numerical models. The cylinders under investigation are suspended on a rigid support through elastic strings, simulating the free-free conditions. The point excitation (white noise signal) is provided onto a face of the panel by means of a shaker (Modal Shop 2100E11), connected to the structure through a stinger (in order to apply the force as much as possible perpendicular to the surface). Five accelerometers - PCB 333B32 - are used to measure the response over the surface of the cylinders, changing their position along the experimental mesh (Fig. 1). The data are recorded using the LMS SCADAS III acquisition system, in the bandwidth 0 – 1024 Hz with a frequency resolution 1 Hz; thus, data are analyzed by using LMS Test.Lab 8.B and Matlab.

The first experimental phase consists on the numerical model up-dates. In fact, the matching between the experimental data and the numerical models is the basic step for the successive similitude analyses: the agreement and/or the assessment of the differences among the data help the successive development of the similitude laws for the stiffened cylinders. In fact, the similitude laws are based on some hypotheses about the mechanical behaviour of the cylinders. The range of validity of these hypotheses can be assessed through the experimental data.

## References

- [1] Morgen G. W.; (1964). Scaling Techniques for Orthotropic Cylindrical Aerospace Structures , Proceedings of AIAA 5th Annual Structures and Materials Conference, Palm Spring CA.
- [2] Leissa, A. W.; (1978). **Vibration of Shells**. NASA SP-288.
- [3] Krayterman B.; Sabnis G. M.; (1984). Similitude theory: plates and shells analysis. Journal of Engineering Mechanics, 110 (9), pp. 1247-1263, 1984.



Figure 1: (Left) Details of the interior of cylinder A. (Right) Test set-up for the forced response of the cylinder A.

- [4] Rezaeepazhand J.; Simites G. J.; (1997). Structural similitude for vibration response of laminated cylindrical shells with double curvature. *Composites Part B: Engineering*, 28(3), pp. 195-200.
- [5] De Rosa S.; Franco F.; Li X.; Polito T.; (2012). A similitude for structural acoustic enclosures, *Mechanical Systems and Signal Processing* 30 330-342.
- [6] De Rosa S.; Franco F.; (2013). Some advances in the definition of exact and distorted similitudes. 9th International Symposium on Vibrations of Continuous Systems, 21-26/07/2013, Courmayeur (AO), Italy, pp.13-15.
- [7] De Rosa S.; Franco F.; Polito T.; (2014). Partial scaling of finite element models for the analysis of the coupling between short and long structural wavelengths, *Mechanical Systems and Signal Processing*, 2015, 52-53, 722–740.
- [8] De Rosa S.; Franco F.; Meruane M.; (2015). Similitudes for the structural response of flexural plates. *Proceedings of the Institution of Mechanical Engineers. Part C, Journal of Mechanical Engineering Science*, doi: 10.1177/0954406215572436.
- [9] De Rosa S.; Franco F.; (2015). Analytical similitudes applied to thin cylindrical shells. *Advances in Aircraft and Spacecraft Sciences*, Vol.2 (4), 403-425, Technopress.
- [10] Meruane V.; De Rosa S.; Franco F.; (2016). Numerical and experimental results for the frequency response of plates in similitude, *J Mechanical Engineering Science*, Vol. 230(18) 3212–3221.
- [11] De Rosa S.; Petrone G.; Franco F., (2016). Similitudes for Acoustic Volumes: Analytical Models for the Response, INTER-NOISE, Hamburg, Germany.
- [12] Robin O.; De Rosa S.; Berry A.; (2016). Similitudes for the Structural Response and Radiated Power from Plates, INTER-NOISE, Hamburg, Germany.
- [13] Robin O.; Franco F.; Ciappi E.; De Rosa S.; Berry A.; (2017). Turbulence induced vibration and acoustic radiated power by flat panels including exact and distorted similitudes, FLINOVIA II - 2017 (<http://www.flinovia.org>).

# The Necessity of the Timoshenko Beam Theory for modeling Gyroscopic Continua

Hu Ding

Shanghai Institute of Applied Mathematics and Mechanics,  
Shanghai University, Shanghai 200072, China  
dinghu3@shu.edu.cn

## Abstract

Axially moving systems and rotating rings are taken as representations of gyroscopic continua. These motional continua are common constituent elements in many machine systems. Large unwanted vibration due to the presence of the motion speed seriously affects the system performance, accuracy and safe operation. In this work, the necessity of the Timoshenko beam theory is studied for modeling gyroscopic continua. Free vibration of a rotating ring supported by an elastic foundation is studied by analytical method, finite element (FE) simulation and experiment. By adopting the ring analogy of Timoshenko beam theory, the nonlinear vibration of the rotating ring on an elastic foundation is modeled based on Hamilton's principle. By solving the generalized eigenvalue problem, natural frequencies and flexural modes are obtained. Moreover, generalized boundary conditions are proposed for the axially moving beam. This generalized boundary constraint can represent all states between the classical boundary conditions. Dynamic stiffness matrixes are created for moving Timoshenko beams and Euler-Bernoulli (E-B) beams with generalized boundary conditions. The validity and utility of the dynamic stiffness method is demonstrated by using numerical simulations. Furthermore, Timoshenko beam theory is applied to study free vibration of high-speed axially moving continua. The weighted residual method (WRM) is employed to solve natural frequencies, which are verified by using the discrete Fourier transform (DFT). For determining the necessity of the Timoshenko theory, the flexural vibration frequencies from two theories are compared. Some interesting conclusions are drawn.

## 1. Introduction

Many researchers and engineers have paid attention to vibration characteristics of the rotating rings. If thick rings are considered, however, the ring analog of Timoshenko beam theory is necessary to obtain accurate results. Thick rings are widely used in engineering systems. Although the effects of shear deformation and rotational inertia on the free vibration of the a rotating ring have been proved, use of the Timoshenko theory for the vibration of a rotating ring resting on an elastic foundation still has not been investigated.

One important problem in the axially moving systems is the occurrence of significant and unwanted resonance. In order to determine when the resonance will occur and the intensity of the resonance, the dynamics of axially moving beams have been widely studied for many decades [1,2]. The dynamic stiffness matrix was introduced for the free transverse vibration of an axially transporting E-B beam [3] and Timoshenko beam [4] with classical boundary conditions. In practical engineering applications,, the boundary of an axially transporting continuum is less likely to strictly satisfy those classical constraints, such as strictly simply supported, or completely fixed or clamped. More likely the boundary conditions will be somewhere between these strict constraints. The generalized boundary conditions are adopted

for studying the vibration characteristics of transporting beams for the first time using either an Euler Beam or Timoshenko Beam model.

The free vibration of the transporting systems at super-critical speed have been studied by the E-B beam theory [5]. The effects of shear force and rotary inertia on the free vibration of the super-critical transporting systems have not been discovered. In other words, the Timoshenko beam theory has not been applied to study the vibration of super-critical transporting systems.

**2. Equations of Motion**

As shown in Figure 1, a rotating elastic ring on an elastic foundation and an axially moving beam with general constraint support boundary conditions are established. The ring and beam are both uniform. In Figure 1(a), the ring rotates at a constant speed  $\Omega$ . The rectangular cross-section has radial thickness  $h$  and the axial width  $b$ .  $k_\theta$  and  $k_r$  are, respectively, the elastic foundation stiffnesses in the tangential and radial directions. The symbols  $u(\theta,t)$  and  $v(\theta,t)$  represent the radial and tangential deformations, respectively.  $\phi(x,t)$  is the slope of the deflection curve due to bending deformation of the ring.  $\rho$  is the density of the ring and  $E$  denotes the elastic modulus.  $\theta$  is the coordinate,  $0 \leq \theta \leq 2\pi$ . This basis rotates at speed  $\Omega$ .  $R$  represents the radius of the ring from the center to the neutral line. In Figure 1(b),  $L$  is the length of the beam between two ends.  $v(x,t)$  is the transverse vibration displacement, where  $x$  and  $t$  stand for the distance from the left end of the beam and the time coordinates, respectively.  $\Gamma$  and  $P_0$  are the axially constant speed and initial axial tension of the transporting beam, respectively. The ends of the beam are supported by vertical springs and constrained by torsion springs.  $K_L$  and  $K_R$  are the spring stiffness coefficients of the vertical elastic support at the left and right ends of the beam, respectively.  $K_{t1}$  and  $K_{t2}$  are the torsion spring stiffness coefficients at the ends.

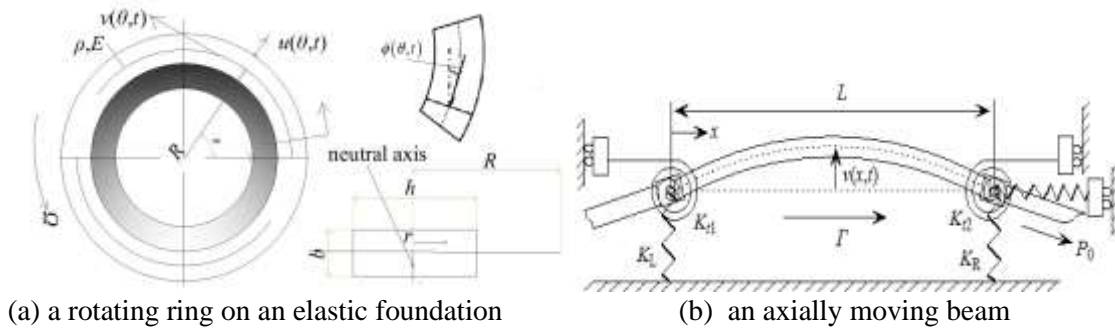


**Figure 1.** Model of a gyroscopic continua.

The non-dimensional equations of the motion of the ring and the axially moving beam with Timoshenko theory have been omitted but will be presented at the symposium.

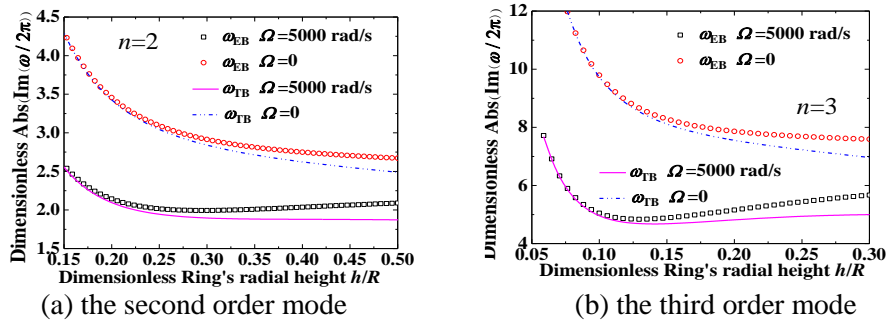


**Figure 2.** Comparison of the natural frequencies of Timoshenko and E-B models changing with the radial height of the ring

The effects of the ratio of radial thickness to the ring radius are shown in Figure 2. The differences between the two ring models emerge with greater increase in the ratio. Indeed, higher order eigenvalues could be totally different for a large thickness-to-radius ratio, no matter whether the ring is stationary or rotating. Interestingly, Figure 3 demonstrates that the vertical spring does not change the critical speed of the moving beam. The effects of the vertical spring stiffness on the E-B beam are larger than for the Timoshenko beam. The difference decreases with the increasing vertical spring stiffness for the first order natural frequency.

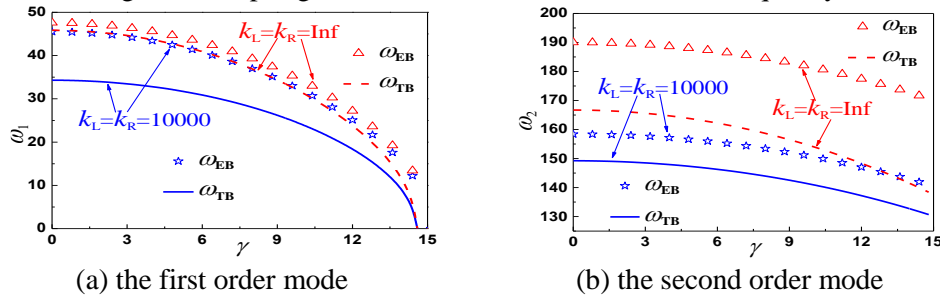


**Figure 3.** Comparisons of the transporting Timoshenko beam model and E-B beam model versus the axial speed and the vertical spring stiffness

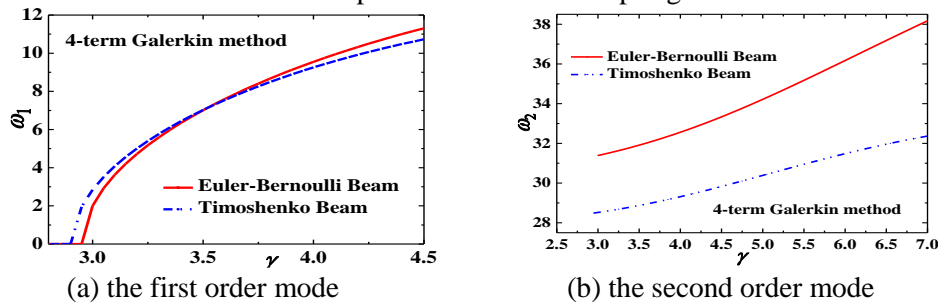


**Figure 4.** Comparisons of the transporting Timoshenko beam model and E-B beam model versus the axial speed and the vertical spring stiffness

Figure 4 illustrates that the second natural frequency of the super-critical vibration from the moving Timoshenko beam theory is much smaller. The fundamental frequency from the moving Euler-Bernoulli beam is smaller than that of the Timoshenko beam theory near the critical speed.

**Acknowledgments**

The authors gratefully acknowledge the support of the National Natural Science Foundation of China (No. 11422214, 11372171, 11232009).

**References**

- [1] Chen, L.Q.: Analysis and control of transverse vibrations of axially moving strings, Applied Mechanics Reviews, Vol.58, pp. 91–116, 2005.
- [2] Marynowski, K.; Kapitaniak, T.: Dynamics of axially moving continua, International Journal of Mechanical Sciences, Vol. 81, pp. 26-41, 2014.
- [3] Banerjee J.R.; Gunawardana, W.D.: Dynamic stiffness matrix development and free vibration analysis of a moving beam, Journal of Sound and Vibration, Vol. 303, pp. 135-143, 2007.
- [4] Lee, U.; Kim, J.H.; Oh, H.M.: Spectral analysis for the transverse vibration of an axially moving Timoshenko beam, Journal of Sound and Vibration, Vol. 271, pp. 685-703, 2004.
- [5] Ding, H.; Chen, L.Q.: Galerkin methods for natural frequencies of high-speed axially moving beams, Journal of Sound and Vibration, Vol. 329, pp. 3484–3494, 2010.

## Vibrations of plates with rectangular cutouts

**Moshe Eisenberger and Aharon Deutsch**

Faculty of Civil and Environmental Engineering

Technion – Israel Institute of Technology

Technion City, Haifa, Israel

e-mail: [cvrmosh@technion.ac.il](mailto:cvrmosh@technion.ac.il)**Abstract**

The vibration analysis of plates is a widely researched area. In many cases, plates with cutouts find a practical use to fulfill requirements of lightweight and dynamic performance. Cutouts can also provide functional access and ventilation or they may occur as damage during service life. A large amount of literature has been devoted to analysis of rectangular plates with cutouts of different shapes ranging from rectangular and polygonal cutouts to round, elliptical, and polygonal ones, as are reviewed in [1].

Starting from the equations of motion of an isotropic rectangular plate we have

$$D_{11} \frac{\partial^4 W(x,y)}{\partial x^4} + 2D_{12} \frac{\partial^4 W(x,y)}{\partial x^2 \partial y^2} + D_{22} \frac{\partial^4 W(x,y)}{\partial y^4} - \omega^2 \rho h W(x,y) = 0 \quad (1)$$

We assume a solution in the following form:

$$\begin{aligned} W(x,y) = & \sum_{m=0}^{\infty} \left( \sin \lambda_a x \sin \frac{m\pi}{2} + \cos \lambda_a x \cos \frac{m\pi}{2} \right) \\ & \cdot (A_m \cosh \alpha_1 y + B_m \cosh \alpha_2 y + C_m \sinh \alpha_1 y + D_m \sinh \alpha_2 y) \\ & + \sum_{n=0}^{\infty} \left( \sin \lambda_b y \sin \frac{n\pi}{2} + \cos \lambda_b y \cos \frac{n\pi}{2} \right) \\ & \cdot (E_n \cosh \alpha_3 x + F_n \cosh \alpha_4 x + G_n \sinh \alpha_3 x + H_n \sinh \alpha_4 x) \\ & + \sum_{m=0}^{\infty} \sum_{n=0}^{\infty} A_m n \xi \eta \cdot \left( \sin \lambda_a x \sin \frac{m\pi}{2} + \cos \lambda_a x \cos \frac{m\pi}{2} \right) \\ & \cdot \left( \sin \lambda_b y \sin \frac{n\pi}{2} + \cos \lambda_b y \cos \frac{n\pi}{2} \right) \end{aligned} \quad (2)$$

With

$$\begin{cases} \lambda_a = \frac{m\pi}{a} \\ \lambda_b = \frac{n\pi}{b} \end{cases}$$

And

$$\left\{ \begin{array}{l} \alpha_1 = \lambda_a \sqrt{\frac{D_{12}}{D_{22}} - \sqrt{\left(\frac{D_{12}}{D_{22}}\right)^2 - \frac{D_{11}}{D_{22}} + \frac{\alpha^4 \omega^2 \rho h}{D_{22} \cdot \lambda_a^2}}} \\ \alpha_2 = \lambda_a \sqrt{\frac{D_{12}}{D_{11}} + \sqrt{\left(\frac{D_{12}}{D_{22}}\right)^2 - \frac{D_{11}}{D_{22}} + \frac{\alpha^4 \omega^2 \rho h}{D_{22} \cdot \lambda_a^2}}} \\ \alpha_3 = \lambda_b \sqrt{\frac{D_{12}}{D_{11}} - \sqrt{\left(\frac{D_{12}}{D_{11}}\right)^2 - \frac{D_{22}}{D_{11}} + \frac{\alpha^4 \omega^2 \rho h}{D_{11} \cdot \lambda_b^2}}} \\ \alpha_4 = \lambda_b \sqrt{\frac{D_{12}}{D_{11}} + \sqrt{\left(\frac{D_{12}}{D_{11}}\right)^2 - \frac{D_{22}}{D_{11}} + \frac{\alpha^4 \omega^2 \rho h}{D_{11} \cdot \lambda_b^2}}} \end{array} \right.$$

$$A_{mn\xi\eta} = \frac{4P}{ab} \frac{\cos \lambda_a \xi \cos \lambda_b \eta}{\pi^4 \left( D_{11} \left(\frac{m}{a}\right)^4 + 2D_{12} \left(\frac{mn}{ab}\right)^2 + D_{22} \left(\frac{n}{b}\right)^4 \right) - \omega^2 \rho h}$$

Using this assumed solution one can find all the unknown parameters for given set of known conditions for deflection, slope, shear, and moment along the four edges, or from the continuity condition for these quantities on the border of neighboring plates. The calculation of the natural frequencies is done by finding the value of frequency for which a zero value of load on the plate will generate infinite deflection, using the method presented in Ref. [1].

For a simply-supported plate with a square cutout as shown in the figure, with  $a=0.5$  the first 4 normalized natural frequencies and the modes shapes were calculated and given below. The values of the natural frequencies are compared with the results from Ref. [2].

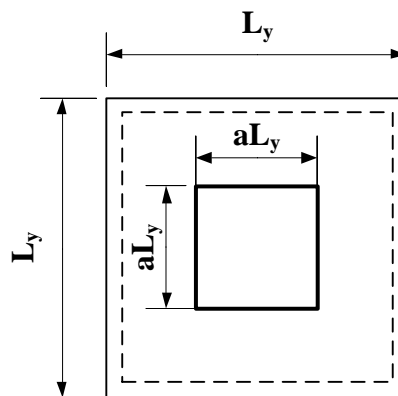


**Figure 1:** square plate with a square cutout,  $a = 0.4$   
 $D_{11} = 1, D_{22} = 1, D_{12} = 1, \nu = 0.3$

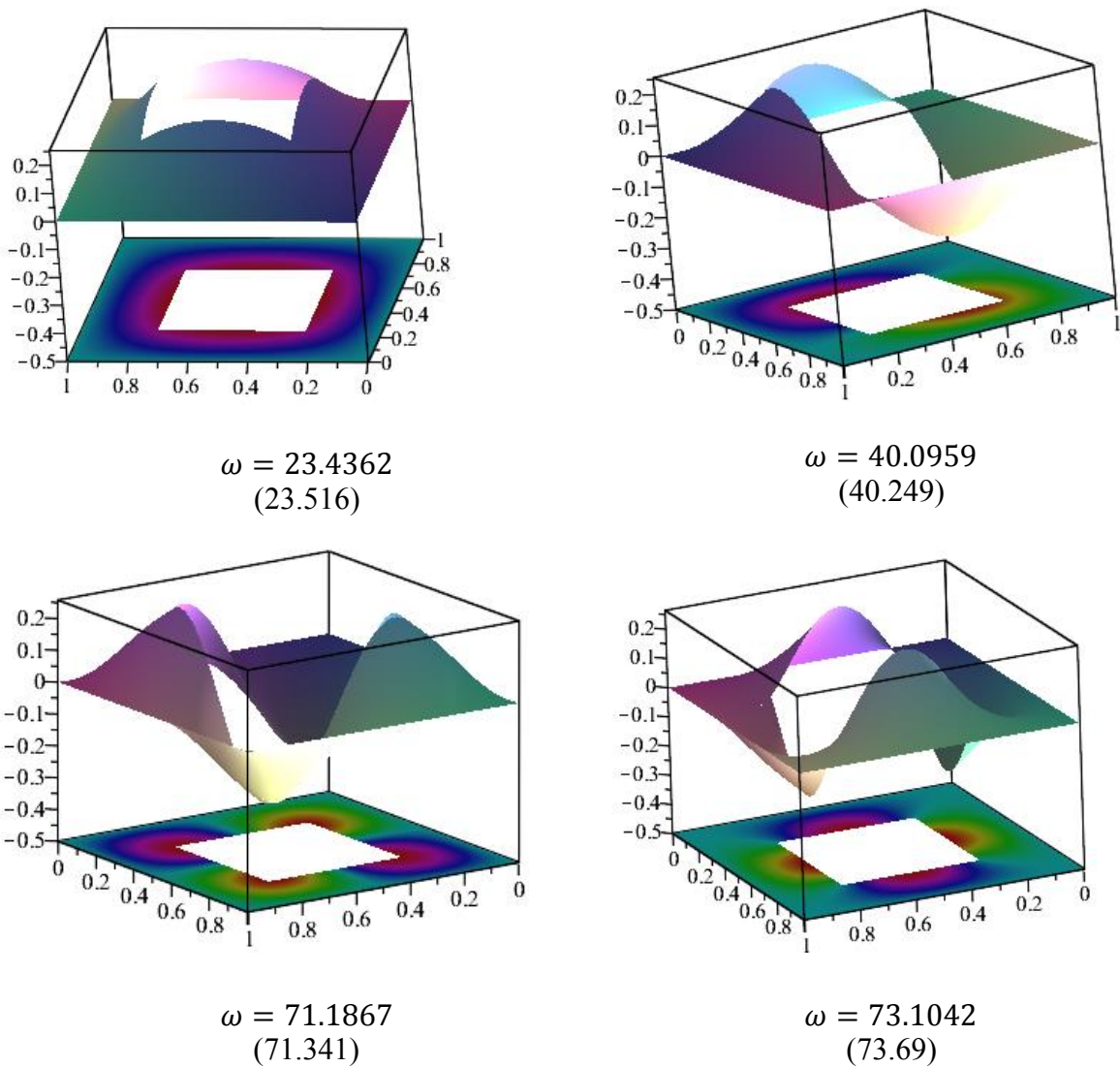


**Figure 2:** The first 4 mode shapes and normalized frequencies for the plate in Figure 1.

**References**

- [1] Eisenberger, M. and Deutch, A., "Static Analysis for Exact Vibration Analysis of Clamped Plates", *Int. Jour. Structural Stability and Dynamics*, Vol. 15, 1540030, 2015.
- [2] Shufrin, I., and Eisenberger, M., "Semi-analytical modeling of cutouts in rectangular plates with variable thickness", *Applied Mathematical Modeling*, Vol. 40, pp. 6983-7000, 2016.

# Shear Coefficients for Symmetric Bending Vibration of Thin, Shallow, Circular Cylindrical, Rectangular-planform Shells

Mark S. Ewing

Aerospace Engineering  
University of Kansas  
Lawrence, Kansas, USA  
[mewing@ku.edu](mailto:mewing@ku.edu)

*This presentation is dedicated to the memory of the late Jim Hutchinson, the past keeper-of-all-knowledge in the realm of beam shear coefficients, and with whom I never took the opportunity to share the results reported here.*

## Introduction

In two previous Symposia, Jim Hutchinson discussed the appropriate selection of shear coefficients for Timoshenko beams of thin-walled [1] and rectangular [2] cross-section, both inspired by his classic 2001 paper on shear coefficients [3]. While these two presentations may have seemed to “close the door” on future discussion on shear coefficients, there is a class of thin-walled “beams” not covered previously: the beam representation of thin, shallow, rectangular-planform shells. Such shells were considered using the author’s 6<sup>th</sup> order vibration beam model [4], characterized by explicit, though not exact, inclusion of bending warping, torsion warping and anticlastic bending effects—both flexibility and restraint.

## Beam Model

The (symmetric) beam vibration model is based on the two-degree of freedom, symmetric Timoshenko model, with the dependent variables  $u_{BS}(z)$ , the total lateral deflection (due to bending and shear) in the  $x$ -direction and  $\psi_x(z)$ , the associated bending slope. To this model is added the bending warping parameter,  $\gamma_x(z)$ , which gives the axial warping deflection,  $(\chi + xy^2)\gamma_x(z)$ , where  $\chi$  is the St. Venant bending warping function, a function of the cross-section shape. After forming the energy functionals and using Hamilton’s principle, the 6<sup>th</sup> order relationship emerges as three, coupled 2<sup>nd</sup> order differential equations of motion:

$$\begin{aligned} G[\Lambda_4\gamma'_x + A(u_{BS} - \psi'_x)] - \rho A\ddot{u}_{BS} &= 0 \\ E[I_{yy}\psi''_x - \Lambda_1\gamma''_x] + G[\Lambda_4\gamma_x + A(u'_{BS} - \psi_x)] - \rho[I_{yy}\ddot{\psi}_x - \Lambda_1\ddot{\gamma}_x] &= 0 \\ E[\Lambda_1\psi''_x - \Lambda_2\gamma''_x] + G[\Lambda_3\gamma_x + \Lambda_4(u'_{BS} - \psi_x)] - \rho[\Lambda_1\ddot{\psi}_x - \Lambda_2\ddot{\gamma}_x] &= 0 \end{aligned} \quad (1)$$

with area-constants

$$\begin{aligned} \Lambda_1 &= \iint_A x(\chi + xy^2)dA & \Lambda_3 &= \iint_A \left\{ \left[ \frac{d}{dx}(\chi + xy^2) \right]^2 + \left[ \frac{d}{dy}(\chi + xy^2) \right]^2 \right\} dA \\ \Lambda_2 &= \iint_A (\chi + xy^2)^2 dA & \Lambda_4 &= \iint_A \left[ \frac{d}{dx}(\chi + xy^2) \right] dA \end{aligned} \quad (2)$$

For a cantilever beam for the case of *total* end fixity,  $u_{BS}(0) = \psi_x(0) = \gamma_x(0) = 0$ , the 3 boundary conditions at the free end emerge as:

$$\begin{aligned} A(u'_{BS} - \psi_x) + \Lambda_4\gamma_x &= 0 \\ I_{yy}\psi'_x - \Lambda_1\gamma'_x &= 0 \\ \Lambda_1\psi'_x - \Lambda_2\gamma'_x &= 0 \end{aligned} \quad (3)$$

This model has been compared with the theories of Cowper [5] who proposed a rational expression for shear coefficients, which characterize cross-section shear deformation, and Levinson [6], who proposed the consideration of cross-section bending warping deformation. Cowper proposed a shear coefficient for thin-walled cross-sections which has been used in the current study of curved shells (and very similar to the formulation by Hutchinson):

$$k = \frac{2(1 + \nu)I_{yy}}{\frac{\nu}{2}(I_{xx} - I_{yy}) - \frac{A}{I_{yy} \iint_A x(\chi + xy^2)dA}}$$

### Results for a thin-walled cantilever beam with a curtate circular sector cross-section

The geometry of the thin-walled beam in question is shown below, left. The shear coefficients for a range of physical parameters is shown below in Table 1, below, right. Note the very small values of shear coefficient for deeper, thin shells.

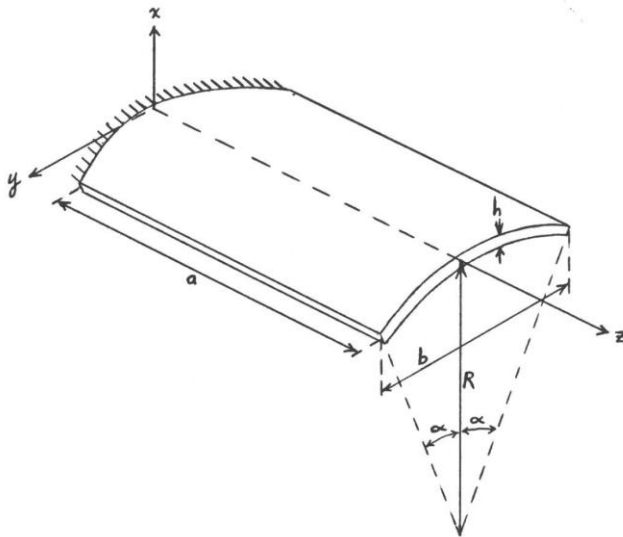


**Table 1.** Shear coefficients for curtate circular sector sections after Cowper ( $\nu = 0.3$ ).

$b/R$	$b/h=20$	$b/h=5$	$b/h=1$
0.01	0.814	0.846	0.850
0.1	0.174	0.839	0.850
0.3	0.0509	0.789	0.845
0.5	0.0510	0.710	0.837

**Figure 1 .** Geometry for the thin-walled "beam".

For rather thick shells ( $b/h \sim 1$ ), the predicted non-dimensional natural frequency results based on Cowper's, Levinson's and the author's beam model (which requires no shear coefficient) match very well (but, are not given here).

But, for thin and deep shells, *e.g.*,  $b/h = 20$  and  $b/R = 0.1$ , the very small values of the shear coefficient corresponds to an *increase* in flexibility, which results in a *decrease* in natural frequency. This makes a significant difference for beam bending vibration (about the minimum principal axis) especially in the case of a very low aspect ratio,  $a/b$ , as is apparent in Table 2. Therein, a comparison is made between shell theory [7] and Timoshenko beam theory (which includes rotary inertia, along with shear deformation). For instance, for the deeper shells,  $b/h = 0.5$ , the **fundamental frequency results** using the Cowper shear coefficient more closely match the results from shell theory, whereas not using the correct shear coefficient results in a beam which is too stiff for  $b/R > 0.1$ . On the other hand, for the 2nd mode, using the "correct", very small shear coefficient, results in frequencies which are uniformly low, and for the case of  $a/b = 1/2$ , are **substantially low**—which one should expect, considering the *lateral* bending restraint in a shell, which a beam model *cannot* accommodate. As such, using beam theory in such cases is ill-advised.

**Table 2.** Comparison of  $\omega a^2 \sqrt{\rho h/D}$  between shell and beam theory for thin ( $b/h = 20$ ) circular cylindrical shells with  $a/b = 1$  and 0.5.

$a/b$	$b/R$	Shell [7]	Timoshenko beam [8]	
			$k = 0.85$	$k$ (Cowper)
1	0.1	3.561	3.456	3.435
		21.48	21.39	20.55
	0.3	4.181	4.229	4.081
		22.76	26.01	21.27
	0.5	5.168	5.484	5.172
		24.66	33.33	24.77
0.5	0.1	3.541	3.434	3.354
		21.88	20.53	17.97
	0.3	3.829	4.18	3.684
		22.12	24.51	14.92
	0.5	4.461	5.400	4.423
		22.58	30.34	16.20

### Conclusion

As shown by Hutchinson, the use of shear coefficients in bending vibration, especially at high frequencies (small wavelengths) requires the right shear coefficient. Further, as noted here, having the right shear coefficient for beam representations of the thin, shallow shell becomes increasingly important for estimating the fundamental vibration frequency as aspect ratio decreases. However, for higher modes, a beam model completely fails—as one should expect.

### References

1. Hutchinson, J.R., “Shear Coefficients for Thin-Walled Timoshenko Beams”, 3<sup>rd</sup> ISVCS, pp 25-27.
2. Hutchinson, J.R., “Timoshenko Beams of Rectangular Cross-Section”, 4<sup>th</sup> ISVCS, pp 11-13.
3. Hutchinson, J.R., “Shear Coefficients for Timoshenko Beam Theory”, ASME J Appl Mech, vol 68, pp 87-92, 2001.
4. Ewing, M.S., “Free Vibration Analysis with Beam Models which include Bending Warping, Torsion Warping and Anticlastic Bending Effects”, PhD dissertation, Ohio State University, 1983.
5. Cowper, G.R., “The Shear Coefficient in Timoshenko’s Beam Theory”, ASME J Appl Mech, vol 33E, no 2, pp 335-340, June 1966.
6. Levinson, M., “Further Results of a New Beam Theory”, J Sound and Vibration, vol 77, issue 3, pp 440-444, Aug 1981
7. Leissa, A.W, Lee, J.K., and Wang A.J, “Vibrations of Cantilevered Shallow Cylindrical Shells of Rectangular Planform”, J Sound and Vibration, vol 78, no 2, pp 311-328, 1981.
8. Leissa, A.W. and Ewing, M.S., “Comparison of Beam and Shell Theories for Vibration of Thin Turbomachinery Blades”, ASME Engineering for Power, vol 105, no 2, pp 383-392, 1983.

## Rotordynamics analyses using a node-dependent unified formulation

Matteo Filippi, Enrico Zappino, Erasmo Carrera

MUL2, Department of Mechanical and Aerospace Engineering  
Politecnico di Torino,  
Corso Duca degli Abruzzi 24, 10129 Torino, Italy  
matteo.filippi@polito.it, enrico.zappino@polito.it, erasmo.carrera@polito.it

### Abstract

In this paper, the dynamics of rotors has been evaluated using refined one-dimensional finite elements developed within the framework of the Carrera Unified Formulation (CUF) and characterized by a node-dependent kinematics. The CUF formalism enables one to express the primary variables (the three displacement components) with an arbitrary number of products,  $M$ , of the cross-sectional functions,  $F_\tau(x,z)$ , and the generalized displacement vector  $\mathbf{u}_\tau(y,t)$ . Such a vector can be, in turn, approximated using the classical shape functions,  $N_i(y)$ , of the Finite Element Method (FEM), and the nodal displacement vector,  $\mathbf{q}_{i\tau}(t)$

$$\mathbf{u} = F_\tau(x,z)N_i(y)\mathbf{q}_{i\tau}(t) \quad \tau = 1, \dots, M \quad (1)$$

The subscript  $i$  of Equation (1) ranges from 1 to the maximum number of nodes of the adopted 1D element, which can be  $N_n = 2, 3$  or 4. According to the node-dependent technique [1], Equation (1) can be particularized for each beam node by modifying either the number or the type of functions  $F_\tau(x,z)$ . For example, let consider a 2-node beam element as shown in Figure 1.

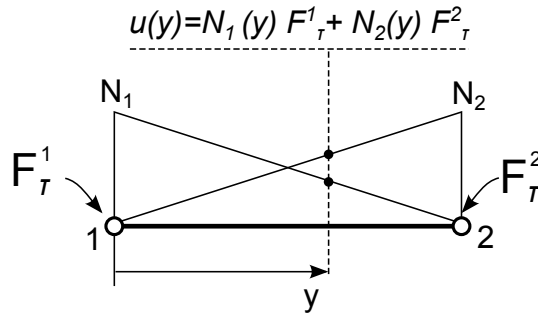


Figure 1: Displacement field of a node-dependent kinematic beam element.

The displacement field corresponding to the node 1 can be written as

$$\mathbf{u}^1 = \mathbf{u}_{1\tau} F_\tau^1, \quad \tau = 1 \dots M^1 \quad (2)$$

while, the kinematics of the second node is

$$\mathbf{u}^2 = \mathbf{u}_{2\tau} F_\tau^2, \quad \tau = 1 \dots M^2 \quad (3)$$

A linear combination of Equations (2) and (3) provides the displacement field of the whole refined beam element as it follows

$$\mathbf{u} = \mathbf{u}_{1\tau} N_1 F_\tau^1 + \mathbf{u}_{2\tau} N_2 F_\tau^2, \quad \tau = 1 \dots M^i \quad (4)$$

In this work, Taylor (TE) and Lagrange (LE) expansions have been used to express the cross-sectional kinematics [2]. For instance, if a first-order Taylor expansion (TE-1) is adopted at the first node, and a 4-node Lagrange element (LE4) is used at the second node, Equation (4) reduces to

$$\mathbf{u} = N_1 \underbrace{[\mathbf{u}_1^1 + \mathbf{u}_2^1 x + \mathbf{u}_3^1 z]}_{1^{st} \text{ node}} + N_2 \underbrace{[\mathbf{u}_1^2 L_1 + \mathbf{u}_2^2 L_2 + \mathbf{u}_3^2 L_3 + \mathbf{u}_4^2 L_4]}_{2^{nd} \text{ node}}$$

Therefore, the displacement field of the 1D-CUF element with a node-dependent kinematics can be written, in a general way, as it follows

$$\mathbf{u} = \mathbf{u}_{i\tau} N_i(y) F_\tau^i(x, z), \quad \tau = 1 \dots M^i; \quad i = 1 \dots N_n. \quad (5)$$

Equation (5) is introduced in the expressions of the potential and kinetic energies of a structure that is rotating about its longitudinal axis [3]. The application of the Hamilton's principle leads to the following equilibrium equations

$$K_{TOT} u + G_\Omega \dot{u} + M \ddot{u} = F \quad (6)$$

where  $K_{TOT}$  includes the stiffness elastic matrix and other contributions due to the rotation (spin softening, convective and geometrical stiffness matrix),  $G_\Omega$  is the Coriolis or gyroscopic matrix depending on which reference frame has been used,  $M$  is the mass matrix, and  $F$  is the vector of the centrifugal force. It is noteworthy that the system 6 has been derived in a fully three-dimensional fashion. The possibility of modifying the number and the nature of the kinematics only at defined regions makes the node-dependent approach appears very effective when rotors are constituted of components with different deformability such as compact shafts and disks. To validate the current approach, the rotor shown in Figure 2 has been considered. The geometrical and material properties can be found in [3].

Figure 3 shows the Campbell diagrams obtained using a full LE model presented in [3], the reference solution proposed in [4], and the node-dependent model TE2-2/LE. According to this mathematical model, the kinematics of the compact shaft has been approximated using a second-order Taylor expansion, while the displacement field related to the disk has been conceived using Lagrange-type elements.

It can be observed that the three solutions strongly agree each other. However, the node-dependent approach required a lower number of degrees of freedom with respect to the full Lagrange approach.

More details about the application of CUF to rotordynamics, and results from a wider range of problems will be provided during the *11<sup>th</sup> International Symposium on Vibrations of Continuous Systems*.

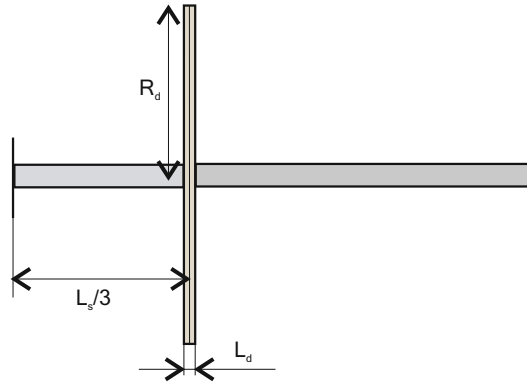


Figure 2: Sketch of the rotor.

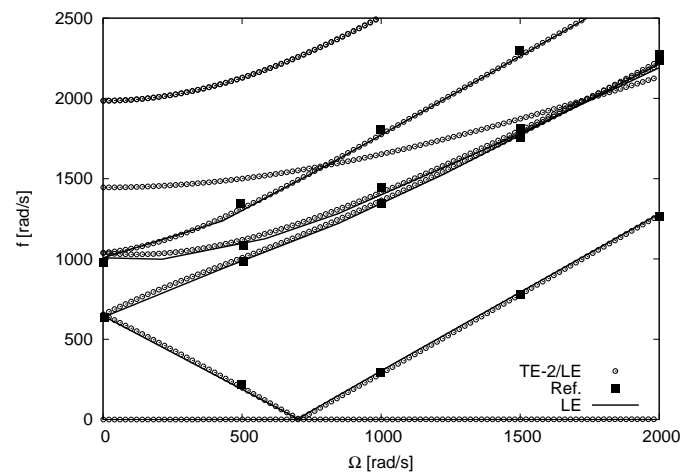


Figure 3: Frequencies vs. spin speed for a rotating disc on a flexible shaft.

## References

- [1] Carrera, E.; Zappino, E.: Analysis of Complex Structures Coupling Variable Kinematics One-Dimensional Models. IMECE2014 - Proceedings of ASME 2014 International Mechanical Engineering Congress & Exposition.
- [2] Carrera, E.; Cinefra, M.; Petrolo, M.; Zappino, E.: Finite Element Analysis of Structures Through Unified Formulation. Wiley & Sons, 2014.
- [3] Filippi, M.; Carrera, E.: A refined onedimensional rotordynamics model with three-dimensional capabilities. Journal of Sound and Vibration, Vol. 366, pp. 343–356, 2016.
- [4] Combescure, D.; Lazarus, A.: Refined finite element modelling for the vibration analysis of large rotating machines: Application to the gas turbine modular helium reactor power conversion unit. Journal of Sound and Vibration, Vol. 318, pp. 1262–1280, 2008.

## Comparison of the Dynamic and Stability behaviour of Guided Spline Circular Saws and Collared Circular Saws

*Stanley G. Hutton*<sup>1</sup>

*Professor Emeritus*

*Ahmad Mohammadpanah*<sup>1</sup>

*PhD, P.Eng,*

<sup>1</sup>*Department of Mechanical Engineering, the University of British Columbia, Vancouver, B.C., Canada, V6T 1Z4*

### Abstract

In the wood processing industry circular saws are widely used in the breakdown of logs to boards of varying dimensions. These circular saws are primarily of two types: a) collared saws; and b) splined arbor saws (Figure 1).

In a collared saw the blade is rigidly fixed to the driving arbor whereas in a splined saw the inner radius of the blade is splined and matches a splined arbor that provides the driving torque for the saw. Lateral constraint for guided saws is provided by space fixed guide pads which constrain the lateral motion of the saw. The maximum cutting speed for a collared saw is determined by the lowest critical speed of the rotating disk whereas the splined saw is able to operate at speeds in excess of the lowest critical speed.

This paper presents a stability analysis of a spinning disk (an idealized representation of the saw) for both saw types, when subjected to radial and tangential in plane forces. This analysis contains an evaluation of the energy transfer from the applied loads to the disk vibrations and is used to examine the role of critical system components on the development of instability.

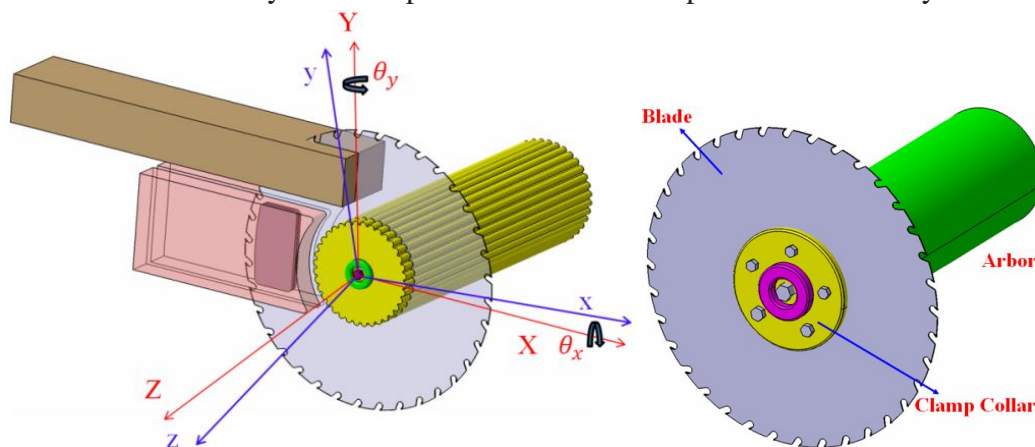


**Figure 1. Schematic of Guided Spline Saw (left), and Clamped Saw (right)**

The works by Chen J.S. [1-4] appear to be the first thorough investigation, concerning the effect of in-plane edge- loads on the natural frequencies of a spinning disk clamped at the inner radius. He concluded that compressive, and conservative in-plane edge-loads result in instability of the clamped disk at critical speeds. In an independent study, Shen [5] predicted the stability

characteristics of a clamped spinning disk subjected to a stationary concentrated in-plane edge load. Recently, Mohammadpanah and Hutton [6-8] discuss the stability of a guided splined disk. They concluded that maximum stable operation speed of a guided splined saw is its flutter instability speed.

The following analysis considers the role of the cutting forces (Figure 2, left) on the stability of the system.

The in-plane radial force  $F_r$  and the in-plane tangential force  $F_t$ , and the lateral force  $F_l$  acting on the outer edge of the disk and the interaction loads on the inner edge of the disk are shown in Figure 2.

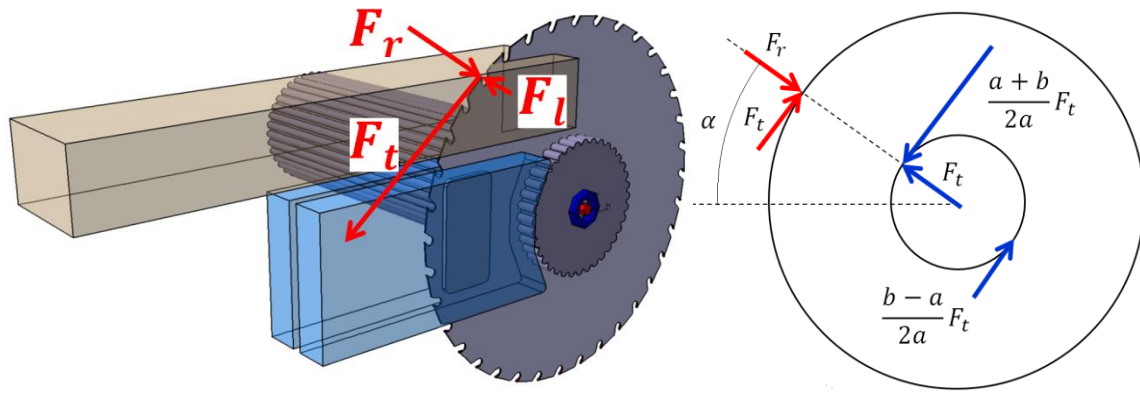


**Figure 2. Schematic of Disk Subjected to In-Plane Edge Loads, and Their Inner Interaction Loads**

In general the rate of work done by a conservative load can be written as [6]:

$$P_{F_r \text{ at Outer Edge}} = F_r \frac{\partial w}{\partial r}(b, \alpha, t) \cdot V(b, \alpha, t) \quad (1)$$



**Figure 3. The Transverse Component of Radial Load**

Where  $F_r \cdot \frac{\partial w}{\partial r}$  is the transverse component of the edge load, and  $V(b, \alpha, t)$  is the transverse velocity of the disk at the point of load application. The work done by this force is found by the integration of Eq. 1 during one complete revolution of the disk. Following the same logic, the rate of work done by applied forces and the inner splined interaction forces can be expressed as in Eq. 2:

$$P_{\text{total}} = F_r \frac{\partial w}{\partial r}(b, \alpha, t) \cdot V(b, \alpha, t) + F_t \frac{\partial w}{\partial \theta}(b, \alpha, t) \cdot V(b, \alpha, t) + F_l \cdot V(b, \alpha, t) + F_r \frac{\partial w}{\partial r}(a, \alpha, t) \cdot V(a, \alpha, t) + \frac{a+b}{2a} F_t \frac{\partial w}{\partial \theta}(a, \alpha, t) \cdot V(a, \alpha, t) + \frac{b-a}{2a} F_t \frac{\partial w}{\partial \theta}(a, \alpha + \pi, t) \cdot V(a, \alpha + \pi, t) \quad (2)$$

As an example consider a clamped and a splined disk of *Inner diameter* = 8 in (200mm), *Outer diameter* = 28 in (700mm), *Thickness* = 0.110 in (2.8mm) ; and subjected to the forces:  $F_r= 100\text{N}$ ,  $F_t= 1000\text{N}$ , and  $F_l= 5\text{N}$ . The rate of work done by in-plane edge loads for the clamped disk, and the splined disk at critical, super critical, and flutter speeds are computed and shown in Figure 3.

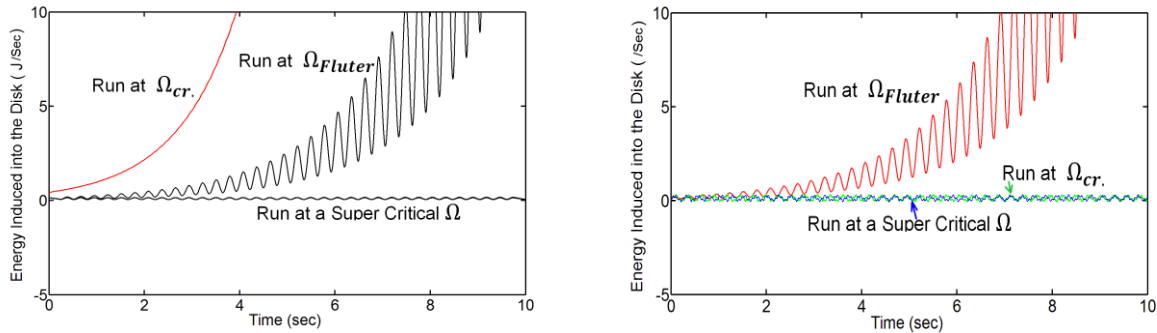


**Figure 3. The rate of work done by in-plane edge loads for a clamped disk (left), and Splined disk (right)**

Comparing the rate of work done by the applied in-plane loads, at the critical speed  $\Omega_{cr}$ , indicates that for a clamped disk, it is positive, and it is zero for a splined disk. The rate of work is positive at flutter speed for both clamped and splined disk.

In conclusion, the rate of work (the energy induced into the system) by in-plane loads is positive at critical (divergence instability) speeds and at flutter instability speeds for a clamped disk. The rate of work (the energy induced to the system) by in-plane loads is only positive at flutter instability speeds for a splined disk. Therefore, a clamped saw cannot be operated at critical speeds, while operation of a splined saw is possible up to its flutter instability speed.

### References:

- [1] Chen J.S., 1994, "Stability Analysis of a Spinning Elastic Disk under a Stationary Concentrated Edge Load", ASME, Vol. 61.
- [2] Chen J.S., 2001, "On the Internal Resonance of a Spinning Disk under Space-Fixed Pulsating Edge Loads", ASME Journal of Applied Mechanics, Vol. 68.
- [3] Chen J.S., 1996, "Vibration and Stability of a Spinning Disk under Stationary Distributed Edge Loads", ASME Journal of Applied Mechanics, Vol. 63.
- [4] Chen J.S., 1997, "Parametric Resonance of a Spinning Disk Under pace-Fixed Pulsating Edge Loads", ASME Journal of Applied Mechanics, Vol. 64/139-143.
- [5] Shen I.Y., and Song Y., 1996, "Stability and Vibration of a Rotating Circular Plate Subjected to Stationary In-Plane Edge Loads", Journal of Applied Mechanics, Vol. 63/121-127.
- [6] Ahmad Mohammadpanah, and Hutton S.G. , 2016, "Vibrations and Dynamics Behaviour of a Guided Spline Spinning Disk, Subjected to Conservative In-Plane Edge Loads, Analytical and Experimental Investigation", ASME, Journal of Vibration and Acoustics, doi: 10.1115/1.4033456
- [7] Mohammadpanah A. and Hutton S.G., 2015, "Flutter Instability Speeds of Guided Splined Disks: An Experimental and Analytical Investigation," Journal of Shock and Vibration, vol. 2015, Article ID 942141, 8 pages, . doi:10.1155/2015/942141
- [8] Mohammadpanah A. and Hutton S. G., 2015, "Maximum operation speed of splined saws", Journal of Wood Material Science and Engineering, doi:10.1080/17480272.2015.1108998

## The effect of roving rotary inertia as it passes a crack

**S. Ilanko<sup>\*</sup>, J. De Los Rios<sup>\*</sup>, S. Caddemi<sup>#</sup>, D. Kennedy<sup>†</sup>**

<sup>\*</sup> The School of Engineering  
The University of Waikato  
Gate 1 Knighton Road Private Bag  
3105 Hamilton 3240 New Zealand  
[ilanko@waikato.ac.nz](mailto:ilanko@waikato.ac.nz);  
[jod1@students.waikato.ac.nz](mailto:jod1@students.waikato.ac.nz)

<sup>#</sup> Dipartimento Ingegneria Civile e  
Architettura  
Università degli Studi di Catania  
Via Santa Sofia 64, 95123 Catania,  
[scaddemi@dica.unict.it](mailto:scaddemi@dica.unict.it)

<sup>†</sup> Cardiff School of Engineering  
Cardiff University  
Cardiff CF24 3AA, United Kingdom  
[KennedyD@cardiff.ac.uk](mailto:KennedyD@cardiff.ac.uk)

### Motivation

While the use of frequency measurements as a means of identifying cracks in a structure has continued to remain a topic of interest for researchers [1-3], it has still not led to a practical way to achieve this, even in laboratory experiments[4]. The reasons for the challenges in implementing this idea include the difficulty in measuring the small changes in the frequency due to the cracks, the lack of a simple way to solve the inverse problem of identifying cracks severity and location, the possibility of multiple cracks which makes the inverse problem even more challenging [5]. In an effort to amplify the effect of the crack on the natural frequencies, Zhong and Oyadiji [6], [7-9] used a roving mass. This resulted in a change in the slope of frequency vs potential crack location plot. Here we explore the use of a roving body possessing inertia and show that as the roving body passes a crack, an abrupt jump in the frequency spectrum can be generally expected. The reason for this assumption is based in the representation of an open crack as a means of slope discontinuity, the inertial property included in the roving mass acts as an amplification element for the mentioned slope discontinuity; the following section will provide a proof to this assumption and present the special case when the amplification effect will not be achieved.

### Proof

Consider two substructures formed by splitting a structure  $A_c$  at a crack location into two component structures, with the possibility of two thin rigid bodies attached to the crack end of each substructure, representing two roving bodies as shown in Fig.1 We will only have a single roving body but to obtain the results for two possible locations (to the left side or the right side of the crack) it is convenient to include two bodies and eliminate one in each special case.

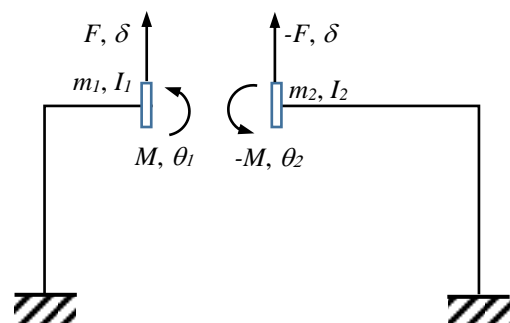


Figure 1. Structure  $A_c$

The internal shear forces and bending moment are given by  $F$  and  $M$  on the left side of the crack and  $-F$  and  $-M$  on the right side of the crack. By Newton's third law, these actions will be equal and opposite, noting that the crack effect represented by a rotational spring does not introduce a discontinuity in moment. Then for the substructures on the left side and the right side of the crack the following DSM equation can be derived:

$$\begin{bmatrix} (K_1 - m_1\omega^2) & K_2 \\ K_2 & (K_3 - I_1\omega^2) \end{bmatrix} \begin{pmatrix} \delta \\ \theta_1 \end{pmatrix} = \begin{pmatrix} F \\ M \end{pmatrix} \quad (1)$$

$$\begin{bmatrix} (K_4 - m_2\omega^2) & K_5 \\ K_5 & (K_6 - I_2\omega^2) \end{bmatrix} \begin{pmatrix} \delta \\ \theta_2 \end{pmatrix} = \begin{pmatrix} -F \\ -M \end{pmatrix} \quad (2)$$

Adding the above equations gives:

$$\begin{bmatrix} (K_1 + K_4 - (m_1 + m_2)\omega^2) & K_2 & K_5 \\ (K_2 + K_5) & (K_3 - I_1\omega^2) & (K_6 - I_2\omega^2) \end{bmatrix} \begin{pmatrix} \delta \\ \theta_1 \\ \theta_2 \end{pmatrix} = \begin{pmatrix} 0 \\ 0 \\ 0 \end{pmatrix} \quad (3)$$

$$\text{But, } M = k(\theta_2 - \theta_1) \quad (4)$$

Substituting Eq. (4) into the second row of eq. (2) gives:

$$K_5\delta + (K_6 - I_2\omega^2)\theta_2 = -k(\theta_2 - \theta_1)$$

$$\text{Rearranging gives: } K_5\delta - k\theta_1 + (K_6 + k - I_2\omega^2)\theta_2 = 0 \quad (5)$$

Combining Eqns. (3) and (5) and subtracting the third row from the second row gives the following equation with a symmetric matrix:

$$D_{c,m,I} = \begin{bmatrix} (K_1 + K_4 - (m_1 + m_2)\omega^2) & K_2 & K_5 \\ K_2 & (K_3 + k - I_1\omega^2) & -k \\ K_5 & -k & (K_6 + k - I_2\omega^2) \end{bmatrix} \begin{pmatrix} \delta \\ \theta_1 \\ \theta_2 \end{pmatrix} = \begin{pmatrix} 0 \\ 0 \\ 0 \end{pmatrix} \quad (6)$$

This is the Dynamic Stiffness Matrix equation for the structure with a crack carrying two bodies on either side of the crack. The roots of the determinant of the above matrix gives the square of the natural frequencies.

Consider the case of the roving bodies without any rotary inertia. Setting  $I_1 = I_2 = 0$ , the determinantal equation for the combined structure becomes:

$$D_{c,m} = \begin{vmatrix} (K_1 + K_4 - (m_1 + m_2)\omega^2) & K_2 & K_5 \\ (K_2 + K_5) & K_3 + k & -k \\ K_5 & -k & (K_6 + k) \end{vmatrix} \quad (7)$$

It may be seen that setting  $m_1 = 0$  and  $m_2 = m$  gives the same expression as setting  $m_2 = 0$  and  $m_1 = m$ . This means whether a roving mass without rotational inertia is on the left of the crack or the right of the crack, the natural frequencies and modes will not change. This is understandable as the crack model being used only permits a relative rotation between the two sides and the imposition of a translatory inertia (mass) immediately adjacent to a crack will have the same effect irrespective of which side it is located. This is not true, when it comes to placement of a rotary inertia, as can be seen from the following derivations.

For the case of  $I_1 = I, I_2 = 0$

$$|D_{c,m,I}| = |D_{c,m}| - I\omega^2 \begin{vmatrix} (K_1 + K_4 - (m_1 + m_2)\omega^2) & K_5 \\ K_5 & (K_6 + k) \end{vmatrix}$$

For the case of  $I_2 = I, I_1 = 0$

$$|D_{c,m,I}| = |D_{c,m}| - I\omega^2 \begin{vmatrix} (K_1 + K_4 - (m_1 + m_2)\omega^2) & K_2 \\ K_2 & (K_3 + k) \end{vmatrix}$$

The change in the expression for the determinant as the roving body passes through the determinant is given by:

$$\Delta D_{c,m,I} = I\omega^2 ((K_1 + K_4 - (m_1 + m_2)\omega^2)(K_6 - K_3)(K_5^2 - K_2^2)) \quad (8)$$

This means that the roots of the determinantal equation would change suddenly as the roving body passes the crack location, unless  $K_5 = K_2$  (or if  $K_5 = -K_2$  which may have no practical meaning) and  $K_6 = K_3$ . This special case would correspond to a crack being located at a point on an axis of structural symmetry. The loss of continuity in the measured frequency as can be seen in Eq.(8) depends mainly of the relative position of the crack which changes the dynamic values of the matrix; regarding to the magnification effect it can be noted from Eq.(8) its dependency of the inertial values of the roving mass.

The natural frequencies will, in general, change abruptly as a thin roving body possessing inertia passes a crack. It can be easily explained that this abrupt frequency shift will occur at each crack location allowing the crack location identification even for a multi-cracked structure.

### Concluding remarks

Using the Dynamic Stiffness Matrix method, it has been shown that the natural frequencies of a skeletal structure with a crack represented by a joint with rotational flexibility carrying a thin roving body possessing rotary inertia will change abruptly as the body passes a crack location. The discontinuity in the natural frequencies versus mass location could indicate a crack location and therefore could possibly be used as a method of damage identification. Numerical experiments show that the magnitude of the discontinuity in the frequency increases with increasing mode number which can be explained by the fact that the inertial moment that affects the vibration is proportional to the square of the frequency. It has also been noted that the shifts in the lower frequencies are relatively small and a cumulative frequency parameter based on the shifts in more than one mode may be a better indicator of the crack location compared to the shift in a single frequency value. Experimental work is required to test the feasibility of using this idea in practice.

### References

- [1] H. Ozturk, A. Yashar, and M. Sabuncu.: Dynamic stability of cracked multi-bay frame structures. *Mechanics of Advanced Materials and Structures*, vol. 23, pp. 715-726, 2016.
- [2] S. Chatzieleftheriou and N. D. Lagaros.: A trajectory method for vibration based damage identification of underdetermined problems. *Structural Control and Health Monitoring*, 2016.
- [3] M. S. Hossain, O. Z. Chao, Z. Ismail, S. Noroozi, and K. S. Yee. :Artificial Neural Networks for Vibration Based Inverse Parametric Identifications: A Review, *Applied Soft Computing*, 2016.
- [4] J. Lei, J. A. Lozano-Galant, M. Nogal, D. Xu, and J. Turmo.:Analysis of measurement and simulation errors in structural system identification by observability techniques. *Structural Control and Health Monitoring*, 2016.
- [5] M. Diaferio and V. Sepe.: Modal identification of damaged frames. *Structural Control and Health Monitoring*, vol. 23, pp. 82-102, 2016.
- [6] S. Zhong and S. O. Oyadiji.: Identification of cracks in beams with auxiliary mass spatial probing by stationary wavelet transform. *Journal of Vibration and Acoustics*, vol. 130, p. 041001, 2008.
- [7] S. Zhong and S. O. Oyadiji.: Analytical predictions of natural frequencies of cracked simply supported beams with a stationary roving mass. *Journal of Sound and Vibration*, vol. 311, pp. 328-352, 2008.
- [8] S. Zhong and S. O. Oyadiji.: Detection of cracks in simply-supported beams by continuous wavelet transform of reconstructed modal data. *Computers & structures*, vol. 89, pp. 127-148, 2011.
- [9] S. Zhong and S. O. Oyadiji.: Sampling interval sensitivity analysis for crack detection by stationary wavelet transform. *Structural Control and Health Monitoring*, vol. 20, pp. 45-69, 2013.

## Exact Strip Modelling and Vibration Based Identification of Damage in Plate Assemblies

**David Kennedy, Carol A. Featherston, Basem Suliman, Yulin Luo**

School of Engineering  
Cardiff University  
Queen's Buildings, The Parade, Cardiff CF24 3AA, United Kingdom  
[KennedyD, FeatherstonCA, SulimanBS, LuoY9]@cardiff.ac.uk

### Abstract

In the exact strip method, vibration modes of a prismatic plate assembly take the form

$$w(x, y, t) = \sum_m W_m(y) \exp(i\pi x / \lambda_m) \sin(\omega t) \quad (1)$$

where  $\omega$  is an undamped natural frequency,  $t$  is time,  $\lambda_m$  are a series of half-wavelengths of response in the longitudinal ( $x$ ) direction and the functions  $W_m(y)$  are obtained from exact solutions of the governing differential equations in the transverse ( $y$ ) direction. A single  $\lambda_m$  suffices for orthotropic plate assemblies with simply supported ends carrying no shear load [1]. Otherwise a series solution is required, the end conditions being modelled by point supports [2]. Natural frequencies are found by assembling a dynamic stiffness matrix which accounts exactly for the continuous distribution of mass, and applying the Wittrick-Williams algorithm [3].

Figure 1(a) shows a plate containing a through-the-length region of reduced stiffness, e.g. due to a reduction in thickness, a degradation in material properties or a delamination [4]. Figure 1(b) shows a plate with a longitudinal crack, which may be represented by a rotational spring by analogy with a cracked beam running in the  $y$  direction [5]. These types of damage can be modelled directly because the plate remains prismatic. The following sections outline methods to model the non-prismatic types of damage illustrated in Figures 1(c, d), as well as vibration-based methods to detect damage in plate assemblies.

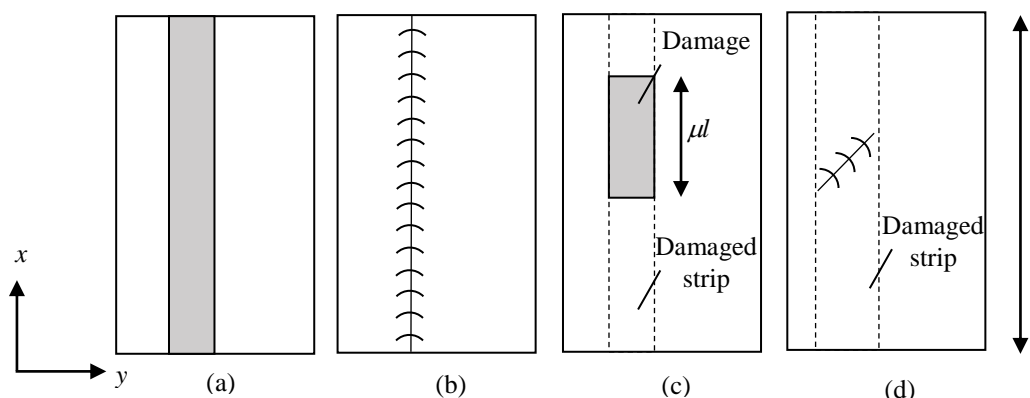


**Figure 1.** Plates containing (a) through-the-length region of reduced stiffness, (b) longitudinal crack, (c) embedded region of reduced stiffness, (d) crack of arbitrary length and alignment.

### Modelling embedded regions of reduced stiffness

A composite plate containing an embedded rectangular delamination, illustrated in Figure 1(c), has previously been modelled using a smearing method [6] in which the dynamic stiffness matrix of the damaged strip for half-wavelength  $\lambda_m$  is given by

$$\bar{\mathbf{K}}_m = \mathbf{K}_m - (\mathbf{K}_m - \mathbf{k}_m)(\mu + \mu') \quad (2)$$

where  $\mathbf{K}_m$  and  $\mathbf{k}_m$  are the dynamic stiffness matrices of its undamaged and damaged regions, respectively,  $\mu$  is the fraction of the length over which the damage occurs and  $\mu'$  is a correction term which allows for the longitudinal position of the damage. This method is computationally efficient and gives accurate results for natural frequencies, but because of the smearing it is unable to capture local effects in the vibration modes.

An alternative approach [7] is to couple a finite element model for the damaged strip with an exact strip model for the rest of the structure. The finite element model is not restricted to prismatic structures, and can therefore include elements of different thickness and material properties, e.g. to represent portions above and below a delamination. The two models are coupled by point constraints which ensure that the displacements and rotations of the finite element nodes along the longitudinal edges of the damaged strip match those in the exact strip model. Natural frequencies, found iteratively using the Wittrick-Williams algorithm, and the corresponding mode shapes agree well with those obtained by a commercial finite element code.

### Modelling cracks of arbitrary length and alignment

Plates containing cracks of arbitrary length and alignment, illustrated in Figure 1(d), may similarly be modelled by coupling a finite element model for the damaged strip with an exact strip model for the rest of the structure. Figure 2 shows a typical element through which the crack passes. The compliance of the rotational spring is resolved into components in the  $x$  and  $y$  directions acting at the mid-point  $(x_c, y_c)$  of the portion of the crack within the element, which are then apportioned to the four nodes of the element. Some numerical results will be presented at the Symposium and compared with those from a conventional finite element model.

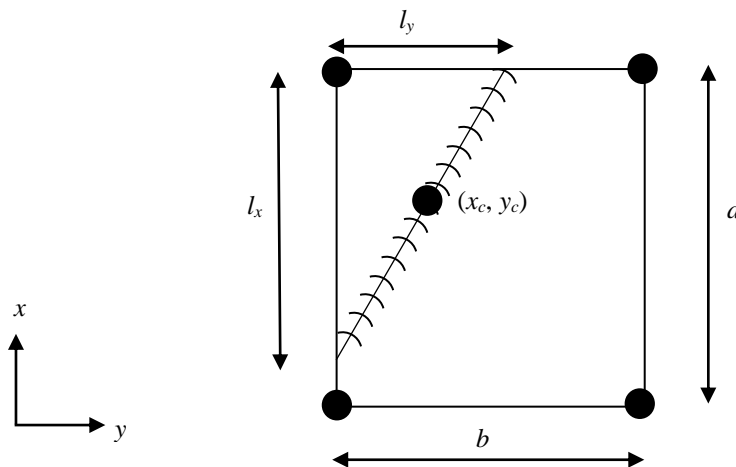


**Figure 2.** Finite element containing a crack of arbitrary length and alignment.

### Detection of damage in plate assemblies

Structural damage can be identified non-destructively by measuring changes in the natural frequencies which, unlike modal changes, do not require a scan of the whole structure. For a single occurrence of damage, normalisation of the natural frequency changes gives a damage vector  $\bar{\delta}$  which is independent of damage severity so that the location is found by solving an inverse problem. For frame structures this amounts to a one-dimensional search along each member, optionally allowing for noise in the natural frequency measurements [8].

For plate assemblies with a single occurrence of damage,  $\bar{\delta}$  is also independent of damage severity, e.g. the area of a delamination or the length and depth of a crack. The through-thickness position of a delamination affects the reduced stiffness  $\mathbf{k}_m$  in Equation (2), while the longitudinal position affects the correction term  $\mu'$ . Thus these are equivalent to size effects so that the transverse location can be found by a one-dimensional search across each plate. Similar arguments apply to cracks, suggesting that the damage can only be located uniquely in the transverse direction along with a generic description of its severity.

If there are multiple occurrences of damage, a multi-dimensional inverse problem must be solved. The search procedure can be adapted to decouple the severity and location effects, and some preliminary results will be presented at the Symposium.

### References

- [1] Wittrick, W.H.; Williams, F.W.: Buckling and vibration of anisotropic or isotropic plate assemblies under combined loadings. *International Journal of Mechanical Sciences*, Vol. 16, No. 4, pp. 209–239, 1974.
- [2] Anderson, M.S.; Williams, F.W.; Wright, C.J.: Buckling and vibration of any prismatic assembly of shear and compression loaded anisotropic plates with an arbitrary supporting structure. *International Journal of Mechanical Sciences*, Vol. 25, No. 8, pp. 585–596, 1983.
- [3] Wittrick, W.H.; Williams, F.W.: A general algorithm for computing natural frequencies of elastic structures. *Quarterly Journal of Mechanics and Applied Mathematics*, Vol. 24, Part 3, pp. 263–284, 1971.
- [4] Damghani, M.; Kennedy, D.; Featherston, C.A.: Critical buckling of delaminated composite plates using exact stiffness analysis. *Computers and Structures*, Vol. 89, Nos. 13–14, pp. 1286–1294, 2011.
- [5] Labib, A.; Kennedy, D.; Featherston, C.: Free vibration analysis of beams and frames with multiple cracks for damage detection. *Journal of Sound and Vibration*, Vol. 333, No. 20, pp. 4991–5003, 2014.
- [6] Damghani, M.; Kennedy, D.; Featherston, C.: Global buckling of composite plates containing rectangular delaminations using exact stiffness analysis and smearing method. *Computers and Structures*, Vol. 134, pp. 32–47, 2014.
- [7] Suliman, B.; Featherston, C.; Kennedy, D.: Vibration analysis of damaged plates by hybrid exact stiffness and finite element method. *Proceedings of 24th UK Conference of the Association for Computational Mechanics in Engineering*, Paper 87637, pp. 1–4, 2016.
- [8] Labib, A.; Kennedy, D.; Featherston, C.A.: Crack localisation in frames using natural frequency degradations. *Computers and Structures*, Vol. 157, pp. 51–59, 2015.

## A novel analytical method for highly efficient and accurate modal analysis of plates and plate assemblies with general boundary conditions

Xiang Liu\*, J. Ranjan Banerjee<sup>#</sup>

\* School of Traffic & Transportation Engineering  
Central South University  
Changsha, China  
xiangliu06@gmail.com

<sup>#</sup> School of Mathematics, Computer Science & Engineering  
City, University of London  
London, UK  
j.r.banerjee@city.ac.uk

### Abstract

The free vibration of plates is a historical problem for over two centuries which has given birth to many fundamental methods like the Rayleigh and the Ritz methods. This problem has also been a standard benchmark for many other analytical and numerical methods. However, the exact solutions for the problem are available only for Navier or Levy-type plates where at least one pair of opposite edges must be simply and/or guided supported. One method in this type is the dynamic stiffness method (DSM) which gives exact dynamic solutions within the whole frequency range of interest, which can be used as benchmark solutions for other methods. However, the DSM is seriously restricted to prismatic plate assemblies with the assumption that two opposite sides of each plate component must be simply supported, which prevents the DSM applications in a wider context. In order to remove the above restrictions and at the same time remain the merits (exactness and super efficiency) of the DSM, this paper will introduce a newly developed method called the spectral dynamic stiffness method (SDSM) [1–5] which accounts for both prismatic and non-prismatic plate assemblies with any arbitrary classical [1–3] and non-classical [4, 5] boundary conditions. The SDSM has been applied to modal analysis to give exact solutions within low, medium and high frequency ranges with remarkable computational efficiency. For instance, the SDSM exhibits two orders of magnitudes of improvement in computational efficiency over the conventional FEM. This superiority is much more pronounced at higher frequencies. The elegance and uncompromising accuracy of the SDSM provide a much wider appeal than the classical DSM.

In essence, the SDSM [1–5] combines the spectral (S) method and the classical dynamic stiffness method (DSM). One of the key points in the SDSM lies in adopting two sets of modified Fourier series. The adopted modified Fourier series for any arbitrary displacement or force boundary condition (denoted by  $h(\xi)$ ) along a plate edge (line node  $\xi \in [-L, L]$  in local coordinates of plate) is given by the following two sets of modified Fourier series

$$h(\xi) = \sum_{\substack{s \in \mathbb{N} \\ l \in \{0,1\}}} H_{ls} \frac{\mathcal{T}_l(\gamma_s \xi)}{\sqrt{\zeta_{ls} L}}, \quad H_{ls} = \int_{-L}^L h(\xi) \frac{\mathcal{T}_l(\gamma_s \xi)}{\sqrt{\zeta_{ls} L}} d\xi, \quad (1a)$$

$$h(\xi) = \sum_{\substack{s \in \mathbb{N} \\ l \in \{0,1\}}} H_{ls} \frac{\mathcal{T}_l^*(\gamma_s \xi)}{\sqrt{\zeta_{ls} L}}, \quad H_{ls} = \int_{-L}^L h(\xi) \frac{\mathcal{T}_l^*(\gamma_s \xi)}{\sqrt{\zeta_{ls} L}} d\xi, \quad (1b)$$

where  $\mathbb{N} = \{0, 1, 2, \dots\}$  is the non-negative integer set, and the subscript ‘ $l$ ’, taking value of either ‘0’ or ‘1’, denotes the corresponding symmetric or antisymmetric functions (and coefficients). Here,  $\zeta_{ls}$  is given as  $\zeta_{ls} = 2$  when  $l = 0, s = 0$  and otherwise  $\zeta_{ls} = 1$ . The corresponding modified Fourier basis functions  $\mathcal{T}_l(\gamma_s \xi)$  and  $\mathcal{T}_l^*(\gamma_s \xi)$  in Eq. (1) are defined as

$$\mathcal{T}_l(\gamma_s \xi) = \begin{cases} \cos(\frac{s\pi}{L} \xi) & l = 0 \\ \sin((s + \frac{1}{2})\frac{\pi}{L} \xi) & l = 1 \end{cases}, \quad \mathcal{T}_l^*(\gamma_s \xi) = \begin{cases} \sin(\frac{s\pi}{L} \xi) & l = 0 \\ \cos((s + \frac{1}{2})\frac{\pi}{L} \xi) & l = 1 \end{cases} \quad (2)$$

with  $\xi \in [-L, L], s \in \mathbb{N}$ . The above two sets of modified Fourier series provide complete and orthogonal sets to described any one-dimensional function  $h(\xi)$  of Eq. (1). Moreover, the above modified Fourier series has strong orthogonality which makes the SDSM numerically stable to compute results within any desired accuracy.

By using the above modified Fourier series, the general solution of the governing differential equation (GDE) for out-of-plane [2] and inplane [3] vibration of plate elements with arbitrary boundary conditions in the frequency domain can be achieved. In the next step, the SDS matrix for an element can be analytically formulated by substituting the above general solution into the general boundary conditions (BC) by algebraic manipulation.

Next, the analytically expressed spectral dynamic stiffness (SDS) matrix of elements can be assembled directly to model complex structures. The assembly procedure is similar to that of the finite element (FE) method with the exception that the FE elements are generally connected at point nodes whereas the SDS elements are connected on *line nodes*. Here the line nodes represent either the plate boundaries and/or the inter-element edges which have the flexibility to describe any arbitrary BC or continuity conditions (either classical [1–3] or non-classical [4, 5]). In general, for an assembly structure, the analytical SDSM formulation can be written in the form:  $\mathbf{f} = \mathbf{K}\mathbf{d}$ , where  $\mathbf{K}$  is the SDS matrix of the complete assembly structure, which relates the modified Fourier coefficient vector of the force  $\mathbf{f}$  to that of the displacement  $\mathbf{d}$  on all of the line nodes (boundaries and inter-element edges) of the assembly structure, so that

$$\mathbf{f} = [\mathbf{f}_1^T, \mathbf{f}_2^T, \dots, \mathbf{f}_i^T, \dots, \mathbf{f}_{N_{lDOF}}^T]^T, \quad \mathbf{d} = [\mathbf{d}_1^T, \mathbf{d}_2^T, \dots, \mathbf{d}_i^T, \dots, \mathbf{d}_{N_{lDOF}}^T]^T. \quad (3)$$

In Eq. (3), the subscript  $N_{lDOF}$  is the total number of *line degrees of freedom (line DOF)* of the plate assembly (Theoretically, each *line DOF* has infinite DOF since each BC function is a continuous function on  $\xi \in [-L, L]$ ). Here,  $N_{lDOF} = ln \times N_{DOF}$  where  $ln$  is the number of total *line nodes* of the plate assembly whereas  $N_{DOF}$  represents the number of *line DOF* of each line node (for instance, an individual rectangular Kirchhoff plate, being a special case of the assembly, has four edges, i.e.,  $ln = 4$  and each edge has two *line DOF*  $W$  and  $\phi$ , i.e.,  $N_{DOF} = 2$ ). Each force  $\mathbf{f}_i$  and displacement  $\mathbf{d}_i$  sub-vectors in Eq. (3) take the following form

$$\mathbf{f}_i = [F_{i00}, F_{i01}, F_{i02}, \dots, F_{i10}, F_{i11}, F_{i12}, \dots]^T, \quad (4a)$$

$$\mathbf{d}_i = [D_{i00}, D_{i01}, D_{i02}, \dots, D_{i10}, D_{i11}, D_{i12}, \dots]^T, \quad (4b)$$

where  $F_{ils}$  and  $D_{ils}$  ( $l \in \{0, 1\}, s \in \mathbb{N}$ ) are respectively the modified Fourier coefficients of the corresponding force  $f_i(\xi)$  and displacement  $d_i(\xi)$  BC (or CC) applied on the  $i$ th *line DOF* of the assembly, which are obtained by applying Eq. (1) onto  $f_i(\xi)$  and  $d_i(\xi)$  respectively to give

$$F_{ils} = \int_{-L}^L f_i(\xi) \frac{\mathcal{T}_l(\gamma_s \xi)}{\sqrt{\zeta_{ls} L}} d\xi, \quad D_{ils} = \int_{-L}^L d_i(\xi) \frac{\mathcal{T}_l(\gamma_s \xi)}{\sqrt{\zeta_{ls} L}} d\xi, \quad (5a)$$

$$\text{or } F_{ils} = \int_{-L}^L f_i(\xi) \frac{\mathcal{T}_l^*(\gamma_s \xi)}{\sqrt{\zeta_{ls} L}} d\xi, \quad D_{ils} = \int_{-L}^L d_i(\xi) \frac{\mathcal{T}_l^*(\gamma_s \xi)}{\sqrt{\zeta_{ls} L}} d\xi. \quad (5b)$$

Therefore, each term of either  $F_{ils}$  or  $D_{ils}$  in Eq. (5) represents a frequency-wavenumber dependent DOF (FWDOF) of the  $i$ th line DOF. In this way, the BC (or CC) can be arbitrarily prescribed along any line DOF, which are directly transformed through Eq. (5) into vector form (i.e.,  $\mathbf{f}_i$  and  $\mathbf{d}_i$ ) of Eq. (4) and eventually into  $\mathbf{f}$  and  $\mathbf{d}$  in Eq. (3).

In essence, the elegance of the SDSM lies in representing a dynamical system very accurately by using an extremely small number of DOF in an analytical and concise manner. This makes the SDSM superior to other numerical or analytical methods in terms of both accuracy and computational efficiency within low, medium and high frequency ranges. The merits of the SDSM are exploited by the application of the well-known Wittrick-Williams (WW) algorithm which is further enhanced by some techniques described as follows. According to the WW algorithm, as the frequency parameter  $\omega$  is increased from zero to  $\omega^*$ , the number of natural frequencies passed ( $J$ ) is given by

$$J = J_0 + s\{\mathbf{K}_f\}, \quad (6)$$

where  $s\{\mathbf{K}_f\}$  corresponds to the negative inertia of the final SDS matrix  $\mathbf{K}_f$  evaluated at  $\omega = \omega^*$ ; and  $J_0$  is given by

$$J_0 = \sum_m J_{0m}, \quad \text{where} \quad J_{0m} = J_{Sm} - s(\mathbf{K}_{Sm}), \quad (7)$$

where  $J_{0m}$  is the number of natural frequencies between  $\omega = 0$  and  $\omega = \omega^*$  for an individual component member when its boundaries are fully clamped. A strategy described in [1–3] is adopted here to provide an efficient and reliable prediction for the above  $J_{0m}$  which is based on the closed-form solution of each members subject to full simple supports. Therefore,  $J_{0m}$  of Eq. (7) can be obtained by applying the WW algorithm in reverse to give  $J_{0m} = J_{Sm} - s(\mathbf{K}_{Sm})$ , where  $J_{Sm}$  is the overall mode count of a certain member with all boundaries subject to simple supports, and  $s(\mathbf{K}_{Sm})$  is the sign count of its formulated SDS matrix  $\mathbf{K}_{Sm}$ . First, the computation of  $J_{Sm}$  in Eq. (7) is accomplished in an analytical manner by solving a number theory problem. Next, the computation of  $s(\mathbf{K}_{Sm})$  in Eq. (7) is achieved in an elegant way by taking advantage of the mixed-variable formulation. The above two techniques of computing  $J_{Sm}$  and  $s(\mathbf{K}_{Sm})$  resolves with conclusive certainty the problem of determining  $J_0$  in a highly efficient, accurate and reliable manner.

## References

- [1] Liu, X. and Banerjee, J. R. Free vibration analysis for plates with arbitrary boundary conditions using a novel spectral-dynamic stiffness method, *Comput. Struct.*, **164**, 108–126, (2016).
- [2] Liu, X. and Banerjee, J. R. An exact spectral-dynamic stiffness method for free flexural vibration analysis of orthotropic composite plate assemblies - Part I: Theory, *Compos. Struct.*, **132**, 1274–1287, (2015).
- [3] Liu, X. and Banerjee, J. R. A spectral dynamic stiffness method for free vibration analysis of plane elastodynamic problems, *Mech. Syst. Signal Process.*, **87**, 136–160, (2017).
- [4] Liu, X., Kassem, H. I. and Banerjee, J. R. An exact spectral dynamic stiffness theory for composite plate-like structures with arbitrary non-uniform elastic supports, mass attachments and coupling constraints, *Compos. Struct.*, **142**, 140–154, (2016).
- [5] Liu, X. Spectral dynamic stiffness formulation for inplane modal analysis of composite plate assemblies and prismatic solids with arbitrary classical/nonclassical boundary conditions, *Compos. Struct.*, **158**, 262–280, (2016).

## Wave propagation in resonant structural metamaterials: continuum and discrete models

**Brian R Mace, Yi Yang, Michael J Kingan**

Department of Mechanical Engineering  
University of Auckland

Private Bag 92019, Auckland 1142, New Zealand

[b.mace@auckland.ac.nz](mailto:b.mace@auckland.ac.nz), [yyan823@aucklanduni.ac.nz](mailto:yyan823@aucklanduni.ac.nz), [m.kingan@auckland.ac.nz](mailto:m.kingan@auckland.ac.nz)

### Abstract

There has recently been significant interest in the vibrational behaviour of continuous structures with attached resonators [1]. In many cases the resonators form periodic arrays. Periodic structures are known to have interesting pass/stop band behaviour. When the dimensions of the periodic cell are comparable to or larger than the wavelength in the continuous structure this is due to Bragg scattering. The resonators introduce the possibility of stop bands around the resonator frequency, which can be tuned to lie in the sub-Bragg frequency range, i.e. when the length of the periodic cell is small compared to the wavelength of the host structure: this is of particular interest in mechanical vibrations where the relevant wavelengths are often quite large. However, as will be seen below, periodicity is not required for this behaviour to occur.

In this paper a general continuum model is developed. The periodic system comprises a uniform thin plate with a 2-dimensional periodic array of point resonators as shown in Figure 1(a). For long wavelength behaviour the system approximates the continuous structure with a limp mass layer attached elastically to the host structure (Figure 1(b)). The pass/stop band characteristics of the continuum model are discussed. An analytical solution using periodic structure theory for plates lying on a 2-dimensional periodic array of point supports [2] is then extended to the system of Figure 1(a). The asymptotic, low frequency (sub-Bragg) limit gives results identical to the continuum model: it is perhaps easier, however, to interpret the underlying behaviour in terms of the continuum model, where periodicity is non-existent.

### Continuum model

The periodic array of resonators in Figure 1(a) are attached at spacings  $L_x$  and  $L_y$  in the  $(x,y)$  directions respectively. The mass and stiffness of each resonator are  $m_r$  and  $k_r$  respectively, so that they have a resonant frequency  $\omega_0 = \sqrt{k_r/m_r}$ . Such a periodic structure has a stop band located at and around  $\omega_0$ , which can be tuned to lie much below the first Bragg band. Now consider the system shown in Figure 1(b), comprising the same host structure to which is attached a limp, layer of mass  $\sigma_2$  per unit area through an elastic connection of stiffness  $\kappa$  per

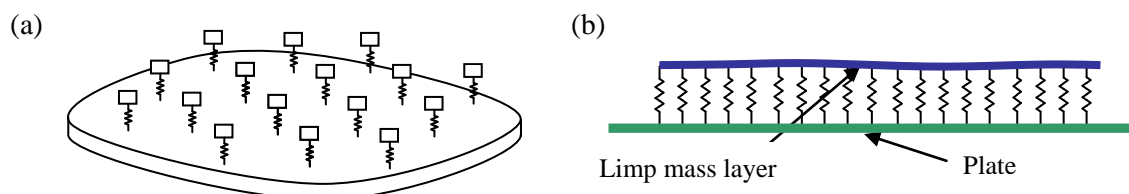


**Figure 1.** Infinite plate with (a) periodic resonators and (b) connected limp mass layer.

unit area. This continuum model is an approximation for the periodic system when the wavelength  $\lambda$  of free wave propagation in the host structure is large compared to the resonator spacing. The low-frequency assumption, when the discrete system can be modelled by the continuous system in Figure 1(b), is valid if  $\lambda \gg \max(L_x, L_y)$ ,  $m_r = \sigma_2 L_x L_y$  and  $k_r = \kappa L_x L_y$ .

Suppose the host structure is a thin plate. The equations of free undamped motion are

$$D \left( \frac{\partial^2}{\partial x^2} + \frac{\partial^2}{\partial y^2} \right)^2 w_1 + \sigma_1 \frac{\partial^2 w_1}{\partial t^2} + \kappa (w_1 - w_2) = 0; \quad \sigma_2 \frac{\partial^2 w_2}{\partial t^2} + \kappa (w_2 - w_1) = 0 \quad (1)$$

where  $w_1$  and  $w_2$  are the displacements of the two layers, and  $\sigma_1$  and  $D$  its mass per unit area and bending stiffness. Time harmonic waves at frequency  $\omega$  and wavenumber  $k$  propagate if

$$Dk^4 (\kappa - \sigma_2 \omega^2) + \sigma_1 \sigma_2 \omega^4 - \kappa (\sigma_1 + \sigma_2) \omega^2 = 0 \quad (2)$$

Introducing

$$\mu = \frac{\sigma_2}{\sigma_1}; \quad \omega_0^2 = \frac{\kappa}{\sigma_2}; \quad k_0^4 = \frac{\sigma_1 \omega^2}{D}; \quad \Omega = \frac{\omega}{\omega_0}; \quad K = \frac{k}{k_0} \quad (3)$$

with  $\mu$  and  $k_0$  being the mass ratio and the wavenumber in the plate, leads to

$$K^4 = \frac{1 + \mu - \Omega^2}{1 - \Omega^2} = 1 + \frac{\mu}{1 - \Omega^2} \quad (4)$$

### Discrete model

An infinite, 2-dimensionally periodically point-supported plate was considered in [2]. If the point supports apply only a translational constraint then free waves propagate if

$$1 - \sum_{m=-\infty}^{\infty} \sum_{n=-\infty}^{\infty} \frac{1}{\left[ a(2m\pi + \mu_x)^2 + (2n\pi + \mu_y)^2 / a \right]^2 - \bar{\Omega}^2} \bar{K}_T = 0 \quad (5)$$

where  $\mu_{x,y} = k_{x,y} L_{x,y}$  are the propagation constants in the  $(x,y)$  directions,  $k_{x,y}$  being the wavenumber components and

$$\bar{\Omega} = \sqrt{\frac{\sigma_1}{D} L_x L_y} \omega; \quad a = \frac{L_y}{L_x}; \quad \bar{K}_T = \frac{L_x L_y}{D} \left( \frac{k_r m_r \omega^2}{k_r - m_r \omega^2} \right) \quad (6)$$

where the last term is the negative of the effective dynamic stiffness of the spring mass attachment. Free waves comprise a series of space harmonics, with the  $(m,n)$ 'th term in the sum in Eq (5) representing the  $(m,n)$ 'th harmonic. At low frequencies, i.e. in the sub-Bragg frequency region, the  $(0,0)$  harmonic is largest and dominates the sum. Neglecting the other terms, as frequency tends to zero, free waves propagate if

$$(L_x L_y)^2 k^4 = \bar{\Omega}^2 + \bar{K}_T = \frac{\sigma_1 L_x^2 L_y^2}{D} \omega^2 + \frac{L_x L_y}{D} \left( \frac{k_r m_r \omega^2}{k_r - m_r \omega^2} \right); \quad k^4 = (k_x^2 + k_y^2)^2 \quad (7)$$

Note that these waves propagate in any direction with the same wavenumber  $k$ . Noting now that  $m_r = \sigma_2 L_x L_y$ ,  $k_r = \kappa L_x L_y$  and  $\omega_0^2 = \kappa / \sigma_2 = k_r / m_r$ , Equation (7) reduces to Equation (4).

**Examples**

Figure 2 shows the positive-real and negative-imaginary solutions for  $K$  (from equation (4)) for various values of mass ratio  $\mu$ . At low frequency ( $\Omega^2 \ll 1$ ),  $K^4 \approx 1 + \mu$  and the wavenumbers approximate those of a plate with a mass per unit area  $(\sigma_1 + \sigma_2)$ . There is a pair of propagating waves ( $k$  real) and a pair of evanescent waves ( $k$  imaginary), as there is at high frequencies ( $\Omega^2 \gg 1 + \mu$ ). The dynamic stiffness of the attached layer thus varies from being mass-like below resonance to stiffness-like above resonance. There is a stop band in the range between  $\omega = \omega_0$  and  $\omega = \sqrt{1 + \mu} \omega_0$ . In this frequency range the solutions to the dispersion equation are complex and of the form  $k(\pm 1 \pm i) / \sqrt{2}$ . The width of the stop band is  $\sqrt{1 + \mu} - 1$ .

**Concluding remarks**

The resonant layer or periodically attached resonators introduce a stop band between the resonator frequency  $\omega_0$  and  $\sqrt{1 + \mu} \omega_0$ . The bandwidth depends on the mass ratio  $\mu$ , and for small  $\mu$  approximates  $\mu/2$ . Note that periodicity is not relevant in the sub-Bragg region. Departure from periodicity makes no difference as long as it is small enough to avoid significant back-scattering. Irrespective of the physical design of the resonators, and many designs have been suggested, the behaviour is determined by their effective mass and stiffness, which together define the tuned frequency  $\omega_0$  and the mass ratio  $\mu$ , which determines the bandwidth.

**References**

- [1] Hussein, M. I.; Leamy, M. J.; Ruzzene, M.: Dynamics of Phononic Materials and Structures: Historical Origins, Recent Progress and Future Outlook. Applied Mechanics Reviews 66(4), (38 pages) Paper No: AMR-13-1027; doi: 10.1115/1.4026911, 2014.
- [2] Mace, B. R.: The vibrations of plates on two-dimensionally periodic point supports. Journal of Sound and Vibration, Vol. 192, No3, pp.629-642, 1996.

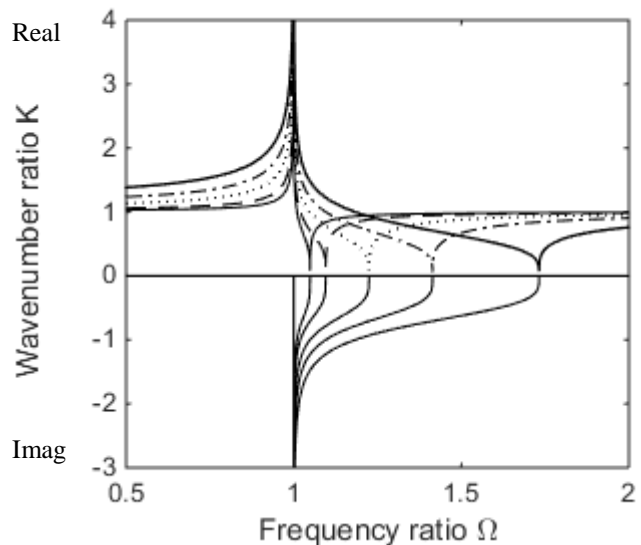


**Figure 2.** Positive real and negative imaginary parts of the wavenumber ratio  $K$ ;  $\mu = 0.1$  (—),  $0.2$  (---),  $0.5$  (···),  $1$  (-·-·-),  $2$  (— — —).

## Stability of in-plane vibration of an elastically supported rotating thin ring, revisited

Tao Lu, Apostolos Tsouvalas, Andrei V. Metrikine

Faculty of Civil Engineering and Geosciences  
Delft University of Technology  
Stevinweg 1, 2628 CN Delft, The Netherlands

### Abstract

Stability of the in-plane free vibration of a rotating thin ring elastically mounted to an immovable axis is revisited in this study. We aim to demonstrate theoretically that the ring can be unstable in contrast to a commonly accepted belief that the instability cannot occur [1].

The inner surface of the ring is assumed to be connected to an immovable axis by means of distributed radial and circumferential springs with stiffness (per unit length)  $k_r$  and  $k_c$ . The outer surface is stress-free.

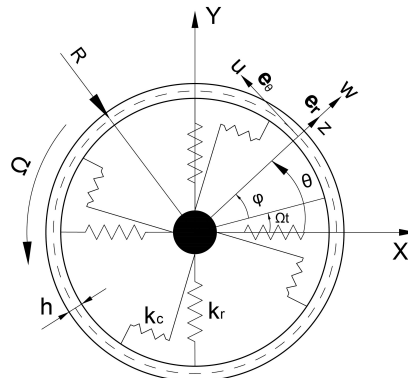


**Figure 1.** A rotating thin ring on an elastic foundation.

The ring parameters and coordinate systems are defined in Figure 1. A space-fixed coordinate system  $(r, \theta)$  is employed. An auxiliary coordinate  $z$  is introduced as  $z = r - R$ . Other parameters, which are not shown in Figure 1, are:  $b$  the width;  $E$  the Young's modulus;  $\rho$  the mass density;  $A$  the area and  $I$  the cross-sectional moment of inertia of the ring. It is assumed that the radial and circumferential displacements  $w(z, \theta, t)$  and  $u(z, \theta, t)$  of a differential element on the ring are defined by

$$\begin{aligned} w(z, \theta, t) &= w_0(\theta, t) + z w_1(\theta, t) + z^2 w_2(\theta, t), \\ u(z, \theta, t) &= u_0(\theta, t) \end{aligned} \quad (1)$$

where  $w_0(\theta, t)$  and  $u_0(\theta, t)$  are the radial and circumferential displacements of the middle surface, respectively;  $w_1(\theta, t)$  and  $w_2(\theta, t)$  are the higher order corrections of the radial displacement. These corrections enable us to take a linear distribution of the through-thickness variation of the radial stress into account. The radial stress at the inner surface of the ring is not zero because of the presence of the radial springs. If the stiffness of the radial springs is large enough, the radial stress at the inner surface cannot be neglected. Thin rings are considered,

thus, the transverse shear deformation and rotatory inertia are not incorporated in the formulation of the governing equations.

The boundary conditions for the inner and outer surfaces of the ring must be satisfied. The material of the ring is considered to be linearly elastic. For the outer surface of the ring, the radial stress should be zero, which implies that

$$\sigma_r \Big|_{h/2} = E\varepsilon_r \Big|_{h/2} = E(w_1 + hw_2) = 0. \quad (2)$$

The inner surface is connected to the springs, thus

$$b\sigma_r \Big|_{-h/2} = Eb\varepsilon_r \Big|_{-h/2} = Eb(w_1 - hw_2) = k_r w \Big|_{-h/2}. \quad (3)$$

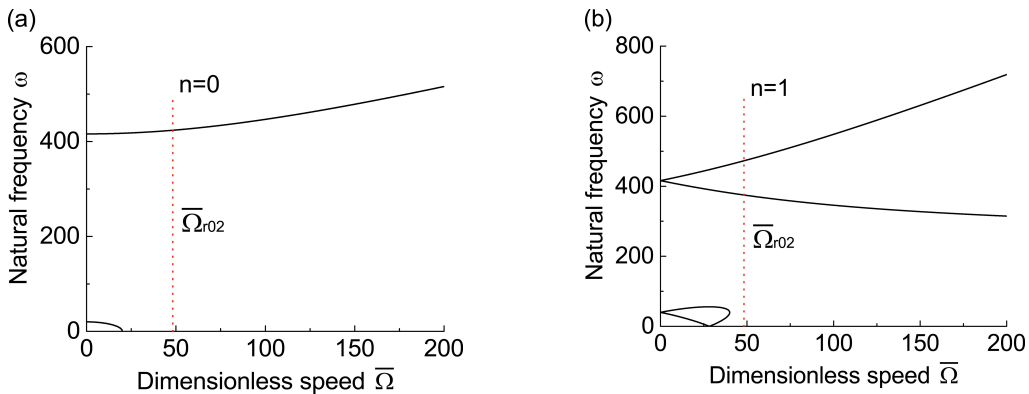
Combining Eqs. (2) and (3),  $w_1(\theta, t)$  and  $w_2(\theta, t)$  can be expressed in terms of  $w_0(\theta, t)$ . To account for the rotation-induced hoop tension, the same nonlinear strain-displacement relation as in Ref. [2] is applied. Using the Hamilton's principle, the nonlinear equations which govern the radial and circumferential motions of the ring are derived in a space-fixed reference system. The linearised governing equations are obtained about the axisymmetric static equilibrium. The latter is derived from the governing equation in the radial direction. Details of the derivations can be found in [3].

To analyse the problem, it is convenient to introduce the following dimensionless parameters and variables

$$t_0^2 = \rho AR^4 / (EI), \tau = t / t_0, \bar{\Omega} = \Omega t_0, \chi = EAR^2 / (EI), \bar{K}_r = k_r R^4 / (EI), \bar{K} = k_c / k_r. \quad (4)$$

Since the radial expansion of the ring grows with the increasing rotational speed, there should be an upper limit of the rotational speed above which the prestresses due to rotation may exceed the allowable strength of the materials. There are two kinds of prestresses which should be examined beforehand. These are: the maximum hoop stress which occurs at the outer surface of the ring and the maximum radial prestress which appears at the inner surface of the ring. To avoid a discussion of the physical behaviour of different materials, the maximum prestress  $\sigma_{\max}^0 \leq 0.2E$  is chosen to define the regime in which the ring material is assumed to behave linearly.

To illustrate that instability can occur prior to material failure, the following dimensionless parameters are chosen:  $\chi = 1200, \bar{K}_r = 4 \times 10^5, \bar{K} = 0.001$ . These parameters correspond to a thin ring with small bending stiffness and stiff foundation.



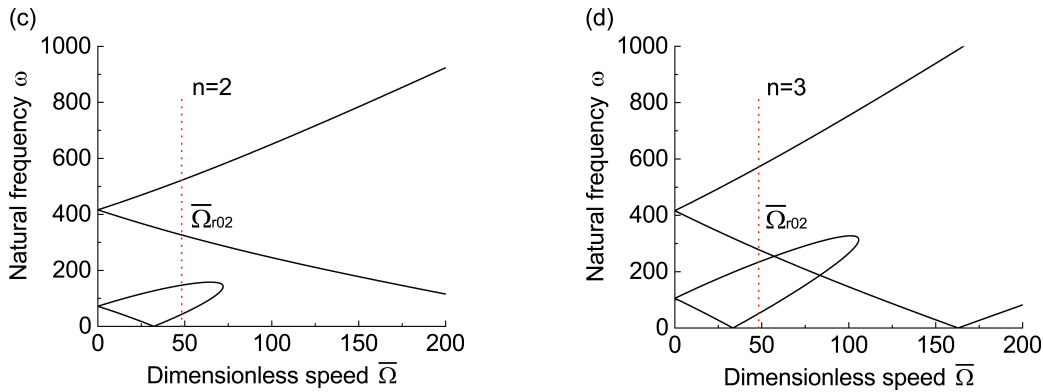


**Figure 2.** Dimensionless natural frequencies versus rotational speeds.

Fig. 2 illustrates the relationship between the rotational speed and the natural frequencies of the first four modes in the space-fixed reference system. We count the modes starting from  $n=0$ , the latter implying an angle-independent deformation. Note that in this mode the rotating ring can and does deform elastically. The vertical dotted line in Fig.2 corresponds to the speed which is determined by  $\sigma_{\max}^0 = 0.2E$ . For mode numbers greater than zero, both the lower and higher natural frequencies split into two branches which result in four distinct natural frequencies per mode. However, for the  $n=0$  modes, the natural frequencies do not bifurcate. The upper branch of the  $n=0$  mode increases monotonically as the speed of rotation grows. The lower branch first descends and then crosses the horizontal axis at a certain rotational speed. It can be shown that above this speed, the natural frequency becomes purely imaginary which indicates the onset of instability of the divergence type. The ring displacement increases exponentially in time in the circumferential direction. For modes  $n \geq 1$  one can see that the lower set of natural frequencies first branches into two curves at  $\bar{\Omega} > 0$ , then the two collide with each other and disappear from the real plane (become complex-valued) after a certain speed. Since the characteristic polynomial has real-valued coefficients, the complex roots appear in conjugate pairs and one may say that flutter occurs after the collision speed. The lowest speed at which instability occurs is for the mode  $n=0$ . Divergence instability of the 0th mode always occurs before flutter could happen.

## References

- [1] Endo, M.; Hatamura, K.; Sakata, M.; Taniguchi, O.: Flexural vibration of a thin rotating ring. *Journal of Sound and Vibration*, Vol. 92, No. 2, pp. 261–272, 1984.
- [2] Cooley, C.G.; Parker, R.G.: Vibration of high-speed rotating rings coupled to space-fixed stiffnesses. *Journal of Sound and Vibration*, Vol. 333, No. 12, pp. 2631–2648, 2014.
- [3] Lu, T.; Tsouvalas, A.; Metrikine, A.V.: The in-plane free vibration of an elastically supported thin ring rotating at high speeds revisited. *Journal of Sound and Vibration*, Vol. 402, pp. 203–218, 2017.

## Vibration Localization of Imperfect Circular Cylindrical Shells

Francesco Pellicano<sup>\*</sup>, Antonio Zippo<sup>\*</sup>, Marco Barbieri<sup>\*</sup>, Matteo Strozzi<sup>#</sup>

<sup>\*</sup> Department of Engineering  
“Enzo Ferrari”,  
University of Modena and  
Reggio Emilia, Modena, Italy  
francesco.pellicano@unimore.it

<sup>#</sup> Department of Industrial  
Engineering,  
University of Bologna  
matteo.strozzi@unimore.it

### Abstract

The goal of the present paper is the analysis of the effect of geometric imperfections in circular cylindrical shells. Perfect circular shells are characterized by the presence of double shell-like modes, i.e., modes having the same frequency with modal shape shifted of a quarter of wavelength in the circumferential direction. In the presence of geometric imperfections, the double natural frequencies split into a pair of distinct frequencies, and the splitting is proportional to the level of imperfection. In some cases, the imperfections cause an interesting phenomenon on the modal shapes, which present a strong localization in the circumferential direction. This study is carried out by means of a semi-analytical approach compared with standard finite element analyses.

### 1. Introduction

Circular cylindrical shells have been proven to be sensitive to initial geometric imperfections. Kubenko and Koval’chuk [1] reviewed many studies on the influence of the initial imperfections on the natural frequencies and mode shapes of elastic shells. They analysed the splitting of the natural frequencies of two conjugate modes as a measure of the initial geometric imperfections imposed. Katawala and Nash [2] studied the influence of the initial geometric imperfections on the vibrations of thin circular cylindrical shells. They found that the natural frequency of the imperfect modes increases with the increase in the amplitude of imperfection on the modal shape. However, the effect of imperfections on mode shapes appears not yet well understood, in particular localization phenomena have been not evidenced in the past.

In the present paper, the linear vibrations and modal localization in circular cylindrical shells are analysed in the framework of the Sanders-Koiter theory (see e.g. [3, 4]). The shell deformation is described in terms of longitudinal, circumferential and radial displacement fields. Clamped-clamped boundary conditions are investigated. The three displacement fields are expanded by means of a double mixed series based on Chebyshev polynomials for the longitudinal variable and harmonic functions for the circumferential variable; the Rayleigh-Ritz method is used to get approximated natural frequencies (eigenvalues) and mode shapes (eigenfunctions). The three displacement fields are re-expanded by using the previous approximated eigenfunctions; conjugate mode shapes are used; geometric imperfections are imposed on the modes in order to investigate the modal localization of the shells.

The semi-analytical approach proposed in the paper is validated in linear field by means of comparisons with finite element analyses.

### 2. Shell theory

In Figure 1, a circular cylindrical shell having radius  $R$ , length  $L$  and thickness  $h$  is represented; a cylindrical coordinate system  $(0; x, \theta, z)$  is considered to take advantage of the axial

symmetry; the origin 0 of the reference system is located at the centre of one end of the shell. Three displacement fields are represented by: longitudinal  $u(x, \theta, t)$ , circumferential  $v(x, \theta, t)$  and radial  $w(x, \theta, t)$ .

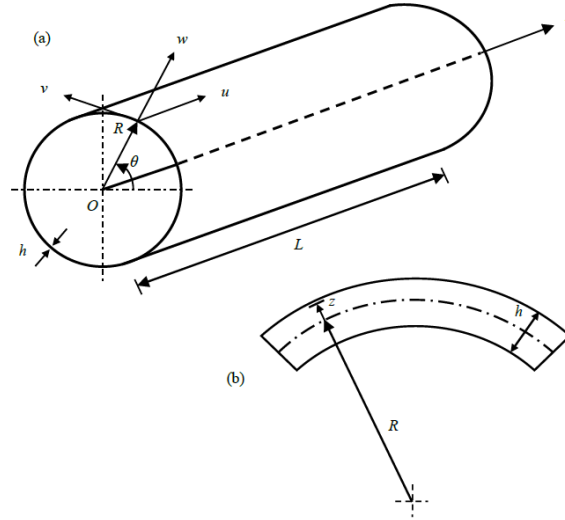


**Figure 1:** Geometry of the functionally graded shell. (a) Complete shell; (b) cross-section of the shell surface.

The Sanders-Koiter shell theory is based on the Love’s first approximation [3, 4]. The strain components  $(\epsilon_x, \epsilon_\theta, \gamma_{x\theta})$  are related to the middle surface strains  $(\epsilon_{x,0}, \epsilon_{\theta,0}, \gamma_{x\theta,0})$  and to the changes in curvature and torsion  $(k_x, k_\theta, k_{x\theta})$  of the middle surface of the shell by the following relationships [3,4]. Isotropic shells are considered.

The elastic strain energy and the kinetic energy of a cylindrical shell are given by [3,4]

$$U_s = \frac{1}{2} LR \int_0^{2\pi} \int_{-h/2}^{h/2} (\sigma_x \epsilon_x + \sigma_\theta \epsilon_\theta + \tau_{x\theta} \gamma_{x\theta}) d\eta d\theta dz \quad T_s = \frac{1}{2} \rho h LR \int_0^{2\pi} \int_0^L (\dot{u}^2 + \dot{v}^2 + \dot{w}^2) d\eta d\theta \quad (4)$$

where  $h, R$  and  $L$  are the thickness, radius and length of the shell, respectively.

*Discretization approach*

In order to carry out the linear analysis of the shell, a two-step procedure is applied [3, 4]: i) the three displacement fields are expanded using a double mixed series and the Rayleigh-Ritz method is applied to obtain approximated eigenfunctions; ii) the displacement fields are re-expanded by using the approximated eigenfunctions and modal geometric imperfections are imposed on the modes.

**3. Numerical results**

The mechanical properties of the circular cylindrical shell considered are reported in Table 1; these data are referred to a PET shell, which are generally used for our lab experiments. In order to validate the semi-analytical approach proposed in this

Table 1: Mechanical parameters of the clamped-clamped circular cylindrical shell.

Young’s modulus E [GPa]	27.58
Poisson’s ratio $\nu$	0.42
Mass density $\rho$ [kg/m <sup>3</sup> ]	1541
Thickness h [mm]	0.25
Radius R [mm]	43.65
Length L [mm]	95.50

Table 2: Natural frequencies of the clamped-clamped circular cylindrical shell of Table 1. Comparisons between Sanders-Koiter shell theory (SKT) and finite element method (FEM).

Mode (j,n)	Natural frequency (Hz)		Difference %
	SKT	FEM	
(1,7)	1850.49	1834.56	0.86
(1,6)	1850.97	1828.80	1.20
(1,12)	4099.48	4087.13	0.30
(1,0)	15303.9	15315.8	0.08

paper, the natural frequencies of the clamped-clamped cylindrical shell of Table 1 obtained by applying the Sanders-Koiter theory are compared with those obtained by FE analyses, see Table 2. These comparisons show that the present semi-analytical method gives results close to the FEM, the differences being less than 2%.

The analysis is carried out considering a clamped clamped shell with small geometric modal imperfections (modes (1,6) and (1,7)) having magnitude  $20\%h$ ; Figure 2 shows the effect of imperfections on modes (1,6) and (1,7,c), where “c” means the “conjugate mode”, a macroscopic localization on mode (1,6) and a slight asymmetry on mode (1,7c) are visible. Results are compared with FEM analyses, see also Table 2. The localization appears when the imperfection is a combination of two distinct modes and the magnitude exceeds the threshold of 10%. Indeed, if the imperfection is considered on mode (1,6) (or (1,7)) only, no localization appears, even if the imperfection magnitude is greatly increased. Moreover, the boundary conditions play a role, e.g. free-free shells do not display localization.

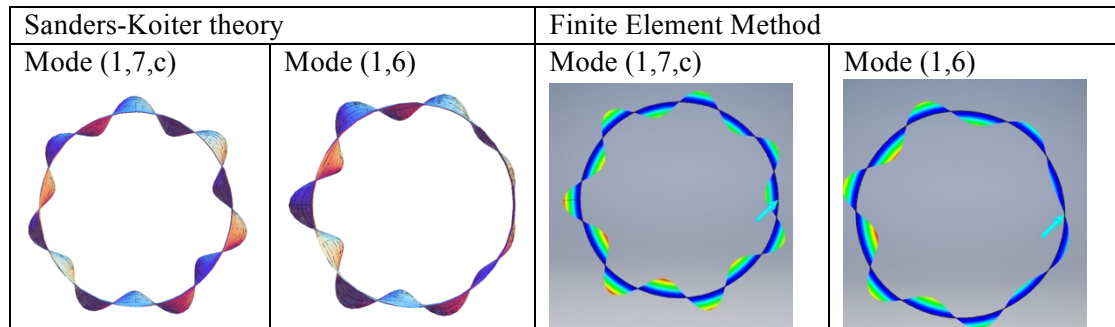


Figure 2: Geometric imperfections  $wp(1,6)=wp(1,7)=0.2h$ ,  $wp(1,6,c)=wp(1,7,c)=0$ . Localization.

#### 4. Conclusions

In this paper, the effect of the geometric imperfections on the modal shapes of cylindrical shells is analysed. The Sanders-Koiter shell theory is used. The shell deformation is described in terms of longitudinal, circumferential and radial displacement fields. Clamped-clamped boundary conditions are applied. Geometric imperfections are imposed to investigate the modal localization of the shells.

The semi-analytical approach proposed in this paper is validated in linear field by means of comparisons with finite element analyses.

It is found that small initial geometric imperfections imposed on single modes or conjugate pairs of modes gives no localization on the modal shape. Conversely, it is seen that small initial geometric imperfections imposed on two non-conjugate modes give modal localization on all the modes; this localization is maximum on the modal shape corresponding to the initial modal imperfection.

#### References

- [1] Kubenko, V.D., Koval'chuk, P.S., Influence of initial geometric imperfections on the vibrations and dynamic stability of elastic shells, *Int. Appl. Mech.*, 40 (8), 847-877, (2004).
- [2] Watawala, L., Nash, W.A., Influence of initial geometric imperfections on the vibrations of thin circular cylindrical shells, *Comp. & Struct.* 16 (1), 125-130, (1983).
- [3] Strozzi, M., Pellicano, F., Nonlinear vibrations of functionally graded cylindrical shells, *Thin-Walled Struct.*, 67, 63-77, (2013). ISSN: 0263-8231.
- [4] Pellicano, F., Dynamic stability and sensitivity to geometric imperfections of strongly compressed circular cylindrical shells under dynamic axial loads, *Comm. on Nonlin. Sciences and Num. Sim.*, 14, 3449-3462, (2009). ISSN: 1007-5704.

## Numerical method to calculate 1D impact problems by approximating the geometry with piecewise constant cross sections and applying d'Alembert's solution

Jens Burgert\*, Wolfgang Seemann<sup>#</sup>

\* Institute for Dynamics/Mechatronics  
Karlsruhe Institute of Technology  
Kaiserstraße 10, 76131 Karlsruhe, Germany  
jens.burgert@kit.edu

<sup>#</sup> Institute for Dynamics/Mechatronics  
Karlsruhe Institute of Technology  
Kaiserstraße 10, 76131 Karlsruhe, Germany  
wolfgang.seemann@kit.edu

### Abstract

Impacting rods are used in various devices in practical life but also for scientific experiments. The typical arrangement is a primary rod with a tool at the end contacting the process material and a free tip, onto which a piston rod is hitting with a given kinetic energy. The hit is followed by a complicated sequence of phenomena. A stress wave starts to propagate along the primary rod to finally reach the tool-process material interface. It is of interest to determine and adjust the stress wave propagating along the rod. Since it is a well-known fact that the cross-sectional profile of the piston rod is shaping the stress wave profile, the idea is to adjust the geometrical form of the impacting piston for an optimized shape of the stress wave. The results can be applied in the field of rock drilling for instance, where researchers revealed, that the efficiency of the drilling process strongly depends on the shape of the longitudinal wave transmitted through the drill rod to the drill bit.

To model 1D impact problems the impacting bodies are described mathematically by the partial differential equation for the displacement  $u_i(x, t)$  as follows

$$\frac{\partial}{\partial x} \left[ EA_i(x) \frac{\partial u_i}{\partial x} \right] = \rho A(x) \frac{\partial^2 u_i}{\partial t^2}, \quad i = 1, 2 \quad (1)$$

with Young's modulus  $E$ , mass density  $\rho$  and area of cross-section  $A(x)$ . For a constant cross-section and for constant material properties the governing equation for each body simplifies to the well-known 1D wave equation

$$\frac{\partial^2 u_i}{\partial t^2} - c_{0i}^2 \frac{\partial^2 u_i}{\partial x^2} = 0, \quad c_{0i} = \sqrt{\frac{E_i}{\rho_i}}, \quad i = 1, 2 \quad (2)$$

with wave propagation speed  $c_0$ . The related solution is given by the d'Alembert solution

$$u(x, t) = f(x - c_0 t) + g(x + c_0 t) \quad (3)$$

with  $f$  and  $g$  being arbitrary functions. The impact between these two bodies leads to the following transition conditions at the contact zone

$$u_1(0, t) = u_2(0, t), \quad (4)$$

$$E_1 A_1 \frac{\partial u_1}{\partial x}(0, t) = E_2 A_2 \frac{\partial u_2}{\partial x}(0, t) \quad (5)$$

assuming that the force between the two bodies is a compressional force and that the spatial coordinate of the impact zone is  $x = 0$ . For an impact between two bodies with constant cross-section

this results in a textbook problem, the solution of which can be seen e.g. in [2]. For non-uniform impacting partners analytical solutions of the differential equations only exist for special shapes of the cross-section. The solutions are obtained by applying the exponential approach

$$u(x,t) = a(x)e^{i(kx-\omega t)} \quad (6)$$

where  $a(x)$  is the wave amplitude and  $k$  is the wave number [1]. With this approach the shape of the cross-sections can be determined for which (6) is a solution in form of a travelling wave.

For arbitrary cross-sections analytical solutions of the wave-problem do not exist and therefore, both the solutions in the impacting parts as well as the impact itself have to be treated numerically. This leads to a variety of problems and is computationally expensive.

At this point it is advantageous to consider the impacting parts with piecewise constant cross-sections. For such rods the simple wave equations can be used and transition conditions between the different sections can be formulated which lead to transmitted and reflected waves at each discontinuity of the cross-section. With such a rod of piecewise constant cross-sections a rod of arbitrary cross-section can be approximated.

The transition conditions at the discontinuities are determined under the assumptions of linear elastic material behavior and force and displacement balance. In the first instance the segment lengths are arbitrary and since each reflected or transmitted wave reflects and transmits at the next change of cross section again, it results in an exponential increase of transmissions and reflections when either the time or the number of cross sections is increased. This causes very high computational costs.

If all cross sections are of the same length however, the reflections and transmissions all occur at the same time at the changes of cross section because the wave propagation speed is constant on the segments. Therefore, a transmitted and a reflected wave can be combined to a new wave traveling along the rod segment. This leads to a linear increase of calculation time which is a noticeable reduction and enables to use a large number of cross section segments in order to approximate any piston rod geometry in good detail.

The benefit of the new method is that the results are more accurate with shorter computation time compared to the FE-approach for example.

## References

- [1] Guo, S.; Yang, S.: Wave motions in non-uniform one-dimensional waveguides. JVC 2011, pp. 92–100, 2011.
- [2] Hagedorn, P.; DasGupta, A.: Vibrations and Waves in Continuous Mechanical Systems. Wiley, 2007.

## Free Vibration of Piezoelectric Composites using NURBS for Geometric and Response Field Functions

Anand V. Singh<sup>#</sup>, Vijai Raj

<sup>#</sup> Department of Mechanical and Materials Engineering  
Western University, London, ON, Canada, N6A 5B9  
avsingh@uwo.ca

### Abstract

Efficient and numerically sound techniques are presented for the free vibration analysis of sandwich plates made of piezoelectric layers supported by a silicon substrate. The in-plane shape of the sandwich plate is assumed to be quadrilateral with four curved edges. Procedures and results from the free vibration analysis for two and three dimensional problems are described below. Two sandwich structure models are considered in the first part of this presentation. Sandwich structure is considered in the first model as a first order shear deformable (FOSD) plate wherein the in-plane displacement varies linearly over the thickness keeping the transverse displacement uniform. Displacement at a point on the middle plane of the sandwich plate is described by three translational  $(u_1, u_2, u_3)$  and two rotational  $(\beta_1, \beta_2)$  components. Electrical charge  $\phi$  which develops during the bending of piezoelectric layers is known to vary nonlinearly in the thickness direction. Therefore, a layer-wise linear scheme is used for this nonlinear distribution in each piezoelectric layer. All components  $u_1, u_2, u_3, \beta_1$  and  $\beta_2$  are expressed by Non-uniform rational B-Spline (NURBS) curves [1]. Also, the four curved boundaries are expressed by NURBS and benefits from the natural coordinates  $-1 \leq \xi_i \leq 1, i = 1, 2$  are fully exploited. For the second sandwich plate model, each layer is taken as a hexahedral solid enclosed by six surfaces. Each hexahedron is defined by NURBS in the natural coordinates  $-1 \leq \xi_i \leq 1$  with  $i = 1, 2, 3$ . Displacement  $u_1, u_2, u_3$  and potential field  $\phi$  are expressed similarly. Control points for the displacement and potential fields constitute the degrees of freedom at a point in the continuum.

Embedded in this paragraph are some of the basic equations, which a researcher working on piezoelectric materials and associated structures routinely applies. Material equations relating stress  $\{\sigma\}$ , electric flux density  $\{D\}$ , mechanical strain  $\{\varepsilon\}$  and electric field  $\{E\}$  are:  $\{\sigma\} = [C]\{\varepsilon\} - [e]^T\{E\}$  and  $\{D\} = [e]\{\varepsilon\} + [\epsilon]\{E\}$ , where  $[C]$  = elastic stiffness matrix,  $[e]$  = piezoelectric coupling matrix, and  $[\epsilon]$  = dielectric matrix [2-4]. Mechanical strains are expressed in terms of  $u_1, u_2, u_3$ , etc. Maxwell's equation  $\{E\} = -\{\nabla\}\phi$  is used to express the electric field  $\{E\}$  in terms of the electric potential  $\phi$ . The displacement field functions and material relations are then used in the energy functional  $\Pi = T - U - W$ , where  $U$  = the strain energy,  $T$  = the kinetic energy and  $W$  = the work done by externally applied electrical and mechanical loads. Two coupled equations are then obtained from the stationary condition of the energy functional  $\Pi$ . By eliminating the electric potential, the two are merged to one equation of motion  $[M]\{\ddot{\Gamma}\} + [K]\{\Gamma\} = \{F(t)\}$  for the forced vibration analysis of a piezoelectric structure. Here, the vector of control points associated with mechanical displacement and

rotation =  $\{\Gamma\}$  and mass matrix =  $[M]$ . The stiffness matrix and the force vector are given by  $[K] = [K_m] - [K_{me}][K_e]^{-1}[K_{em}]$  and  $\{F(t)\} = \{F_m(t)\} - [K_{me}][K_e]^{-1}\{Q(t)\}$  respectively.

In this section, results are presented and discussed for the free vibration of a square ( $150\text{ mm} \times 150\text{ mm}$ ) cantilevered sandwich plate of thickness  $h$  and stacking layout ZnO/Si/ZnO [5]. The three layers are assumed to have the same thickness. Numerical simulations are performed using both two and three dimensional models mentioned above. Patches and blocks for various aspect ratios and mesh configurations are considered keeping order of the NURBS curves at four. Control knots inside the two domains are generated through linear interpolation. A basic plate patch has  $6 \times 6$  control points for the middle plane, whereas a mesh of  $5 \times 5 \times 5$  control points is considered in a hexahedral continuum. A  $3 \times 3$ , i.e. nine patch plate model each having 36 control points and six sub piezoelectric layers has 1280 mechanical degrees of freedom and 1792 electrical degrees of freedom. Degrees of freedom in one solid module, for example, amount to 375 corresponding to  $(u_1, u_2, u_3)$  and 125 to  $\phi$ . Hence, in  $3 \times 3 \times 3$  solid modules and 125 control points per module, there are 6591 mechanical and 2197 electrical degrees of freedom to a total of 8788. Eigenvalues and eigenvectors are obtained from the homogeneous equation of motion, i.e. without the force vector, by the direct iteration method. Table 1 shows values of the first five natural frequencies in radian per second for  $a/h = 100$  and 50 respectively. Columns for cases 1 and 2 present results from the plate and 3D models respectively. A third model is built in ANSYS using solid 226 coupled-field-elements for the piezoelectric material and solid 185 for the silicon core. The assembled model in this case has 129546 degrees of freedom, which is approximately fifteen times the NURBS based solid model. The results from ANSYS are given in the last column of Table 1. A huge advantage of the present method over the conventional finite element method is seen here. Results in Table 1 from different formulations show a resounding agreement between the frequencies and modes shapes from the present NURBS based solid and ANSYS models. However, the mode shapes are not included in this summary paper because of the space limitation. While comparing the frequencies between the plate and solid models, it is found that there is a very good agreement in the fundamental frequencies from the plate and solid NURBS models. By examining the mode shapes, it was observed that the odd modes showed reasonably good agreement, while it was not so for the even modes. The difference in fundamental frequencies, as expected seems to be increasing with the thickness.

Table 1. Natural frequencies (rad/sec) of rectangular sandwich plate.

a/h	Mode Number	Case 1	Case 2	ANSYS
100	1	389	385	385
	2	1432	1222	1221
	3	2371	2445	2443
	4	4746	4214	4215
	5	5999	5979	5977
50	1	803	798	799
	2	2846	2433	2431
	3	4730	4874	4874
	4	8419	8377	8375
	5	11935	11905	11913

Some results for a 50 cm long cantilevered homogeneous prismatic PZT4 piezoelectric bar [5] are also presented as the benchmark. The cross section of this bar is uniform and given by  $50\text{mm} \times 50\text{mm}$ . The condition of  $u_1 = u_2 = u_3 = 0$  is taken at the fixed end. Similarly, the electrical potential  $\phi = 0$  is applied by grounding the top and bottom surfaces. The model from the present method is created with a grid of  $5 \times 5 \times 5 = 125$ . Each module has 125 control points, 6591 mechanical degrees of freedom corresponding to  $(u_1, u_2, u_3)$  and 2197 electrical degrees of freedom pertaining to the electrical potential function  $\phi$  to a total of 8788. The model created in the ANSYS environment using 226 coupled field elements has a total of 65066 degrees of freedom. Values of the first eight natural frequencies in radian per second are given in Table 2. Results from the two sources show very close agreement. The mode shapes though not presented in this summary were found to match closely in pattern.

Table 2. Natural frequencies (rad/sec)for PZT4 bar .

Mode Number	3D Solid	3D ANSYS	Difference (%)
1	1125.6	1121.8	0.34
2	1141.5	21151.4	0.87
3	2980.1	2981.7	0.06
4	4947.5	4939.7	0.16
5	5124.1	5134.9	0.21
6	5684.2	5554.9	2.33
7	8936.1	8910.2	0.29
8	10681.6	10740.9	0.56

Efficient computational two and three dimensional methods are developed for piezoelectric laminates with full electro-mechanical coupling. NURBS curves are used to represent geometric coordinates, displacement and electric charge fields. Free vibration analysis is performed on a rectangular sandwich plate to validate the efficiency of the present NURBS based method. The fundamental frequencies from the plate and solid models of the piezoelectric sandwich plates are close. Hence, the use of the first order shear deformable plate model should be quite adequate in sensing, actuating and power harvesting devices, where only the fundamental mode of vibration is triggered to a significant extent. The present three dimensional NURBS based approach and ANSYS yield very close results. However, there is a huge difference in the numbers of the degrees of freedom in the two models. This can be significant particularly if the transient response analyses are performed.

## References

- [1] Piegl, L. A.; Tiller, W: The NURBS book, Springer, Berlin, New York, 1997.
- [2] Tiersten, H. F.: Linear Piezoelectric Plate Vibrations, Plenum, New York, 1969.
- [3] Allik, H.; Hughes, T.J.R.: Finite Element Method for Piezoelectric Vibration, International Journal for Numerical Methods in Engineering 2, 151-157, 1970.
- [4] EerNisse, E.P.: Resonances of One-Dimensional Composite Piezoelectric and Elastic Structures, Sonics and Ultrasonics, IEEE Trans, 14, 59-66H,1967.
- [5] Singh, A.V., Raj, V. : Numerical Studies of Piezoelectric Composites using NURBS for Geometry and Field Functions, Proc. Indian National Sc. Academy, 82(02),361-367,2016.

## Eigenvalues and eigenvectors of a system of Bernoulli Euler beams connected together in a tree topology

Andrew Watson<sup>\*</sup> and W. Paul Howson<sup>#</sup>

<sup>\*</sup> Dept. of Aero and Auto Engineering  
Loughborough University  
Loughborough, LE11 3TU, UK  
a.watson@lboro.ac.uk

<sup>#</sup> Independent Consultant  
Gwanwyn, Craig Penlline, CF71 7RT, UK  
w.p.howson@gmail.com

### Abstract

Consideration is given to determining the exact solutions of the eigenproblem posed by a graph with linear tree topology on which the fourth order Sturm Liouville operator is acting. However, this purely mathematical problem in Quantum Graph theory can be solved straightforwardly using a structural mechanics analogy, namely that its solution corresponds precisely to the free vibration problem of a network of beams with identical topology. It is interesting to note that this parallels previous work in which a similar analogy, but with bars rather than beams, was made to establish exact solutions to the simpler problem of the second order Sturm Liouville operator acting on similar tree topologies [1,2]. Such problems remain a continuing source of mathematical interest [3,4].

The exact free vibration of a single, uniform Bernoulli Euler beam can be described by the following fourth order Sturm-Liouville equation

$$\frac{d^2}{dx^2} \left( v_2(x) \frac{d^2 y}{dx^2} \right) - \frac{d}{dx} \left( v_1(x) \frac{dy}{dx} \right) + v_0(x) y = \lambda w y \quad (1)$$

where  $v_2(x)$  is the flexural rigidity of the beam;  $v_1(x)$  is the static axial load;  $v_0(x)$  is the distributed foundation stiffness per unit length;  $w$  is the mass per unit length of the beam; and  $\lambda$  is  $\omega^2$ , ( $\omega$  is the circular frequency). The exact solution of Eq.(1) is most conveniently achieved in the form of a dynamic stiffness matrix, e.g. [5]. This allows any number of tree topologies to be modelled, while use of the Wittrick-Williams algorithm [5] enables any desired eigenvalue to be converged upon to any desired accuracy with the certainty that none have been missed.

The remainder of this paper examines the eigenvalues and corresponding eigenvectors of a series of trees typified by the one drawn to enhance clarity in Fig. 1. However, it should be noted that: every tree must have one or more levels ( $n \geq 1$ ); within any given tree the branching number,  $b$ , must be constant with  $b \geq 1$ ; and that any members (edges) at the same tree level are theoretically collinear in terms of the structural mechanics analogy. Subject to these constraints, the use of theoretical relationships for eigenvalue multiplicity and efficient coding techniques, trees of virtually any complexity can be solved. For brevity in the results presented herein, each member is assumed to be a uniform Bernoulli Euler beam and the effects of static axial load and distributed foundation stiffness are ignored.

The results given in Table 1 are for a tree with clamped boundary conditions at the left hand side (the root of the tree) indicated by the letter 'A' in Fig. 1 and at the right hand side indicated by the letters 'O' to 'W'. The table shows the set of fundamental, normalised eigenvalues and their corresponding multiplicities, that completely describe the family of repetitive trees of length  $n = 1, 2, \dots, 5$ . The index,  $r$ , defines the subtree length in which a fundamental eigenvalue first occurs, denoted by a '1' in the appropriate column. Any multiplicities are then calculated from Eq.(2). As examples, consider the following: (a) the tenth eigenvalue of the  $n = 5$  tree is given as  $\lambda \approx (0.5087\pi)^4$ . This fundamental eigenvalue first appears in subtree  $r = n = 5$  and Eq.(2a) gives its multiplicity  $M_n$  as 1; (b) the 15th eigenvalue for the same tree lies in a group of multiplicity 18, where  $\lambda \approx (0.7314\pi)^4$  and its multiplicity of the fundamental eigenvalue is

given by Eq.(2b) with  $b = 3, n = 3, r = 2$ , as  $M_2 = 2 \times 3^{5-2-1} = 18$ ; (c) the 16th eigenvalue for an  $n = 4$  tree is given as  $\lambda \approx (1.192\pi)^4$  whose multiplicity is given by Eq.(2b) as  $M_3 = 2 \times 3^{4-3-1} = 2$ . The last eigenvalue given in the table corresponds to the clamped clamped eigenvalue of a single beam. For  $n = 5$  this eigenvalue has multiplicity 54. For the notation adopted in this paper this multiplicity is defined as  $M_1=54$ . The subscript refers to the subtree that is vibrating. The multiplicites of each eigenvalue  $M_r$  are given by

$$M_n = 1; M_r = (b-1)b^{n-r-1} \text{ for } 1 \leq r \leq n-1 = 1 \tag{2a,b}$$

**Table 1.** Normalised eigenvalues of a tree with  $n=5$  and  $b=3$ . For each eigenvalue the associated subtree length is given by the index  $r$  corresponding to a mulitplicity of ‘1’.

Eigenvalues		Multiplicities				
$k$	$\sqrt[4]{\lambda_k}/\pi$	$r =$				
		5	4	3	2	1
1	0.3234581	1				
2	0.3896334	2	1			
3	0.5040498	6	2	1		
4	0.5087078	1				
5	0.6242067	2	1			
6	0.6965265	1				
7	0.7314065	18	6	2	1	
8	0.8103492	6	2	1		
9	0.8506574	2	1			
10	0.8746724	1				

Eigenvalues		Multiplicities				
$k$	$\sqrt[4]{\lambda_k}/\pi$	$r =$				
		5	4	3	2	1
11	1.127646	1				
12	1.151974	2	1			
13	1.192491	6	2	1		
14	1.272673	18	6	2	1	
15	1.307907	1				
16	1.380471	2	1			
17	1.499681	1				
18	1.499999	6	2	1		
19	1.505618	54	18	6	2	1

For the tree shown in Figure 1 with  $n = 4$  the results in the column  $r = 5$  can be ignored. The first eigenvalue for this tree has a multiplicity 1 and is the fundamental eigenvalue. Higher harmonics of this fundamental eigenvalue exist higher up the spectrum as shown by the multiple occurrences of the value 1 in the  $r = 4$  column. Other multiplicites exist such as 2 and 6. These are different fundamental eigenvalues and are harmonics of subtrees. The first occurrence of the multiplicity 2, in this column, is the fundamental eigenvalue for a subtree  $r = 3$ . Any eigenvalue with multiplicity greater than unity will have unique eigenvector characteristics. Looking at Figure 1, we can see that if the subtree of length 3 emanating from vertex B to tips OPQ is vibrating with its root clamped then it can be only achieved if the subtree B to RST is vibrating in antiphase or if B to UVW is vibrating in antiphase or a combination of the two subtrees vibrating in antiphase. Hence there exist two independent orthogonal modes and the  $n = 4$  tree has an eigenvalue of the subtree of length  $r=3$ . This argument can be followed for all subtrees.

The rapid growth in the multiplicities can be seen by looking at eigenvectors of the individual member for a clamped clamped eigenvalue. Figure 2a indicates that any pair of beams which emanate to the right of a vertex at level  $n-1$  of Figure 1 can vibrate flexurally in antiphase and with their modes having equal amplitude, so that, remembering that the beams are collinear, equilibrium of moment and of transverse force exists at their common vertex. Because there is equilibrium with the force vector results in zero rotation and zero translation which, in effect, is the equivalent of a clamped supprt. Hence the common node is shown as a clamped boundary condition at the left hand side. It is only possible to get equilibrium by examining modes that have members vibrating in antiphase. An eigenvector to a path such as P,GCBA (t: top) is no longer possible at the same eigenvalue because the associated mode would have to involve zero deflection and rotation at G, C and B and such modes cannot give both moment and transverse force equilibrium at G, C and B (they can only give either moment equilibrium or transverse force equilibrium). Figure 2(b) shows a mode for a subtree of length  $r = 2$ . The approximate mode and the relative amplitudes shown for the upper four beams give force and moment

equilibrium both at their common vertex and, because the lower four beams are in anti-phase, at the left-hand vertex on the figure. Therefore, this is clearly a possible mode for the set of  $b$  subtrees emanating to the right from any vertex at level  $n-2$ . Hence it may be deduced that the mode multiplicities are again the same as those described in equation (1).

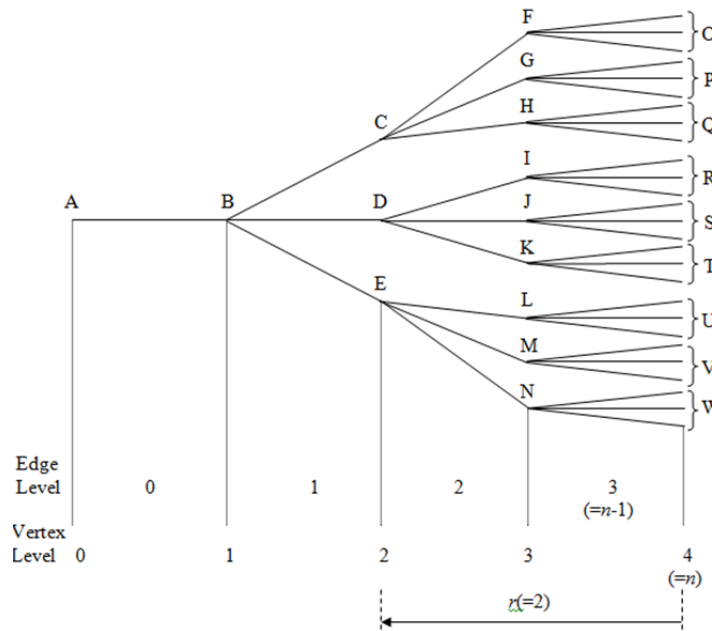


**Figure 1.** Four level tree with  $b=3$ .

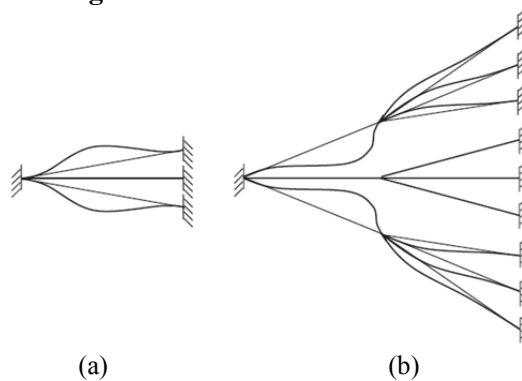


**Figure 2.** Eigenvectors corresponding to (a)  $M_1$  and (b)  $M_2$  for trees of beams which form the analogous structural mechanics problem of trees of the Sturm-Liouville differential equations.

**References**

- [1] Williams, F.W., Howson, W. P. & Watson, A., Application of the Wittrick–Williams algorithm to the Sturm–Liouville problem on homogeneous trees: a structural mechanics analogy., Proc. R. Soc. A, Vol. 460, pp. 1243–1268, 2004.
- [2] Williams, F.W., Watson, A. Howson, W. P. & Jones, A.J., Exact solutions for Sturm–Liouville problems on trees via novel substitute systems and the Wittrick–Williams algorithm., Proc. R. Soc. A, Vol. 463, pp. 3195-3224, 2007.
- [3] Kurasov, P., Malenova, G. & Naboko, S., Spectral gap for quantum graphs and their edge connectivity, J. Phys. A: Math. Theor., Vol. 46, 275309, 2013.
- [4] Band, R., The nodal count  $\{0, 1, 2, 3, \dots\}$  implies the graph is a tree., Phil. Trans. R. Soc. A, Vol. 372, 20120504, 2014.
- [5] Howson, W. P. & Williams, F.W., Natural frequencies of frames with axially loaded Timoshenko members., Vol. 26, 503-515, 1973.

## Prof. Haim Abramovich

<p>Faculty of Aerospace Engineering Technion, I.I.T., 32000, Haifa, ISRAEL. Email: <a href="mailto:haim@technion.ac.il">haim@technion.ac.il</a>; <a href="mailto:abramovich.haim@gmail.com">abramovich.haim@gmail.com</a> Tel : +972 544 696566</p>	
---	--

Obtained his B.Sc., M.Sc. and Ph.D. degrees from the Faculty of Aerospace Engineering, Technion, in 1975, 1979 and 1983, respectively.

His Ph.D. thesis was entitled “The behavior of the Blade of a Darrieus Wind Turbine”, while his M.Sc. thesis title was “Correlation between Vibrations and Buckling of Stiffened Shells with Realistic Boundary Conditions and Combined Loading”.

He has been with the Technion since 1987, and currently he is the head of the Aerospace Structures Laboratory.

He spent three years with the Israeli industry and between 1996-1998 he was Guest Professor at ETH Zurich Institut fur Leichtbau und Seilbahntechnik, Switzerland.

His main fields of interest are: static and dynamic stability of thin walled structures, piezoelectric materials, laminated composite structures, dynamic buckling of thin walled structures, smart structures technologies, structural mechanics and energy harvesting using piezoelectric and pyroelectric materials .

He has published more than 103 papers in well-known international journals on these quoted subjects. He is the author of 10 patents on piezoelectric harvesting devices. He is also the author of two new books with another one in progress:

1. H. Abramovich, *Intelligent Materials and Structures*, © 2016 Walter de Gruyter GmbH, Berlin/Boston, 386 p.
2. H. Abramovich, *Stability and Vibrations of Thin Walled Composite Structures*, © 2017 Woodhead Publishing Limited, 540 p.
3. H. Abramovich, *Advanced Aerospace Materials – Aluminum-based and Composite Materials*, in progress, to be published by Walter de Gruyter GmbH, Berlin/Boston.

Since 2013, editorial board member of the International Journal of Composite Materials

Since 2014, editorial board member for International Journal of Aeronautical Science & Aerospace Research (IJASAR).

## **Professor Ranjan Banerjee**

After receiving his Bachelor's and Master's Degree in Mechanical Engineering from the University of Calcutta and the Indian Institute of Technology, Kharagpur, respectively, Ranjan Banerjee joined the Structural Engineering Division of the Indian Space Research Organisation, Trivandrum in 1971 and worked there for four years, first as a Structural Engineer and then as a Senior Structural Engineer. He was involved in the dynamic analysis of multistage solid propellant rocket structures using the finite element method. He also carried out research on the response of rocket structures to acoustic loads. Later in the year 1975 he was awarded a Commonwealth Scholarship to study for a PhD degree at Cranfield University where he conducted research within the technical areas of structural dynamics and aeroelasticity. He received his PhD in 1978. An important spin-off from his PhD was the development of an aeroelastic package in Fortran, called CALFUN (CALculation of Flutter speed Using Normal modes) which was originally written for metallic aircraft, but later extended to composite aircraft. CALFUN has been extensively used as a teaching and research tool in aeroelastic studies. After completing his PhD, he joined the Structural Engineering Division of the University of Cardiff in 1979 and worked there for six years first as a Research Associate and then as a Senior Research Associate to investigate the free vibration and buckling characteristics of space structures using the dynamic stiffness method. During this period he worked in close collaboration with NASA, Langley Research Center, and he was principally involved in the development of the well-established computer program BUNVIS (BUckling or Natural Vibration of Space Frames) which was later used by NASA and other organizations to analyse spacecraft structures. He joined City University London in 1985 as a Lecturer in Aircraft Structures and he was promoted to Senior Lecturer and Reader in 1994 and 1998 respectively. In March 2003 he was promoted to a Personal Chair in Structural Dynamics. His main research interests include dynamic stiffness formulation, aeroelasticity, unsteady aerodynamics, composite structures, functionally graded materials, aircraft design, symbolic computation, free vibration and buckling analysis of structures and associated problems in elastodynamics. He has been responsible for supervising various research contracts as Principal Investigator, involving EPSRC, American Air Force Base, Embraer Aircraft Company, amongst others. To date he has published around 200 papers from his research. He serves in the Editorial Boards of a number of international journals and established conferences and he has been a member of the EPSRC Peer Review College since its inception. He is a Fellow of both the Royal Aeronautical Society and the Institution of Structural Engineers in the UK and an Associate Fellow of the American Institute of Aeronautics and Astronautics. He teaches the subjects of mechanics, strength of materials, aircraft structures, composite materials, computational structural mechanics and aeroelasticity, and he has acted as external examiner in five British universities for their undergraduate and postgraduate programmes in aeronautical and aerospace engineering. In recognition to his contributions in structural dynamics, aeroelasticity and material science, he was awarded the degree of Doctor of Science (DSc) in 2016 by City, University of London.

After earning two degrees (Aeronautics, 1986, and Aerospace Engineering, 1988) at the Politecnico di Torino, Erasmo received his PhD degree in Aerospace Engineering jointly at the Politecnico di Milano, Politecnico di Torino, and Università di Pisa in 1991. He became Associate Professor of Aerospace Structures and Computational Aeroelasticity in 2000, and Full Professor at the Politecnico di Torino in 2011.

Erasmo has been visiting professor at the Institute of Static and Dynamics of the University of Stuttgart (6 months in 1991 and 15 months in 1995-1996); he spent 3 months at the department of Engineering Science and Mechanics of Virginia Tech in 1996; 3 months at Supmecca, Paris, in 2006; and 3 months at the Centre of Research Public H Tudor (Luxembourg) in the summer of 2009. In 2013 he has got a joint appointment at School of Aerospace, Mechanical and Manufacturing Engineering at Royal Melbourne Institute of Technology of University of Melbourne, Australia. In 2013 as HiCi Scientist Erasmo became member of Distinguished Professor Committee of King Abdulaziz University, Jeddah, Saudi Arabia.

Carrera has been author and coauthor of about 600 papers on the above topics, most of which have been published in first rate international journals, including six recent books, three of these published by J Wiley & Sons. Erasmo's papers have had more than 13000 citations with h-index=62 (data taken from Google-Scholar). Most of the papers, in particular those concerning the activities of the last decade, have been coauthored by Master students, PhD students, Italian colleagues, foreign professors and scientists from industry. Due to his international reputation, Erasmo has held Invited Seminars in various European and North- American Universities, as well as plenary talks in international conferences. Erasmo serves as Associate Editor for Composite Structures, J Thermal Stress, Computer and Structures, International Journal of Smart and Nano Materials and the International Journal of Aeronautical and Space Sciences. He is founder and Editor-in-Chief of Advances in Aircraft and Spacecraft Science, first Issue January 2014. He acts as Editor-in-Chief of Mechanics of Advanced Structures. He acts as reviewers for about 100 journals and is on the Editorial Board of many international conferences. He has in charge of the Chapter on 'Shells' for the Encyclopedia of Thermal Stress published by Springer as well as of the Section 'Composites' on the coming Springer Encyclopedia of 'Computational Mechanics'. Erasmo is the founder of the non-profit International Conference DeMEASS whose V Edition is scheduled for October 2012 in Austria and main organizer of the following conferences: ICMNMMCS, Torino, June 2012, co-chaired by Prof A Ferreira; the ECCOMASS SMART 13 conference, Torino, June 2013; ISVCS IX, Courmayeur, July 2013. He is General Chairman of ISVCS 11. He has been member of PhD and Habilitation committees in Germany, France, The Netherlands and Portugal.

He is president of the Piedmont Section of AIDAA (Associazione Italiana di Aeronautica ed Astronautica) and Senior Member of AIAA. Erasmo has been Highly Cited Researchers (Top 100 Scientist) by Thompson Reuters in the two Sections: Engineering and Materials. He has been confirmed HiCI in 2015 in the Section Engineering. The only aerospace Engineering worldwide. Due to his scientific commitments professor Carrera has been recently awarded by the President of Italian Republic, as 'Honoray Commendator'. It consist of one of the highest award in Italy and it has been given to only 73 Italian Scientists from 2003.

## **Weiqiu Chen**

**Weiqiu Chen** is a Chair Professor and the Dean of the Department of Engineering Mechanics at Zhejiang University. He received his BS and PhD degrees from Zhejiang University in 1990 and 1996, respectively. He worked as a postdoctoral research associate at The University of Tokyo during 1997-1999. After he went back from Japan, he was immediately promoted to be an associate professor, and became a full professor in 2000. His research interests include mechanics of smart materials/structures and vibration/waves in structures. Now he is working mainly on mechanics of soft active materials and structures, particularly addressing wave propagation in soft periodic materials and structures subjected to large deformation. He has co-authored over 350 peer-reviewed journal articles with a total number of citations about 5500 and H-index 39 according to WoS, as well as three English books on elasticity of transversely isotropic elastic materials, three-dimensional analysis of piezoelectric solids, and Green's functions of anisotropic media, respectively. He now serves as the editorial member of several academic journals including Journal of Thermal Stresses, Theoretical and Applied Mechanics Letters, and Applied Mathematics and Mechanics (English Edition). Furthermore, he reviews more than 100 manuscripts per year for more than 50 journals including Journal of the Mechanics and Physics of Solids, International of Solids and Structures, Journal of Applied Mechanics, International Journal of Engineering Science, International Journal of Mechanical Sciences, European Journal of Mechanics A/Solids, Acta Mechanica, Archive of Applied Mechanics, Proceedings A of Royal Society, Composite Structures, Mechanics of Advanced Materials and Structures, Composites Science and Technology, Composites Part B, Journal of the Acoustical Society of America, Journal of Sound and Vibration, etc.

**Prof. Li Cheng**  
(<http://www.mypolyuweb.hk/mmlcheng/>)



Li Cheng is currently a Chair professor and Director of Consortium for Sound and Vibration Research (CSV), The Hong Kong Polytechnic University.

He received his BSc degree from Xi'an Jiaotong University in 1984. He was then selected through national selection process and went France to start postgraduate studies. He got his DEA and Ph.D. degrees from the Institut National des Sciences Appliquees de Lyon (INSA-Lyon), France in 1986 and 1989, respectively, in the area of vibration and acoustics. During that period of time, he had chance to work with the then Aerospatiale on sound and vibration problems of the Aerial 5 launcher. He then moved to Canada, working as a post-doctorate fellow and a research fellow at Sherbrooke University in Canada. His research endeavor focused on aircraft noise and vibration control, supported by Canadair.

Li started his academic career in Laval University, Canada in 1992, rising from an assistant professor to Associate/Full Professor till 2000. During that period of time, he undertook a few large-scale research projects with various industries, including the one with Bombardier Ltd, on active control of Dash-8 floor panels. Li joined the Hong Kong Polytechnic University in 2000, establishing a research group in sound and vibration, and becoming its founding director.

Li published extensively, with over 350 publications including book/book chapters and journal/conference papers, receiving over 4000 citations. He is an elected fellow of the Acoustical Society of America, Acoustical Society of China, IMechE and the Hong Kong Institution of Engineers. He currently serves as an Associate Editor for the Journal of Acoustical Society of America, Associate Editor of Structural Health Monitoring: An International Journal, and an editorial board member of the International Journal of Applied Mechanics, ACTA ACUSTICA Sinica, Chinese Journal of Acoustics and four other international journals.

Li is now the president of the Hong Kong Society of Theoretical and Applied Mechanics. He also served as the Chair/Co-Chair and as a scientific committee member (30+ times) in various international conferences, including the general Chair of the 46th International Congress on Noise Control Engineering (Inter-noise), Vice-chair of the World Congress on conditioning Monitoring 2017 and Chair of 14<sup>th</sup> and 17<sup>th</sup> Asia Pacific Vibration Conference. He has been the plenary/keynote speaker in over 25 international conferences, including the 23<sup>rd</sup> International Congress on Sound and Vibration in Greece and 15<sup>th</sup> Asia Pacific Vibration Conference in South Korea.

**Piotr Cupiał**

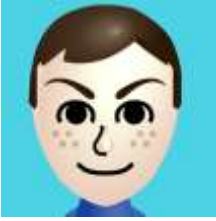
**AGH University of Science and Technology, Kraków, Poland**

I graduated in 1987 from the Cracow University of Technology, in the field of applied and computational mechanics. My MSc thesis considered the problem of the optimum design of a circular plate subjected to non-conservative compressive loading. In 1997 I obtained my PhD in the area of the application of damping polymers in the vibration suppression of layered composite plates. In 2008 I published a monograph “Coupled electromechanical vibration problems for piezoelectric distributed-parameter systems”, and in the following year I obtained the DSc title (habilitation). I hold a professorship position at the Faculty of Mechanical Engineering and Robotics, at the AGH University of Science and Technology.

I spent three years (1998-2001) at the European Organization for Nuclear Research (CERN), in Geneva. My activities at CERN focused on the finite element analysis and dynamic measurements, in connection with the Large Hadron Collider (LHC) and the four particle physics experiments, being designed then. After leaving CERN I have continued my contacts with particle physicists. In recent years, I have been taking part in several research projects within the European neutrino physics collaboration. In this framework, I coordinated the design of specialized equipment used in advanced physics experiments, subjected to very-short-duration pulses of magnetic and thermal character.

Since 2007 I have been a member of the editorial board of the Journal of Sound and Vibration. I am the editor-in-chief of the quarterly Mechanics and Control, and a member of the editorial board of the Journal of Theoretical and Applied Mechanics. Starting from this year, I am the chairman of the biennial conference on Active Noise and Vibration Control Methods; for several years now I have been a member of the advisory committee of ISVCS. I am a member of the Section of the Dynamics of Systems, working under the auspices of the Polish Academy of Science.

I am married to Gabriela and we have one son. I have always been very fond of the mountains, hiking in the summer and skiing during winter.



## Sergio De Rosa

Professor

Department of Industrial Engineering – Aerospace Section  
University of Naples “Federico II”, Italy

From the beginning of my research activity, I was involved in the engineering fields concerning the structural dynamics, the vibroacoustics and the fluid-structure interaction in large sense.

The thesis work concluded the five-year Italian degree in aerospace engineering in 1998. It was focused on the assembling of a predictive vibroacoustic model for the ATR-42 fuselage. Large part of that time was usefully spent on the pages of vibration of plates and shells. In the same year, I became researcher at the Italian Aerospace Research Center, CIRA, where continued my studies and applications in the vibroacoustic fields.

In 1992, I arrived as researcher at University of Naples “Federico II” at the Department now named Industrial Engineering - Aerospace Section: my entire academic career was spent in the Aerospace Structures sector. In parallel with the research activity, I was also guided to the teaching stuff, having from 2001 the full responsibility of courses.

I belong to a group named **pasta-Lab: laboratory for promoting experiences in aeronautical structures and acoustics**.

Since 1990 I was involved in the main research programmes funded by the European Union in the aerospace sector. The actual H2020 projects are:

- 2016-2019 MSCA-EJD, VIPER (Vibroacoustics of periodic structures, European Joint Doctorate): <http://vipер.ec-lyon.fr>
- 2016-2019 Clean Sky 2 action Airframe-ITD, CASTLE (Cabin system design toward passenger wellbeing)

The targets of the research activities were to study, investigate and define numerical and experimental procedures and/or tools to be used as predictive methods, all inside the paradigm of increasing complexity:

- *Definition of SAMSARA, Similitudes and Asymptotical Modelling for Structural Acoustics Researches and Applications.*
- *Stochastic response of structural and fluid-structural systems under random and convective excitations.*
- *Convective effect on the acoustic radiated power by structural components.*
- *Influence of the uncertainties on the dynamic system response.*

I am still convinced that only a full interaction among human beings can promote the knowledge at highest levels. The research and teaching mechanics can't be a passive process but requires that all the involved persons play (and risk) something, hopefully with a smile ☺.

This is the 3rd time for me to be at ISCVS, and I will be very glad to meet again some of the persons who guided my adventure.

Nevertheless, I am (very) lazy researcher but I know to be a loquacious friend, being passionate of photography, blogging and micro-blogging, music, modern literature, comics.

[Many things: too much, maybe.]

## **Hu Ding, Ph.D.**

Shanghai Institute of Applied Mathematics and Mechanics,  
Shanghai University  
149 Yan Chang Road, Shanghai 200072, China  
Email: dinghu\_3@hotmail.com  
<http://www.dvc.shu.edu.cn>

### **Education:**

09, 1998 - 09, 2002 HeFei University of Technology, Bachelor Degree;  
09, 2002 - 09, 2005 HeFei University of Technology, Master Degree;  
09, 2005 - 03, 2008 Shanghai University, Doctor Degree: Mechanics;  
04, 2012 - 04, 2013 University of Toronto, Visiting Professor;  
09, 2016 - 03, 2017 Duke University, Visiting Scholar.

### **Conducted research activities and research interests:**

Nonlinear vibration of axially moving continua; nonlinear vibration and control of continua.

### **Message:**

Two years ago, in Colorado, I spent a fantastic week. Met a lot of very nice people. Able to discuss research work with these kind people. Talk about the problems encountered in the research work and the significance of the study. Really very interesting and helpful. I am very excited and look forward to being able to attend the ISVCS series international symposium again.

A photo from ISVCS10 in Colorado in 2015:



ISVCS11

Professor Moshe Eisenberger

The Sigmund Sommer Chair in Structural Engineering

Faculty of Civil and Environmental Engineering

Technion – Israel Institute of Technology

Haifa, Israel

BSc. Technion (1977), MSc. Stanford University (1978), PhD. Stanford University (1980).

Since 1980 on the faculty at the Technion.

Visiting positions: Carnegie Mellon, PA (1987-9, 1993), City University, Hong Kong (2006), Waikato University, NZ (2015), University of Lisbon, Portugal (2015), and Bologna University, Italy (2015).

Research: Computational Structural Analysis – Static, Vibration, Stability of Beams, Plates and Shells, made from isotropic, composite and FGM.

My professional interests have shifted within the broad discipline of computational mechanics: in the early 80's, at the beginning of the PC era I was mostly involved in structural analysis and computer methods for frames and finite elements calculations. Then I became more interested in stability and vibration analysis of continuous systems, starting with rods and beams with variable cross section, and moving to plates and shells with variable thickness, made of isotropic, composite, and functionally graded materials. All these analyses were performed using the dynamic stiffness method and thus produced exact results, which have since served as benchmark values for comparison by other researches that developed various computational methods. Currently I am working on getting "exact" results for vibration and buckling of plates, and hopefully a super convergent plate element.

I am married to Dorit and have two children, Gilad and Yarden, and all have been with me in some of the previous ISVCS meetings. For many years I have been biking (mostly road), and hiking and climbing mountains. I am satisfied with the way I can combine work and travel in my life!

**Mark S. Ewing**  
**University of Kansas**

*I grew up interested in science and mathematics, largely due to my fascination with the U.S. spacecraft I used to watch launch from Cape Canaveral—when I lived in nearby Orlando, Florida. I received my BS in Engineering Mechanics from the U.S. Air Force Academy, then began a 20-year career in the Air Force. I served for four years in turbine engine stress and durability analysis where I was an “early” user of finite element analysis for hot, rotating turbomachinery. I then served a two-year assignment in turbine engine maintenance and support, which was less technical, but eye-opening. During these early years—in my spare time—I earned an MS in Mechanical Engineering from Ohio State University.*

*With an MS in hand, I returned to the Air Force Academy to serve on the faculty as an Assistant Professor. After two years, I returned to Ohio State to complete a PhD. As a student of Art Leissa’s, I focused on the combined bending, torsion and axial vibrations of “stubby” beams, thereby establishing my interest in the vibrations of continuous systems.*

*After returning to and teaching at the Academy for six years, I was assigned to the Air Force Flight Dynamics Lab, where I worked on two interesting projects. The first was the development of a structural design algorithm capable of, among other things, “maximizing” the separation of two natural frequencies. The utility of this endeavor was to allow the design of aircraft wings for which the bending and torsional natural frequencies are sufficiently separated (in frequency) to avoid flutter. The other interesting project was the analysis of the effect of convected aerodynamic loads on a missile.*

*I am now on the Aerospace Engineering faculty at the University of Kansas. My current research interests are in structural acoustics, which is a topic of increasing interest to aircraft manufacturers. In recent years, I have focused on the best way to characterize and estimate structural damping for built-up structures. All the test articles I’ve used to validate my work through experimentation are simple structural elements, namely beams and plates.*

*I have a great love of the outdoors, and of the mountains in particular. When Art Leissa asked me to help organize the first International Symposium on Vibrations of Continuous Systems—held in 1997—and he told me he wanted to meet in the mountains, I really got excited. I look forward to the 11<sup>th</sup> Symposium in Llanberis as a time to visit with long-time friends and colleagues.*

## Biographical Information

### Matteo Filippi

MUL2, Department of Mechanical and Aerospace Engineering  
Politecnico di Torino,  
Corso Duca degli Abruzzi 24, 10129 Torino, Italy  
matteo.filippi@polito.it



Matteo Filippi is currently a research fellow of the research group MUL2 (<http://www.mul2.polito.it>) at Politecnico di Torino. From the same university, he received a Bachelor's (March 2009) and a Master's (December 2011) Degree in Aerospace Engineering. Afterward, he started his Ph.D. that has been received in March 2015. During this period, he spent three months at School of Aerospace, Mechanical, and Manufacturing Engineering at Royal Melbourne Institute of Technology of University of Melbourne, Australia.

From the beginning of his research activity, Matteo was involved in the development of high-fidelity finite elements for dynamic and stress analyses of a wide range of structures. In particular, great attention has been given to response of structures made of composite, functionally graded, and viscoelastic materials. He extended the higher-order one-dimensional theories obtained through the Carrera Unified Formulation to the rotor dynamics field. The versatility of the proposed approach enables the study of dynamics of axial rotors and rotary-wing configurations. Furthermore, aeroelastic studies have been performed by combining the structural models with steady and unsteady aerodynamic theories.

Matteo Filippi has authored more than 25 scientific papers most of which have been published in first rate international journals. He is serving as reviewer for a number of international journals such as "Journal of Sound and Vibration", "Journal of Vibration and Acoustics", "Composite Structures", and "Mechanics of Advanced Materials and Structures". He is involved in many research programs supported by the European Space Agency and the European Union in cooperation with many European industrial and academic partners.

## **Stan Hutton**

1941 Born in Kidderminster England;

1960 Undergraduate studies at Nottingham University in Civil Engineering;

1963 Site Engineer, Wilfa Nuclear Power Station, Angelsey, Wales;  
Site survey, concrete design engineer, construction supervision.

1965 MAsc in Civil Engineering, Calgary University, Canada;  
Thesis: The behaviour of partially prestressed concrete;

1966 Structural Design Engineer, H.A. Simons Ltd, Vancouver, Canada;  
Design and analysis of pulp and paper mills;

1968 Ph D in Applied Mechanics, UBC, Vancouver, Canada;  
Thesis: The finite element method - a Galerkin approach.

1972 Lecturer in Civil Engineering, Adelaide University, South Australia;  
Research into the behaviour of bridges subjected to moving loads and earthquake response of buildings.

1978 Professor in Mechanical Engineering, UBC, Vancouver, Canada  
Research into the behaviour of wood machining equipment.

2003 Emeritus Professor, Mechanical Engineering, UBC  
Continued supervision of graduate students and consulting work with FPInnovations.

**Sinniah Ilanko**  
**The University of Waikato**  
**Te Whare Wananga o Waikato**

e-mail: <Ilanko@Waikato.ac.nz>

Ilanko was born in the north of Sri Lanka (Jaffna), and according to the common Tamil practice, he does not have/use a family name. Ilanko is his given name and Sinniah is his late father's given name and conveniently remains informal.

He graduated from the University of Manchester (U.K) with a BSc in civil engineering and also obtained an MSc from the same university under the supervision of late Dr S.C. Tillman, investigating the effect of initial imperfections on in-plane loaded rectangular plates. His move to England at an early age was the result of his late brother Senthinathan's foresight on the Sri Lankan political situation. After working as an assistant lecturer at the University of Peradeniya in Sri Lanka for about two years, he commenced doctoral studies at the University of Western Ontario under the supervision of Professor S.M. Dickinson, continuing his earlier research on vibration behaviour of initially imperfect in-plane loaded plates. Soon after completing his PhD, he worked as a postdoctoral fellow at the UWO for about six months until he joined the University of Canterbury in 1986. He continued his academic career at Canterbury for nearly 20 years, in various positions, as lecturer, senior lecturer and associate professor until he joined the University of Waikato in 2006. In 2012 he became a full professor. He has served as the Chairperson and later the Head of School of Engineering from January 2013 to December 2015. He has also served as the Head of Mechanical Engineering Department at Canterbury for a year (2001-2202) and worked as a visiting professor at the Annamalai University (India) and Technical University of Hamburg-Harburg during his study leaves. In 1997, he was awarded the Erskine Fellowship and visited several universities in Australia, Canada, Singapore and the U.K.

His research areas include vibration and stability of continuous systems, numerical modelling and adaptive mechanisms. He has published 41 journal papers and in 2014 authored a book "The Rayleigh-Ritz Method for Structural Analysis" jointly with Dr Luis Monterrubio and Dr Yusuke Mochida. Since January 2009, he is serving as the Subject Editor for Journal of Sound and Vibration, for analytical methods for linear vibration.

He is also interested in computer-aided learning and has developed and used several interactive lectures and tutorials for teaching Mechanics of Materials and Vibration, as well as computer based tutorials and games for learning/teaching Tamil language.

He is married to Krshnanandi and they have two daughters, Kavitha and Tehnuka. Ilanko's birth family is scattered across the globe (Australia, Canada, New Zealand, the U.K. and the U.S.A.) because of the civil war in Sri Lanka which has now ended.

**David Kennedy**  
**Professor of Structural Engineering**  
**School of Engineering, Cardiff University, United Kingdom**

David Kennedy obtained a First Class Honours degree at the University of Cambridge in 1978 and a PhD in the area of efficient transcendental eigenvalue computation from the University of Wales, Cardiff in 1994.

From 1978 to 1983 he was employed as an Analyst/Programmer for the computer services company Scicon Ltd, where he worked on the development of the Mathematical Programming software SCICONIC/VM. In 1981 he was awarded a 2-year BP Venture Research Fellowship in Non-linear Optimization, supervised by the late Professor Martin Beale.

In 1983 he was appointed as a Research Associate in the University of Wales Institute of Science and Technology, which was merged into Cardiff University in 1988. Working under the supervision of Professor Fred Williams and funded under a collaborative agreement with NASA, he coordinated the development of the space frame analysis software BUNVIS-RG which was released by NASA to US users in 1986/87. Further collaboration with NASA and British Aerospace (now BAE Systems) led to the development and successive releases, starting in 1990/91, of VICONOPT, a buckling and vibration analysis and optimum design program for prismatic plate assemblies. Both of these programs use analysis methods based on the Wittrick-Williams algorithm.

He was appointed to a Lectureship in the School of Engineering in 1991, promoted to Senior Lecturer in 2000, Reader in 2005 and Professor in 2009. He has continued to manage the collaborative development of VICONOPT, successfully co-supervising 16 PhD students and holding Research Council grants on parallel computing, aerospace panel optimization, local postbuckling and mode finding. He has visited NASA Langley Research Center several times, and in 2007 he undertook a 6-month secondment to Airbus UK, funded by a Royal Society Industry Fellowship. Since 2010 he has been a Deputy Head of the School of Engineering with responsibility for staff matters.

Through the Cardiff Advanced Chinese Engineering Centre, Professor Kennedy has participated for over 25 years in collaborative research projects with leading Chinese universities, including Tsinghua University, Dalian University of Technology and Shanghai Jiao Tong University.

Professor Kennedy is the author of nearly 200 publications of which approximately 50% are in refereed journals of international standing.

He lives with his wife Helen in a village near Cardiff, where he plays the church organ and sings in a community choir. David and Helen are both learning Welsh and will try to teach you some basic words during the Symposium.

**Xiang Liu, PhD**  
**Specially-appointed Professor**  
**School of Traffic & Transportation Engineering, Central South**  
**University, China**

Xiang Liu (XL) was born in Changsha, a city in the central south of China, in 1985. His research interests include elastodynamics, vibro-acoustics, structural instabilities, aeroelasticity, composite structures and metamaterials.

XL received his Bachelor's and Master's degrees with First Class in Civil and Geotechnical Engineering respectively. Then he joined University of Glasgow in 2010 to work for his PhD in Applied Mechanics which was fully funded by an EPSRC grant. His PhD research was on surface instabilities of membranes, plates and solids which are essentially instabilities of continuous systems by using asymptotic and direct numerical simulations. The research was focused on both the mathematical and physical aspects of the problems and important insights were gained. Three journal papers were published by XL from his PhD. The project enabled XL to acquire valuable knowledge and expertise in structural instabilities and eigenvalue problems both from mathematical and mechanical perspectives.

After completing his PhD, XL joined City, University of London in 2013. He worked as a Research Fellow with Prof. J. Ranjan Banerjee (RB) on an EPSRC project entitled "Dynamic Stiffness Formulation for Plates with Arbitrary Boundary Conditions through the Solution of the Biharmonic Equation". This project is against the background that the exact solution of the biharmonic equation with any arbitrary boundary conditions has always been a challenging task not only for the engineers but also for the mathematicians for well over two centuries. To this end, a novel method called the spectral dynamic stiffness method (SDSM) has been proposed by XL and RB for exact free vibration analysis of isotropic and anisotropic plate assemblies with arbitrary boundary conditions (BCs). A set of novel related techniques have been developed so that the new SDSM becomes unconditionally stable with remarkable accuracy and computational efficiency. It has been established that the SDSM has as much as two orders of magnitude computational efficiency when compared with the conventional FEM. The superiority of the SDSM over the FEM will be even more pronounced within the medium to high frequency ranges when the FEM can be prohibitively expensive in computer time and the results can become unreliable. Additionally, a general theory has been developed to account for plate assemblies with arbitrary non-uniformly distributed elastic supports, elastic coupling constraints as well as mass attachments. This theory has no-doubt broadened the applicability of the SDSM for real life structures. More recently, the SDS theory has been generalised to be applied to general plane elastodynamic problems. So far, the SDSM has been applied to many engineering structures such as aircraft wings, multi-span bridge decks, optical beam pointing system, shear-walls, ultrasonic motors, amongst many others.

In February 2017, XL received a specially-appointed professorship from Central South University (China), and now his main work lies in the vibration and noise control, structural instabilities and aeroelasticity in rail transportation engineering.

## **Brian Mace**

Brian is Professor of Mechatronics in the Department of Mechanical Engineering at the University of Auckland, which he re-joined in 2011. Prior to that he was Professor of Structural Dynamics at the Institute of Sound and Vibration Research, University of Southampton. Brian's research interests fall into two general areas. The first concerns structural dynamics. Interests include wave methods, a hybrid wave and finite element approach to noise and vibration modelling, periodic structures and uncertainty modelling, including energy methods and SEA. The second general area concerns smart structures and noise and vibration control using active, semi-active or adaptive-passive methods. Examples include control of vibration transmission, active vehicle suspensions, active constrained layer damping, energy harvesting and the use of smart materials in self-tuning, adaptive vibration control devices.

BRM, 30 March 2017

***ANDREI MITRAKIN***

Andrei Metrikine is Antoni van Leeuwenhoek Professor at the Faculty of Civil Engineering and Geosciences of the Delft University of Technology, the Netherlands. He holds the chair of Dynamics of Solids and Structures and is Head of the Offshore Engineering Section. He is also Deputy Editor-in-Chief of the Journal of Sound and Vibration and holds the part-time International Chair of Offshore Engineering at the Norwegian University of Science and Technology, Trondheim, Norway.

Andrei graduated in radio-physics from the State University of Nizhniy Novgorod, Russia in 1989 and received his PhD and DSc in 1992 and 1998 in St.Petersburg, Russia. In 1994-1998 he held a number of post-doctoral positions, including one at the Institute for Mechanics of the Hannover University, Germany awarded by the Alexander von Humboldt foundation. Since 1999 Andrei is employed by TU Delft. Currently Andrei's research interests focus on vibrations of and waves in structures that are in contact with solids and fluids. The main engineering application areas of his research are Offshore Engineering, including Offshore Wind and Ocean Energy, and Railway Engineering.

## **Wolfgang Seemann**

Wolfgang Seemann was born on 31 March, 1961 in Kelttern (Germany, Baden-Württemberg). After school he studied mechanical engineering at the University of Karlsruhe from 1980 to 1985. After civil service (1985-1987) he worked as a PhD-student at the Institute of Applied Mechanics at the University of Karlsruhe (now Karlsruhe Institute of Technology). The PhD under the supervision of Prof. Jörg Wauer was finished in 1991 with a thesis on 'Wave propagation in rotating or prestressed cylinders'. In 1992 he joined the group of Peter Hagedorn at Darmstadt University of Technology to work in a post-doc position until 1998 when he got a professorship on machine dynamics in Kaiserslautern. In 2003 he got an offer to go back to the University of Karlsruhe on the chair of Applied Mechanics.

His previous and current research interests are in fluid bearings, ultrasonic motors, nonlinear vibration, multibody dynamics, vibration of continuous systems, active materials, nonlinear phenomena in piezoelectric materials, humanoid robots, dynamics of human motion, mechatronic systems, road-vehicle interaction, rotor dynamics and wave propagation.

Besides his duties in teaching and research he is responsible for the French-German cooperations of the KIT.



Alfonso Pagani  
Assistant professor  
MUL<sup>2</sup>, Department of Mechanical and Aerospace Engineering  
Politecnico di Torino, Italy  
[www.mul2.com](http://www.mul2.com)

Alfonso Pagani is professor assistant at the Department of Mechanical and Aerospace Engineering, Politecnico di Torino. He earned a Ph.D. in Structural Dynamics at City University of London in 2016 and, earlier, a Ph.D. in Fluid-dynamics at Politecnico di Torino.

Pagani is a member of the MUL<sup>2</sup> group ([www.mul2.com](http://www.mul2.com)) since 2011 and his research activities are related to the development of refined models for aerospace structures, composites, bio- and fluid-mechanics, post-buckling. He also spent research periods at Purdue University in 2016, where he worked on the implementation of advanced models for micro-structural analysis of composite materials with Prof. W. Yu; at RMIT Melbourne in 2014, where he developed models for flutter analysis and gust response of composite lifting surfaces; at Universidade do Porto in 2013, where he carried out investigations about the use of RBFs for the solution of equations of motion of refined beam models; and at London City University in 2012, where he formulated higher-order, exact, DSM-based 1D models. Together with Prof. Carrera and his research group, Pagani recently extended CUF for the geometrical nonlinear response and post-buckling analysis of metallic and composites structures.

He is involved in the Marie Skłodowska-Curie actions FULLCOMP and COMPOSELECTOR. Moreover, Pagani acts as team member and co-investigator for a number research projects together with International partners and Institutions, such as ENSAM Bordeaux for the development of advanced optimization methodologies for VAT composites, and EMBRAER S.A. for the tailoring of composite wing structures and global/local analysis.

Pagani is the co-author of some 40 articles in International Journals and currently serves as assistant editor for Advances in Aircraft and Spacecraft Structures.

**Francesco Pellicano**

Francesco Pellicano is Aeronautical Engineering and Ph.D. in Theoretical and Applied, he is currently Associate Professor, vice-Head of the Centre Intermech MoRe and committee president of 2 BsC and 3 MsC programmes. He is coordinator of EU Regional projects: METaGEAR (Gears, Materials, Robotics), INDGEAR (condition monitoring) and HPGA Fortissimo (applications of high performance computing); he was coordinator of several international and national projects. He published 2 Books, more than 50 Journal papers and more than 100 conference papers. Bibliometry: h-index 23, more than 1500 citations. His research activities are: gears experimental and numerical stress and vibration analysis; nonlinear vibrations of structures; vibration control; axially moving systems; nonlinear vibration of shells with fluid structure interaction, vibration of carbon nanotubes; non-smooth dynamics; Chaos; Nonlinear Time Series Analysis; Forecasting Methods in Oceanography.

## **Anand V. Singh**

After graduating with B. Sc. in Mechanical Engineering from Ranchi University, I came to Canada in September 1969 to join the school of graduate studies at the University of Ottawa and completed M. A. Sc. (1971) and Ph. D. (1975) degrees. The research area was the free vibration of sandwich spherical shells.

After graduation from the University of Ottawa, I worked as a Defence Scientist at the Defence Research Establishment Suffield (DRES) near Medicine Hat Alberta from January 1978 to April 1981. Then, I accepted a design engineer position in the Civil Design Department of Ontario Hydro in Toronto and worked there until December 1984. That is when I came to the Western University to teach machine component design and the finite element methods. At Western, I taught other courses viz. graphics and engineering drawings, dynamics, kinematics and dynamics of machines, modern control systems, theory of plates and shells, continuum mechanics, computational methods in engineering to name a few. I worked with some remarkable graduate students in the field of computational solid mechanics dealing with the linear and nonlinear vibrations of plates and shells. I retired as of July 01, 2016 and am a Professor Emeritus at the Western University.

About the family: I was married to Bimla about 50 years ago and we have two grown up children. Bidhi, our son, is married to Swati and they have a son named Akshaj. Our daughter Shikha just completed Ph. D. in Fisheries and Wildlife from the Michigan State University, East Lansing. Bimla and I attended eight of the last ten ISVCS symposia. This is the ninth.

**Andrew Watson**  
**Lecturer of Aerospace Structures**  
**Department of Aeronautical and Automotive Engineering**  
**Loughborough University, United Kingdom**

Andrew obtained his undergraduate and higher degrees from Cardiff University. His PhD looked at the stability analysis and optimisation of light weight structures. After two post-doctoral appointments at Cardiff Andrew joined Loughborough University as a member of academic staff in 2004.

His research includes buckling and postbuckling of aerospace panels; vibration of beams and quantum graphs. Buckling, vibration and quantum graph problems can all be approached by using the Dynamic Stiffness Method along with the Wittrick-Williams algorithm. Andrew is currently developing a set of tools to provide the user with eigenvalue and eigenvector solutions to any shaped graph with a differential operator.

Other research includes experimental and numerical modelling of damage in composite panels and numerical simulation of geometric nonlinear beams subject to bending and compression. More recently Andrew has been looking at fossil fuels and other finite resources. To facilitate this he is developing analytical methods to optimise structures where the objective function can be mass, energy costs or environmental degradation. His interest in resource demand reduction is opening a new area of research and is a subject area for delivering talks on the subject at various academic institutions and schools.

In his spare time he likes to keep up with current affairs and enjoys walking and sailing.